HOCHSCHULE FRESENIUS
UNIVERSITY OF APPLIED SCIENCES

Department of Chemistry & Biology
International Bachelor Applied Chemistry
Idstein

Synthesis of a Depsipeptide with Photolabile Protective Group and Fluorescence Label

Approved BACHELOR THESIS
for the achievement of an academic degree as
Bachelor of Science

Lara Alix Kaczmarek
born in Frankfurt/Main

Matriculation number: 400051655

1st Reviewer: Prof. Dr. Monika Buchholz
2nd Reviewer: Prof. Dr. Thorsten Hofe

12.06.2019

This Thesis was written between 01.02.2019 and 12.06.2019 at the Max Planck Institute for Polymer Research under support and supervision of Prof. Dr. Tanja Weil.

Acknowledgements

I would first like to thank Prof. Dr. Tanja Weil for offering the opportunity to work on this thesis at the Max Planck Institute for Polymer Reasearch. Furthermore I would like to thank Prof. Dr. Monika Buchholz for repeated advice and corrections during this work. Additionally, I would like to acknowledge Prof. Dr. Thorsten Hofe as the second reader of this thesis. I am also grateful to Dr. Christopher Synatschke for continuous feedback, advice and handling of organisational matters. I would particularly like to thank Adriana Sobota for her supervision and advice, provision of compounds and proofreading as well as the funny moments in the lab and for answers to every one of my even so tedious questions. Furthermore I would like to express my sincere thanks to Sarah Backfisch for her patience in recording various spectra during the NMR study and provision of a compound. Additionally, I would like to thank the entire research group for the pleasant working atmosphere and help with any kind of issues and the "Coffee Gang" for the cheerful breaks. Finally, I wish to thank my family and friends who have always accompanied and supported me on my path of life.

Contents

Abbreviations

ACN	Acetonitrile
Aβ	Amyloid β peptide
Boc	*Tert*-Butoxycarbonyl
DBF	Dibenzofulvene
DCM	Dichloromethane
DIC	*N,N'*-Diisopropylcarbodiimide
DIPEA	*N,N*-Diisopropylethylamine
DMAP	4-(Dimethylamino)pyridine
DMF	*N,N'*-Dimethylformamide
DMSO	Dimethyl sulfoxide
DPBS	Dulbecco's phosphate buffered saline
DSC	*N,N'*-Disuccinimidyl carbonate
E1cB	Elimination Unimolecular conjugate Base
ESI-MS	Electrospray ionisation–mass spectrometry
EtOAc	Ethyl acetate
FA	Formic acid
Fmoc	Fluorenylmethyloxycarbonyl
FTIR	Fourier-transform infrared spectroscopy
HPLC	High performance liquid chromatography
LC-MS	Liquid chromatography – mass spectrometry
m/z	Mass-to-charge ratio
MALDI-TOF-MS	Matrix-assisted laser desorption ionisation – time of flight mass spectrometry
NCA	α-Amino acid *N*-carboxyanhydride
NHS	*N*-Hydroxysuccinimide
NMR	Nuclear magnetic resonance
Oxyma	Ethyl cyano(hydroxyimino)acetate
PBS	Phosphate-buffered saline
PEG	Polyethylene glycol
PES	Polyether sulfone
PS	Polystyrene
PyBOP	Benzotriazol-1-yl-oxytripyrrolidinophosphonium hexafluorophosphate
ROP	Ring-opening polymerisation
SPPS	Solid phase peptide synthesis
TBAF	Tetra-*n*-butylammonium fluoride
TBDMS	*Tert*-Butyldimethylsilyl ether
***t*Bu**	*Tert*-Butyl
TEA	Triethylamine
TEM	Transmission electron microscopy

TFA	Trifluoroacetic acid
THF	Tetrahydrofuran
TIPS	Triisopropyl silane
TLC	Thin layer chromatography
Trt	Triphenylmethyl

List of Figures

List of Schemes

List of Tables

1 Introduction

In nature, biological systems with a tendency to self-assemble into ordered structures and molecular scaffolds play a vital role in physiological processes. On the other hand, disruption of these assemblies can cause pathological alterations leading to disorders like Alzheimer's Disease. A deeper understanding of such processes and their possible applications has therefore been within the focus of science for a long time.
Peptides present one of the various classes of self-assembling structures. Due to their biocompatibility, aggregation characteristics, and easily accessible and relatively cheap synthesis, peptides have gained a remarkable interest for application in a vast variety of fields. These include the rather obvious nanotechnologies in biomedicine where applications include drug delivery, tissue engineering, biosensors and antibacterial agents, but even among renewable energies peptides have gained recognition for example as microrod power generators. [1]
Through various non-covalent intra- and intermolecular interactions like hydrogen bonding, van der Waals and electrostatic forces, π–π-stacking and hydrophobic interactions, peptides exhibit self-assembling properties that can be modified and adapted to various needs. While these structures are crafted by nature with remarkable precision and efficiency, the complexicity of these self-assembling mechanisms and their dependency on one another complicates the artificial design of longer and more difficult peptide sequences. Control over spatial arrangement, solubility and ultimately the process of self-assembly has therefore been in the focus of synthetic chemistry for several decades. However, prediction of structures, properties and assembly behaviour still provides one of the major obstacles in peptide chemistry. Development and analysis of different self-assembling peptide systems aims for a deeper understanding of the various complex processes and might provide vital data for studies of biological phenomena. In the future, these could provide cure for diseases based on self-assembly mechanisms and create other various applications.[2–4]

By now, various experiments have revolved around the design of molecules that can "respond" to their surrounding in terms of self-assembly. A shift in their spatial arrangement can be triggered by changes in the environment like pH, temperature, ionic strength and mechanical force. One of the key developments in peptide synthesis has been the incorporation of a kink in the peptide's backbone *via* so-called depsipeptides to lessen non-covalent interactions and therefore increase solubility and lessen aggregation phenomena. [3, 5]

Previous work by members of the group of Prof. Dr. T. Weil involved studies of the self-assembling properties of an amphiphilic peptide sequence. Development of a kinked peptide sequence that would linearise upon change in pH and its resulting change in morphology were explored by Gačanin *et al*. [6] Based on this, further research by Pieszka *et al.* [4]showed that the triggering mechanism could be altered *via* incorporation of a protective group.
Other work by Wegner *et al.* [7] focused on photo-triggered release of bioactive molecules *via* a photocleaveable linker molecule. Combination of this triggering mechanism with previous research by the group of Prof. Dr. T. Weil will be the objective during this work and might provide further insight into morphology and spatial arrangement of peptides as well as possible applications in the field of biomedicine like photo-responsive tissue regeneration or drug-release.

1.1 Aim of the Project

The aim of this project will be to synthesise a photoresponsive depsipeptide and analyse its morphology and kinetics of a photoinduced deprotection as illustrated in Scheme 1.

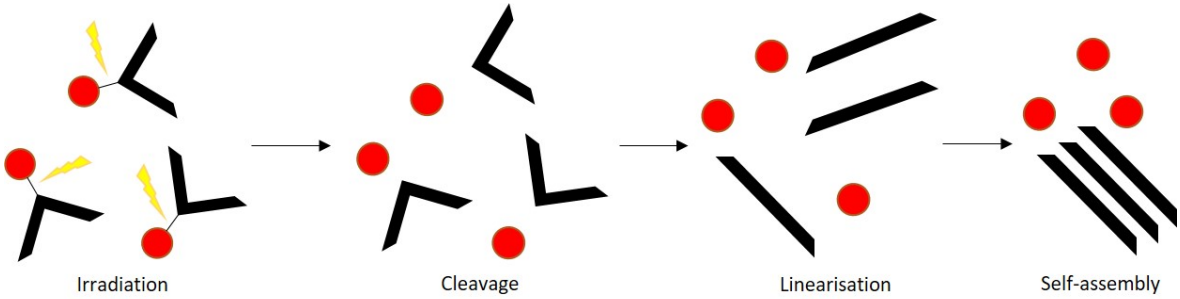

Scheme 1: Illustration of the photocleavage of a protected depsipeptide. The red circles display the protective group, the kinked and linear peptide sequence is displayed in black.

In more detail, this project will combine the aforementioned researches by synthesising protected KIKISQINM depsipeptide **1** (see Figure 1) wherein the serine's amino group is protected by a photocleaveable linker (highlighted in red). The linker will be synthesised during the course of the project in 6 steps following the procedures by Mizuta *et al.* [8] and Kaneko *et al.* [9] and successively coupled to the peptide. The depsipeptide will be synthesised in automated solid phase peptide synthesis (SPPS) according to protocols already established in previous works by the group of Prof. Dr. T. Weil (Gačanin *et al.* [6], Pieszka *et al.* [4]). Analysis of the photoinduced cleavage and fibrillation behaviour will involve transmission electron microscopy (TEM) imaging, high performance liquid chromatography (HPLC) and nuclear magnetic resonance (NMR) spectroscopy studies. To visualise cleavage of the linker, labelling with an azide dye is planned (green in Figure 1).

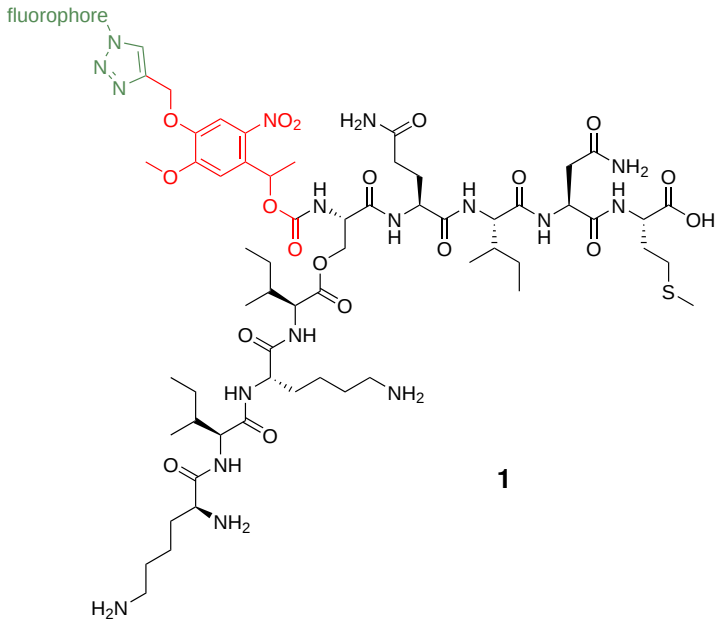

Figure 1: Structure of a fluorescence-labelled photoresponsive depsipeptide. The photoceaveable linker is highlighted in red, a possible fluorophore bound to the linker is highlighted in green.

2 Theory

2.1 Peptides

Peptides are a crucial part of life as we know it. In living organisms they make up essential molecules and structures like enzymes and transporters and regulate various processes. In all biological systems, these are composed of a variation of the same 20 standard amino acids linked *via* amide bonds to create a typically linear backbone bearing manifold side-chains – a so-called peptide. The structural constitution of peptides and their connection *via* amide bonds were first characterised independently by Emil Fischer and Franz Hofmeister in 1902. [10]

Amino acids contain an α-carboxyl and an α-amino group, the moiety R substituted on the α-carbon varies within each of the residues. An amide bond is formed in a condensation reaction between the carboxyl and amino groups (see Scheme 2). Since the hydroxyl group is a poor leaving group, the reaction will not occur readily at physiological pH.

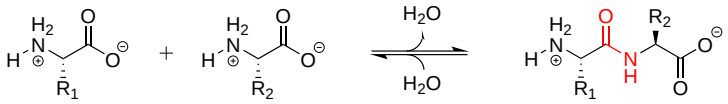

Scheme 2: Formation of an amide bond in a condensation reaction [10, 11]

Due to the electric dipole (carbonyl oxygen partially negative, amide nitrogen partially positive) the amide bond posseses a slight double bond character (see Scheme 3a). This limits free rotation around the binding axis of the peptide bond, resulting in a linear structure with 6 atoms in the same plane (see Scheme 3b). For the $N-C_\alpha$ and $C_\alpha-C$ bonds rotation (defined as angles ϕ and ψ) is not as restricted, though certain angles are thermodynamically more stable.

(a)

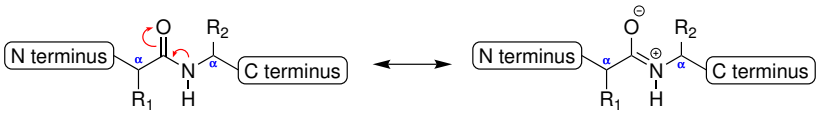

(b)

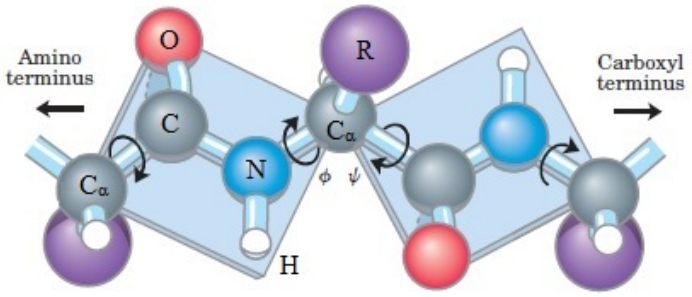

Scheme 3: (a) Double-bond character of the amide bond in peptides. (b) Structural planarity of the amide bond. Figure taken from *Lehninger's Principles of Biochemistry* and edited [11]

The amino acid sequence, or rather covalent bonds (including disulfide bonds), in a peptide define its so-called primary structure. As peptides grow longer recurring arrangements with higher stability

begin to form, defining the aforementioned thermodynamically more stable angles of ϕ and ψ. Due to rotation around the $N-C_\alpha$ and $C_\alpha-C$ bonds and hydrogen-bonding of not adjacent functional groups there are two preferred arrangements: α-helix and β-sheet. These arrangements can occur in multiple locations along the amino acid chain. The interactions of multiple of such structures in the same peptide create a threedimensionally folded molecule. This spatial arrangement is termed the tertiary structure, describing the entire arrangement of all atoms in the peptide. It includes the longer-range interactions of the amino acids among themselves. Larger proteins (e. g. haemoglobin) are composed of multiple seperate polypeptide subunits, creating a fourth level of structural arrangement: the quaternary structure. [11]

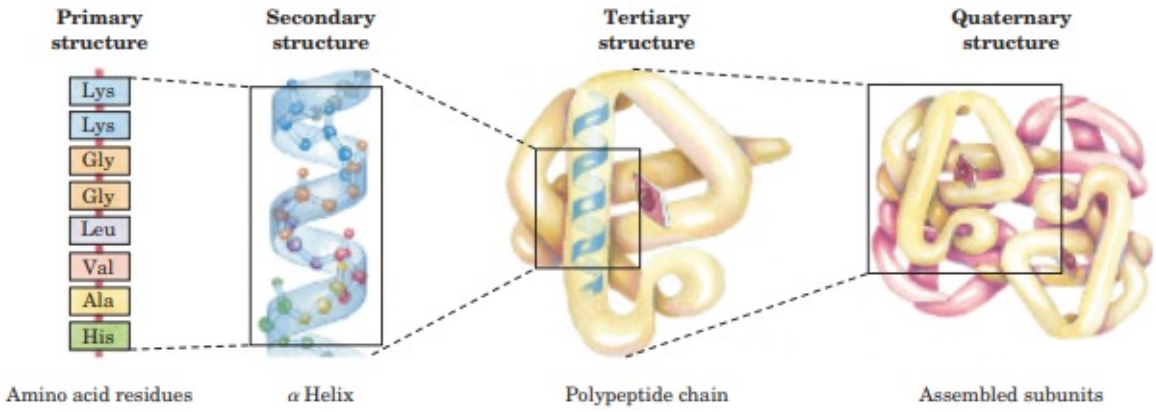

Figure 2: Four levels of protein structures. Figure taken from *Lehninger's Principles of Biochemistry* [11]

Additionally, many peptides exhibit self-assembling properties, i. e. form highly ordered threedimensional structures though non-covalent interactions depending on surrounding conditions like concentration, pH, temperature or presence of salts. Many of these are observed in nature e. g. as micelles, vesicles or fibrils. Figure 3 illustrates formation of some of these self-assembled structures.

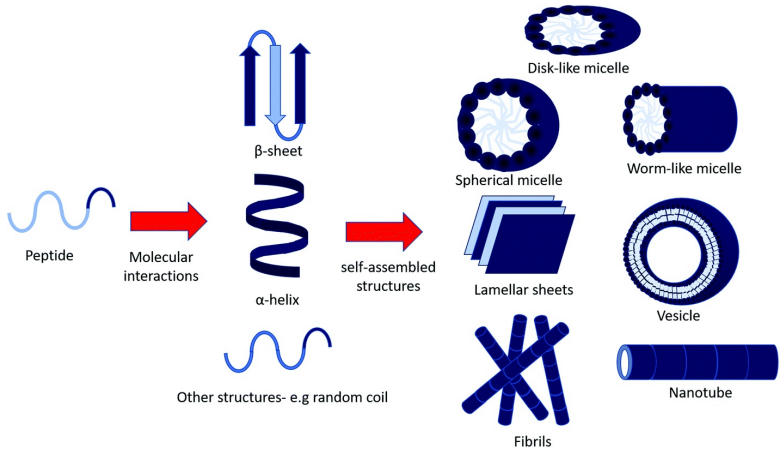

Figure 3: Formation of self-assembled structures of peptides. Figure taken from an article by Edwards-Gayle and Hamley. [12]

One of these self-assembling systems that has gained much recognition are amyloid fibrils. These are based on cross-β-sheet arrangements and are often associated with neurodegenerative diseases such as Alzheimer's or Parkinson's disease, but they also exhibit interesting traits for applications in e. g. biomedicine, tissue engineering, renewable energy and nanotechnology. [4, 13]

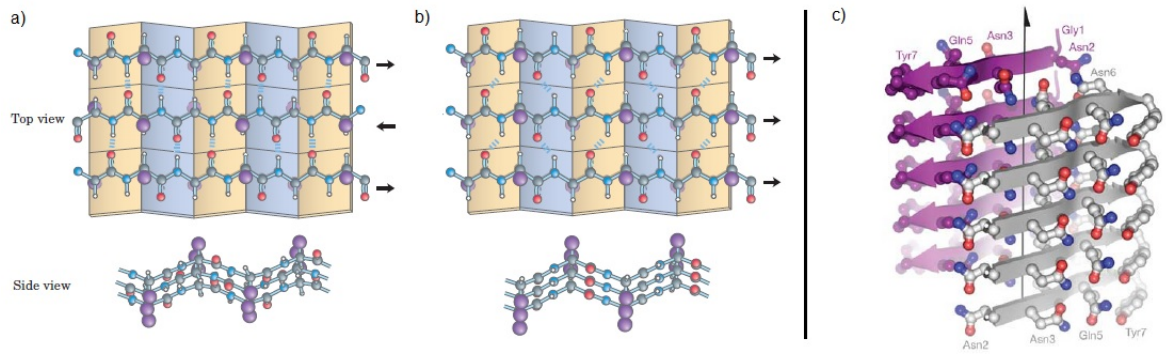

Figure 4: β-sheet structures in peptides. The residues R extend out of the β-sheet structure. (a) Antiparallel arrangement of strands. (b) Parallel arrangement of strands. (c) Examplary structure of a peptide with cross-β-sheet arrangement. The parallel β-sheet backbones are displayed as arrows. The black arrow between the β-sheets displays the fibril axis. Figures taken from *Lehninger's Principles of Biochemistry* [11] and a publication by Nelson *et al.* [14] and edited

In β-sheet arrangements, hydrogen bonds between amide bonds stabilise the zigzag structure of the peptide's backbone. The segments forming the β-sheet structure are often close to each other, in larger peptides interactions between distant sequence parts are also possible. The strands making up the secondary structure can either run parallel or antiparallel in terms of orientation of N and C termini (see Figure 4a and b) and can self-assemble into higher ordered structures like fibrils. According to Harris *et al.* antiparallel β-sheet formation is expected to be more stable since it reduces electrostatic repulsion and forms more hydrogen bonds, but hydrophobic interactions between the side chains seem to play a vital role in self-assembly of peptides. [15] Wang *et al.* reported that in peptides with strong hydrophobic side-chains, formation of parallel sheets is preferred. [2] Research on amyloid fibrils showed that they are made up of two stacked parallel β-sheet arrangements with the peptide's backbones being perpendicularly ordered to the fibril axis – a so-called cross-β-sheet structure (see Figure 4). [11, 14, 16]

Ordered structures like these β-sheets and the resulting threedimensional arrangement are requirements for hydrogel formation. A hydrogel is a cross-linked polymer that is unsoluble in water, but possesses the ability to retain water in its structure. Cross-linkage in the polymeric structure can be formed either *via* chemical bonds like disulfide bridges or physical interactions such as hydrogen bonds and hydrophobic interactions in peptides. Depending on their threedimensional structures, peptides can exhibit such hydrogel formation properties in aqueous solutions. The ability to swell in water is responsive to various stimuli which allows for controllable designs of hydrogels. Usually, swollen hydrogels contain a much higher mass fraction of water in their network than the actual polymer's mass, resulting in a significant increase in volume. [17]

2.1.1 Synthesis of Peptides

Due to their biocompatibility peptides are attractive for many biochemical, medicinal and pharmacological purposes which is why organic chemistry has focused on their synthesis for over 100 years. In nature, bioorganisms synthesise peptides in short time with high accuracy on ribosomes, which is why one of the three frequently used methods to obtain peptides is genetic engineering. This method allows for monodispers peptide preparation of large proteins like collagen, silk or even newly designed sequences.[11, 18]

The second mainly used method is synthesis *via* ring-opening polymerisation (ROP) of α-amino acid *N*-carboxyanhydrides (NCAs) to create homo- and block copolymer peptides. Many NCAs are commercially available, or can alternatively be prepared by phosgenation of side-chain protected α-amino acids. During ROP carbon dioxide is expelled in the presence of an initiator (e. g. primary and tertiary aminos, alkyl oxides) to produce a primary amino as active species for further ring-opening and subsequent polymerisation (see Scheme 4). [19, 20]

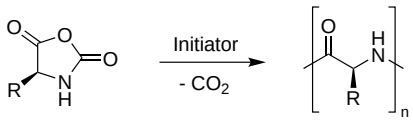

Scheme 4: Ring-opening polymerisation of α-amino acid *N*-carboxyanhydrides for the synthesis of homopolymer peptides [20]

In 1903 Emil Fischer published his first explorations on the synthesis of peptides wherein he successfully coupled two amino acids using acyl chlorides. [21] However, this method was at the time limited by the inability to protect the amino terminus for creation of longer peptide chains. Further research and exploration allowed for du Vigneauds synthesis of oxytocin in 1954 [18, 22], but it was not until 1963 that the total synthesis of peptides became a commonly used technique. At this time Robert B. Merrifield achieved a major breakthrough by binding the peptide to a solid phase at one end while successively coupling amino acids at the other. [23] Today this so-called SPPS is the most widespread and accessible method for creation of peptides composed of up to 50 amino acid residues. [18, 24]

In SPPS peptides are built from C to N terminus. To obtain a peptide of the desired amino acid sequence, protection of the N_α-terminus is crucial. Thus, the standard protocol for SPPS involves four steps: (1) deprotection of the main chain, (2) washing, (3) coupling of a protected amino acid to the main chain and (4) washing. These steps are repeated until the final peptide is deprotected (5) and cleaved from the resin (6). The most common method nowadays utilises an orthogonal protective group strategy (i. e. successively cleaveable protective groups) involving the base-labile fluorenylmethyloxycarbonyl (Fmoc) protective group (see Scheme 5), which will be studied more closely in the following. [24] Scheme 5 illustrates the standard protocol in SPPS.

In 1972 Carpino and Han reported the development of the new base-labile N-Fmoc protective group. [25] It can be removed follwing an Elimination Unimolecular conjugate Base (E1cB) mechanism. Due to the electron-withdrawing effect of the fluorene system, the β-hydrogen is very acidic. Exposed to piperidine (the typical removal reagent for the N-Fmoc protective group), the proton is easily removed owing to the aromaticity of the cyclopentadienyl anion. [26] A further β-elimination generates a reactive dibenzofulvene (DBF) intermediate (which can be quenched with excess base), CO_2 and the free amino group (see Scheme 6). [24]

Since most amino acids posess reactive side chains (e. g. amino group in lysine), respective protective groups must be incorporated to omit unwanted side reactions. These have to be stable at the Fmoc cleavage conditions, hence acid-labile protective groups are used predominantly. Table 1 lists the side chain protective groups of amino acids used for synthesis during this work.

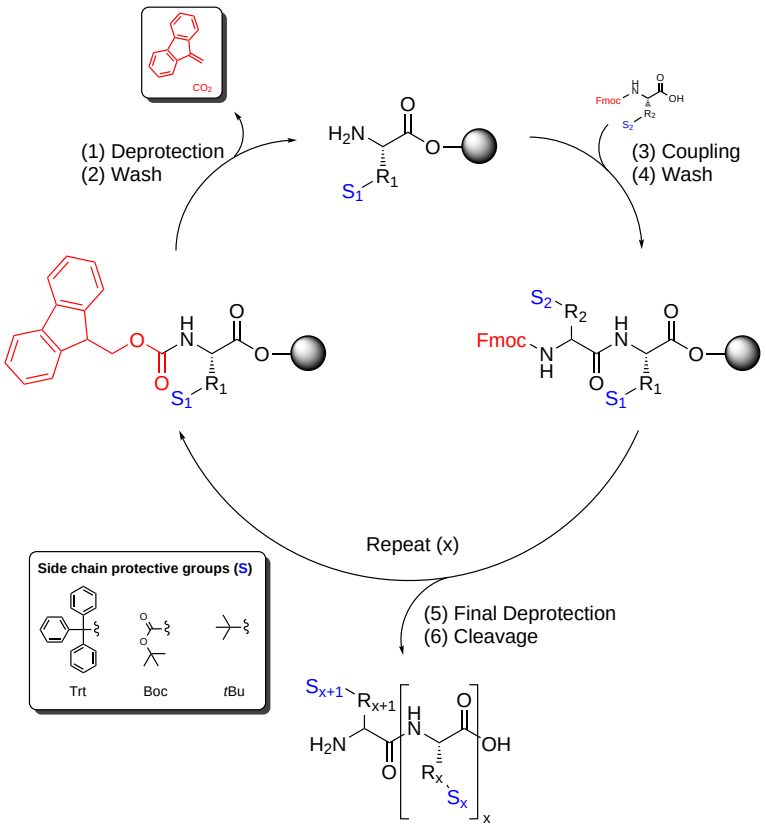

Scheme 5: Standard protocol in SPPS. The N_α-terminal protective group (Fmoc) is coloured red. [24]

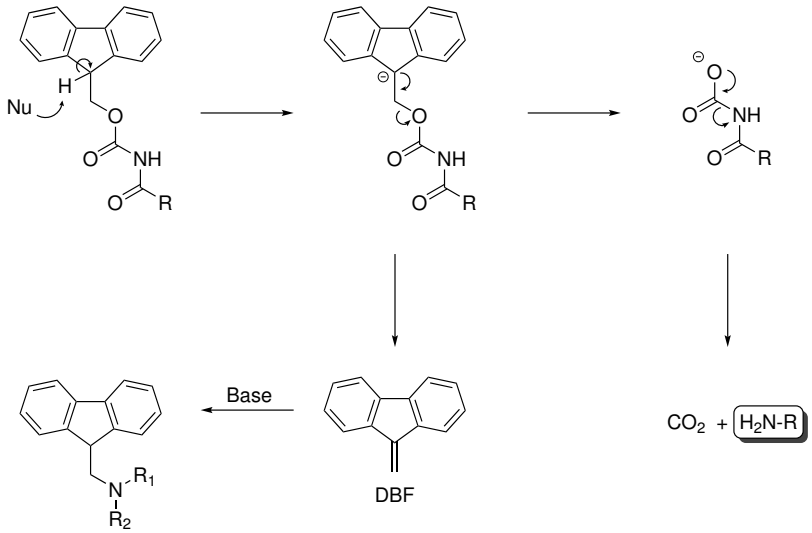

Scheme 6: E1cB mechanism: Fmoc deprotection generating a reactive DBF intermediate, CO_2 and the free amino group. DBF can be quenched by excess base. [24]

Table 1: Side chain protective groups of amino acids used in this work. The side-chain protective groups are triphenylmethyl (Trt), *tert*-butoxycarbonyl (Boc) and *tert*-butyl (*t*Bu).

Amino Acid	Functionality	Protective Group
Asn	$-CONH_2$	Trt
Gln	$-CONH_2$	Trt
Lys	$-NH_2$	Boc
Ser	$-OH$	*t*Bu

All of the protective groups listed in Table 1 can be cleaved with trifluoroacetic acid (TFA) as shown exemplarily in Scheme 7 for the Boc group. The Boc group is a carbamate protective group and will hydrolyse in presence of dilute aqueous acids like aqueous 3 M HCl solution. [26]

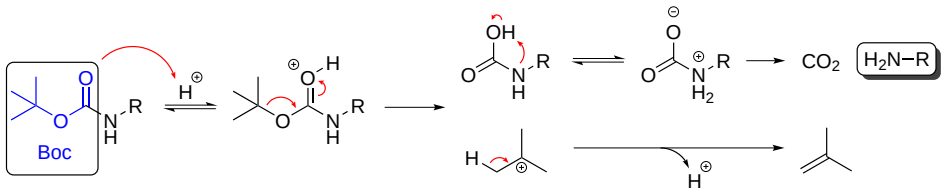

Scheme 7: Boc deprotection [26]

To induce the coupling of amino acids to the peptide chain, the amino acid's carboxylic acid needs to be activated. Activators used during this work were benzotriazol-1-yl-oxytripyrrolidinophosphonium hexafluorophosphate (PyBOP) and *N,N'*-diisopropylcarbodiimide (DIC) whose mechanisms will be explored further in the following.

Onium-salt promoted coupling requires the use of a base to create a carboxylate ion and start the activation mechanism to create the active ester. A sterically hindered base like *N,N*-diisopropylethylamine (DIPEA) is preferred as it limits α-proton abstraction of the active ester, though this side reaction cannot be omitted entirely. [24]
After deprotonation by the base (**A**), a nucleophilic attack of the carboxylate ion at the phosphorus atom of the activator (PyBOP) follows (**B**). An (acyloxy)phosphonium salt and a deprotonated 1-hydroxybenzotriazole (OBt^-) are generated in the process and further react with each other. The OBt^- attacks the carbonyl-carbon of the (acyloxy)phosphonium salt nucleophilic to generate the desired active ester and tri(pyrrolidin-1-yl)phosphine oxide as a side product (**C**). The active ester will form a new peptide bond *via* aminolysis. [27, 28]

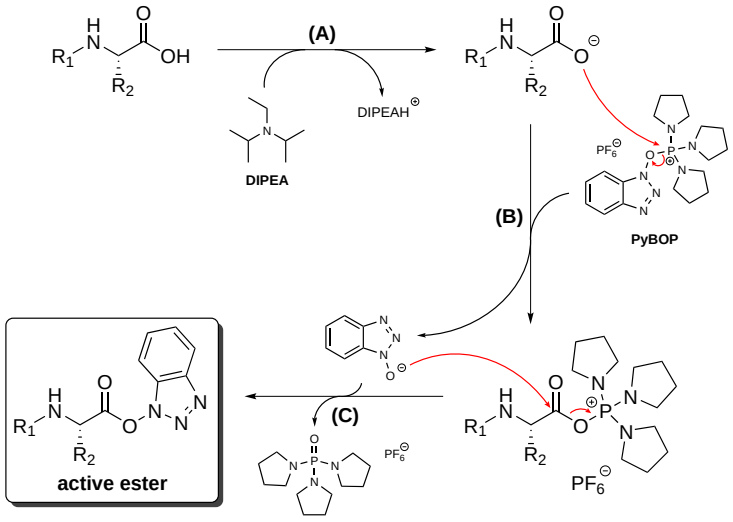

Scheme 8: Mechanism of PyBOP activation

A second very common activation method involves use of carbodiimides like DIC (see Scheme 9). For these compounds a base to initiate deprotonation is not necessary. The slight basicity of the nitrogen atoms promote formation of an *O*-acylisourea from the amino acid's carboxyl group. It will

subsequently react with the free amino group at the peptide's N_α terminus to create a new amide bond.

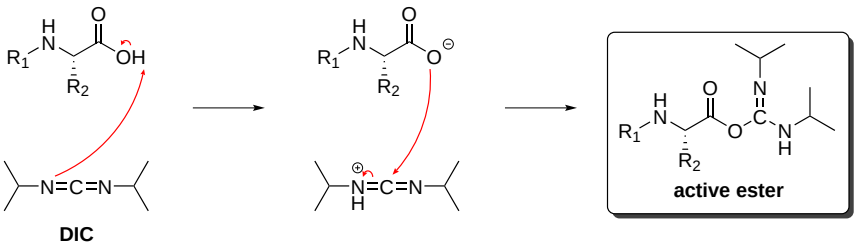

Scheme 9: Mechanism of DIC activation

However, the high reactivity of the *O*-acylisourea makes it prone to unwanted side reactions like conversion to a less reactive *N*-acylurea and racemisation. Addition of ethyl cyano(hydroxyimino)acetate (Oxyma) shall reduce base-induced side reactions like aspartimide formation during deprotection cycles in aspartic acid or asparagine residues due to its strong acidity (pK_a 4,60). While HOBt has the same pK_a, research showed that benzotriazole-based additives exhibit potentially explosive properties. Oxyma has proven to give lower racemisation rates and higher efficiency during SPPS. Scheme 10 shows the proposed base-catalysed aspartimide formation in aspartic acid and asparagine residues and the subsequent racemisation *via* a nucleophilic attack. It is believed that Oxyma lessens this side-reaction by competing with the peptide for the base. [24, 28, 29]

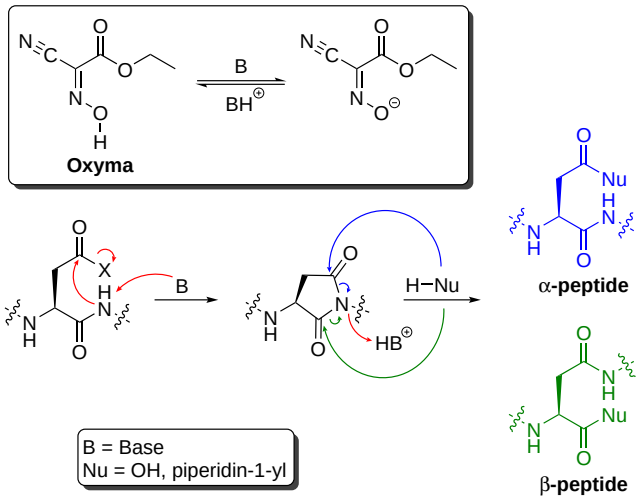

Scheme 10: Mechanism of aspartimide and α/β-peptide formation during SPPS

For the automated synthesis on a solid phase, the resin has to meet certain requirements. These include high chemical stability to allow for longer reaction times and good swelling properties to omit steric hindrances and reduced reaction times. There are many different resins available for use in solvents with different polarities. Most of the resins used in SPPS nowadays are polystyrene (PS) based and can be further functionalised with spacers and linkers. The resin used for this work is the PS based resin shown Figure 5 which is functionalised with a Wang linker. Upon cleavage it releases the peptide acid. Other resins such as Rink amide resins relase peptide amides upon cleavage. The Wang resin exhibits good swelling properties in *N,N'*-dimethylformamide (DMF) and dichloromethane (DCM), the two mainly used solvents during this work.

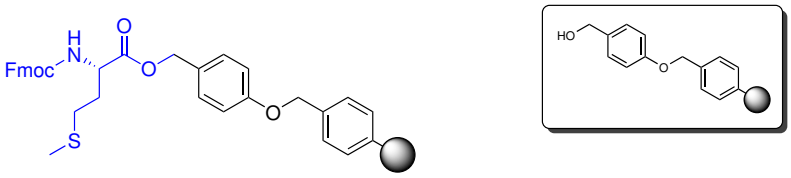

Figure 5: Depiction of the used Wang resin preloaded with Fmoc-*L*-methionine (blue) and the plain resin (box).

After synthesis the finished peptide is cleaved from the resin. For this work a methionine-preloaded Wang resin was used (structure shown in Figure 5) which can be removed in a solution of 95 % TFA, 2.5 % triisopropyl silane (TIPS) and 2.5 % H_2O. The peptide acid is released from the resin *via* acidic ester hydrolysis. Typically, side chain protective groups are removed simultaneously to resin cleavage, though some other resins that are highly acid-sensitive may allow cleavage from the resin without removal of the side chain protective groups. [24, 30]
When protective groups are simultaneously cleaved from the peptide as the peptide is from the resin, a variety of reactive side-products (i. e. carbocations) are produced. When sensitive residues are exposed to these species, a manifold of unwanted derivatives of the desired peptide can form, creating lower yields as a result. Other problems include irreversible modifications of the peptide, oxidations or incomplete removal of protective groups as well as cleavage in an undesired position of the resin's linker. To suppress side-reactions, scavengers are added to the cleavage cocktail. The choice of scavengers is adapted to the respective probability of different side-products. TIPS (or trialkylsilanes in general) has proven to be effective especially as scavenger for Trt cations that occur during removal of the protective group. Water can also act as a scavenger and for example inhibit formation of adducts. [31, 32]

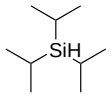

Triisopropylsilane

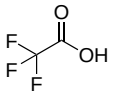

Trifluoroacetic acid

Figure 6: Structures of TFA and TIPS used in the cleavage cocktail

2.2 Depsipeptides

Depsipeptides – a special form of peptides – can be found in many forms in nature, the most of them being cyclic. The term is a combination of the words "depside" and "peptide", indicating their structural peculiarity: Depsides are esters of hydroxy acids, i. e. esters of two or more different or same phenolic benzoic acids. An example is shown in Figure 7a. A depsipeptide is therefore a peptide containing the previously discussed amide bonds as well as one or more ester bonds. The term was first introduced by Shemyakin in 1953 to cover compounds as the one shown in Figure 7b. [33, 34]

The term depsipeptide does not include information on the location of the ester bond in a peptide. Some amino acids contain carboxy or hydroxy functionalities in their side chains which are also prone to esterification. These molecules are termed "isopeptides" (example in Figure 7c). Furthermore, "isopeptide bonds" are amide bonds formed between an amino and a carboxyl group with at

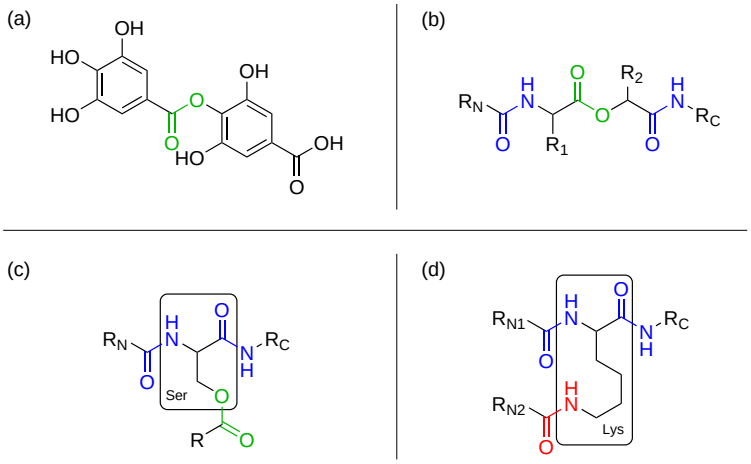

Figure 7: (a) Example of a depside (4-*O*-galloylgallic acid). The ester bond is highlighted in green. (b) Exemplary structure of a depsipeptide with an ester bond in the backbone. The amide bonds are blue, the ester bond is highlighted in green. (c) Exemplary structure of an isopeptide with an ester bond in the serine's side-chain. The amide bonds are blue, the ester bond is highlighted in green. (d) Exemplary structure of an isopeptide with an amide bond (*isopeptide bond*) in the lysine's side-chain. The amide bonds (*eupeptide bonds*) are blue, the isopeptide bond is highlighted in red.[33–35]

least one of them being located at the side-chain of an amino acid (Figure 7d). The corresponding counterpart (i. e. the C – N bond between two α carbons) is sometimes called "eupeptide bond". [35]

2.2.1 Secondary Structures of Depsipeptides

As already discussed in section 2.1, peptides can fibrillise and induce hydrogel formation depending on their structure. Isopeptides connecting peptide backbones *via* ester bonds in a side chain present a different behaviour. Originally those depsipeptides were used to improve solubility of synthesised peptides and allow for easier purification. Another side effect of the kink in the structure is the reduced aggregation of peptide chains due to disruption of the β-sheet structure. According to Sohma *et al.* this process is reversible. The *O*-acyl isopeptide can undergo an intramolecular *O,N*-acyl shift (*via* a five-membered ring intermediate) shown in Scheme 11 to rearrange into the native linear peptide structure. This shift is pH-dependent and can therefore be controlled. Previous work by Gačanin *et al.* showed that for depsipeptide **2** this shift occurs at pH $>$ 2. [4, 5, 36]

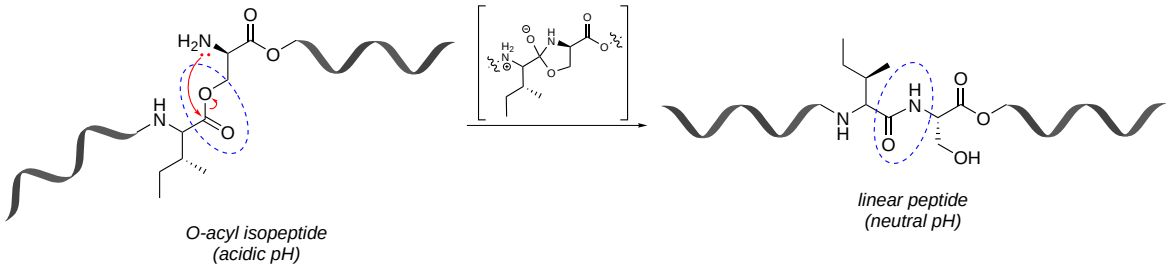

Scheme 11: pH-induced *O,N*-acyl shift in *O*-acyl isopeptides [5]

Previous work by the group of Prof. Dr. T. Weil showed that the amphiphilic peptide sequence KIKISQINM **3** quickly forms cross-β-sheet peptide nanofibers in aqueous solution. This fibrillation occurs even at low pH when incubated in aqueous 0.1 % TFA solution. To evaluate whether the fibrillation could be selectively triggered, depsipeptide **2** was prepared. In this depsipeptide an ester bond

between the serine's side-chain and the carboxy-group of the isoleucine residue replaces the regular amide bond in the peptide's backbone, providing a kink in the structure. Both structures are shown in Figure 8. TEM imaging proved that the kinked structure of the depsipeptide will prohibit formation of peptide nanofibers when incubated at low pH. Physiological pH will cause an *O,N*-acyl shift (linearisation) of the depsipeptide, therefore exhibiting fibrillation behaviour. This pH controlled mechanism did even sustain human serum albumin was functionalised with the peptide and polyethylene glycol (PEG) to create a fibrous soft polymer hydrogel. Due to these self-assembling properties and their continued occurence even after functionalisation, the KIKISQINM peptide sequence was chosen for functionalisation during this work. [6]

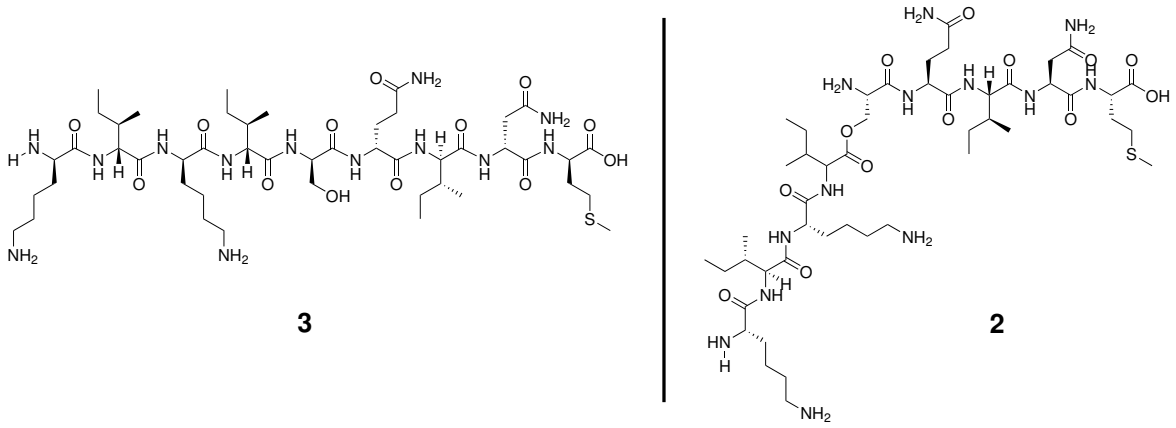

Figure 8: KIKISQINM peptide sequence in linear (**3**) and depsipeptide (**2**) configuration

Further research concerning the triggering mechanism of the *O,N*-acyl shift involved synthesis of boronic acid protected depsipeptide **4**. Pieszka *et al.* showed that the synthesised protected depsipeptide is stable in pure water and will therefore not form fibrils visible in TEM imaging. Upon exposure to kosmotropic agents (i. e. "order-generating" agents like phosphate salts) the carbamate bond will cleave, leaving the free depsipeptide **2** which will then linearise and fibrillise due to neutral pH (see Scheme 12). Additionally, parallel β-sheets were observed in fourier-transform infrared spectroscopy (FTIR) analysis, meaning that the protected peptide formed the aforementioned amyloid-like fibrils and could therefore be used to investigate respective fibrillation behaviour. [4]

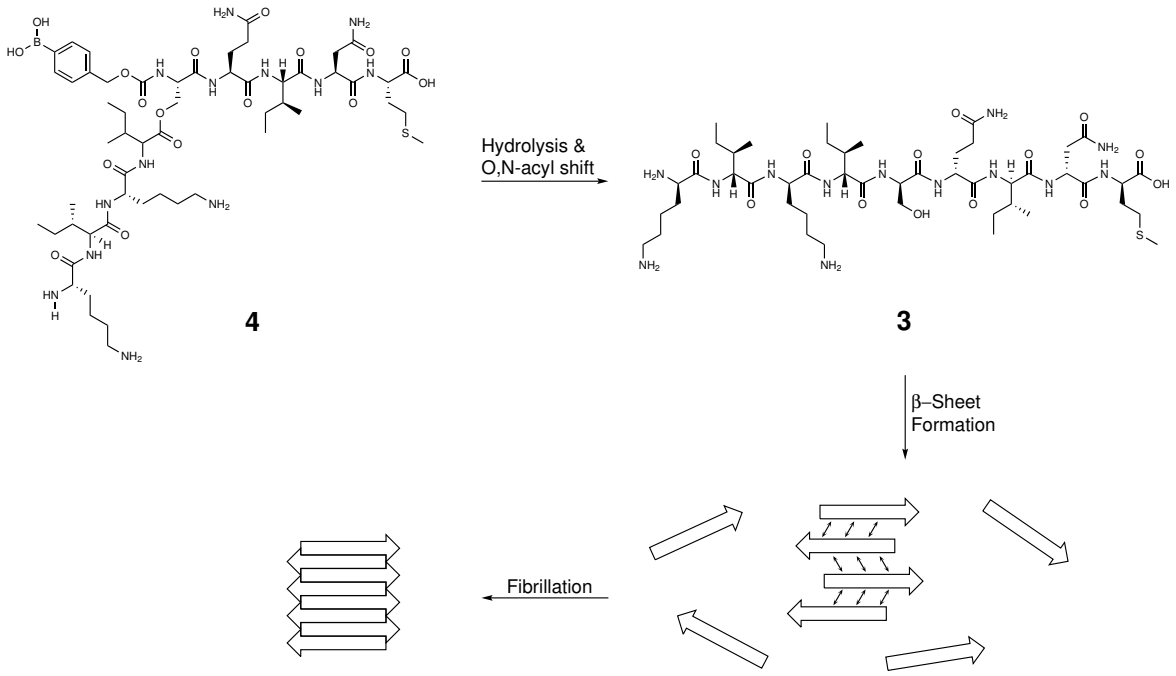

Scheme 12: Previous research on a boronic acid caged depsipeptide by Pieszka *et al.* [4]

The reaction conditions of the coupling of 4-nitrophenyl (4-(4,4,5,5-tetramethyl-1,3,2-dioxaborolan-2-yl)benzyl) carbonate to the resin (shown in Scheme 13) were adapted in this work.

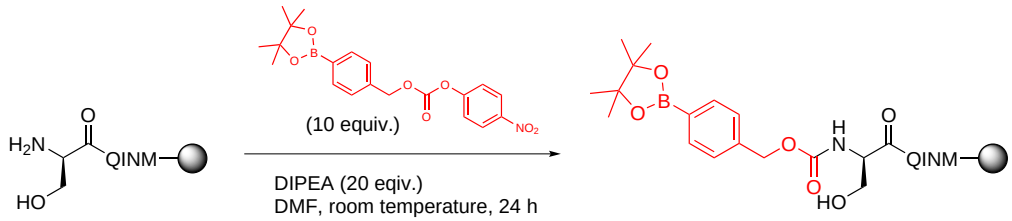

Scheme 13: Incorporation of boronic acid protective group in depsipeptide synthesis as reported by Pieszka *et al.* [4]

2.3 Cleavage Mechanism of the Photolabile Protective Group

One aspect of this work is the photocleavage of protective group **PhotoSG6** from the synthesised depsipeptide and the corresponding kinetics. The mechanism behind this cleavage is described as the Norrish reaction mechanism. In Norrish type I and II reactions carbonyl compounds are cleaved photochemically. The reactions were first described as the main two decomposition types in aldehydes and ketones by Norrish *et al.* in 1932. [37] Type I describes an α-cleavage creating an acyl and alkyl radical (or diradical in case of cyclic compounds). Through various fragmentations and recombinations of the radical species the final product for type I reactions can be a variety of hydrocarbons. Type II – the one that photolinker **PhotoSG6** follows – refers to the abstraction of a γ-hydrogen to produce a 1,4-diradical. Cyclobutanoles can be produced through a subsequent ring closure reaction (Norrish-Yang reaction). Alternatively, the intermediate can undergo fragmentation to yield an enol and an alkine. [38, 39] As type II is the desired mechanism in the synthesised photolabile peptide, it will be explored further in the following.

As shown in Scheme 14 the double bond between nitrogen and oxygen in the synthesised photolinker's structure is split homolytically upon exposure to UV-light to produce a biradical species (**A**). A γ-hydrogen is abstracted by the electron-deficient oxygen to create the 1,4-biradical intermediate (**B**). *Via* intramolecular electron migration (**C**) and a five-membered cyclic intermediate (**D**) the final cleavage of the photolabile group and the ligand (R_3) is achieved (**E**). Carbon dioxide is produced as a side product during the reaction. [40]

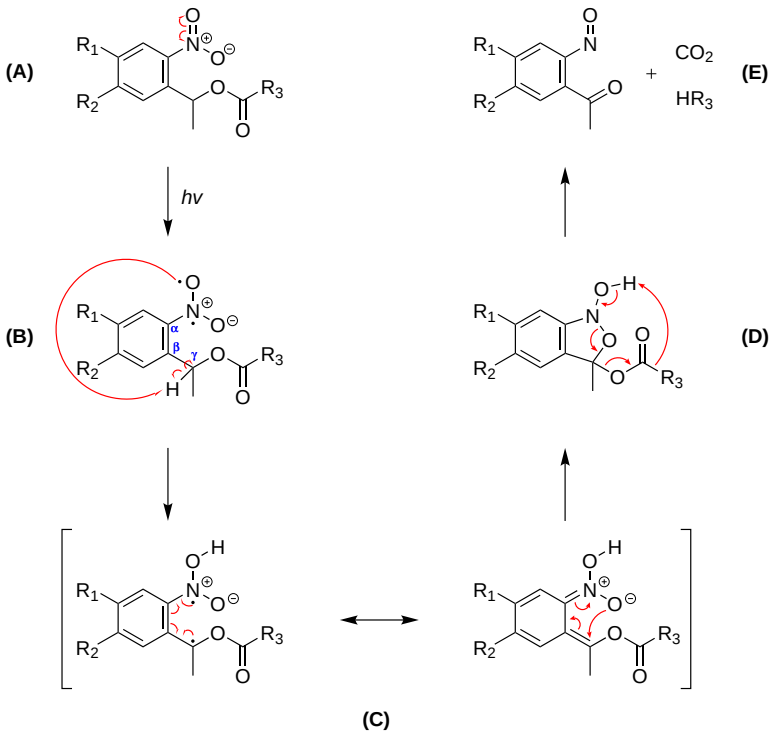

Scheme 14: Proposed Norrish type II reaction mechanism for the cleavage of a photolabile depsipeptide [40]

2.3.1 Photoresponsive Depsipeptides

Combining a photolabile protective group with a depsipeptide creates a "click"-peptide in which fibrillation can be controlled by external stimuli. Previous work by Sohma *et al.* involved the synthesis of a click-peptide analogue of the amyloid β peptide (Aβ) 1–42 which is related to Alzheimer's disease (see Scheme 15). This structure featured a kink in the main chain and protection of the amino function *via* a photolabile protective group. The click-peptide did not self-assemble as observed in the regular Aβ 1–42 structure under physiological conditions. However, an intact Aβ 1–42 structure could be obtained from the click-peptide after photo-triggered cleavage of the protective group and *O,N*-acyl migration thus proving that the self-assembly can be induced upon irradiation. [5]

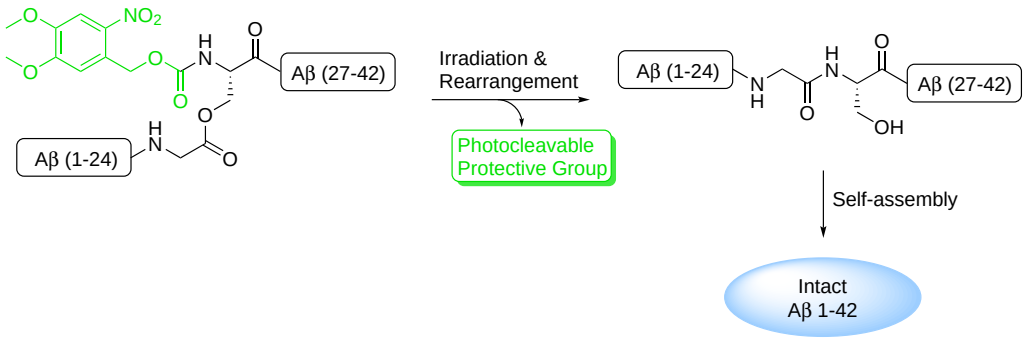

Scheme 15: Photo-triggered click-peptide analogue of Aβ 1–42 reported by Sohma *et al.* [5]

Furthermore, research by Wegner *et al.* focused on photo-triggered release of biomolecules. [7] Photosensitive linker **PhotoSG6a** was used to attach bioactive molecules with an amino group to a surface. The NHS moiety of the linker can react with the amine group of a biomolecule while the alkyne moiety can undergo a click reaction with one of various azide functionalised materials. Wegner *et al.* showed that the biomolecules can be cleaved from the surface *via* irradiation at 365 nm. Depending on the time of irradiation and intensity, the amount of cleaved molecules can be controlled to the extent of creating gradients. Since the linker can easily be bound to the free amino group in (KIKI)SQINM depsipeptide **2** and allows for simple labelling with azide dyes on the alkyne functionality, **PhotoSG6a** was chosen as the photolabile protective group in this work.[7]

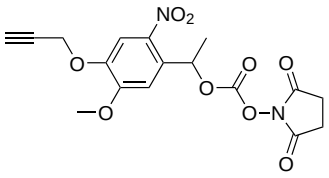

PhotoSG6a

Figure 9: Structure of photolinker **PhotoSG6a**

2.4 Transmission Electron Microscopy

One of the analysis methods used during this work was TEM. Basic principles of this method will be explained in the following.

Optical microscopes have been used for a long time throughout history. However, the restrictions in resolution due to the wavelength of visible light initiated the search for spectroscopic methods that would be able to surpass these boundaries. After deBroglie's presentation of the wave-particle duality of electrons in 1925, the first attempts on utilisation of this priciple led to the first functional electron microscope in 1936. With this technology, pictures up to atomaric resolution became possible which could obtain information on chemical composition and crystal structures.

Figure 10 shows the general setup of a transmission electron microscope. In vacuum, a tungsten filament on top of the microscope emits electrons upon heating up. The electrons are directed through a hole in the anode from the electron source towards the condenser lens system. The wavelength of the electrons can be influenced by variation of the accelerating voltage. A higher

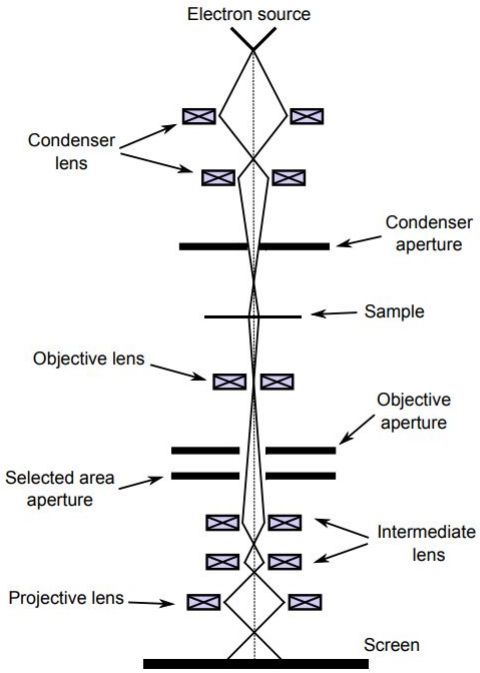

Figure 10: General setup of a transmission electron microscope. Figure taken from dissertation of N. Marturi. [41]

voltage results in a lower wavelength, but will also cause less scattering. Since high energy beams might destroy the specimen, typical accelerating voltages for biological compounds range from 80 to 125 kV compared to 200 kV and higher for materials science. The lenses influence the electron beam to create a uniform intensity and energy distibution within the beam. The electrons will then hit the specimen and interact with it *via* diffraction and scattering effects. Samples have to be as thin as possible to allow for proper imaging. When passed through the specimen, electrons are focused by another magnetic lens system onto an imaging plate. Imaging is achieved *via* impact on fluorescent or phosphorescent plates or a charge-coupled device. Depending on the adjustment of the objective aperture, images or diffraction patterns can be observed on the imaging plate.

Upon impact of the electron beam on the specimen, electrons can interact with its atoms *via* elastic and inelastic, coherent and incoherent scattering and diffraction due to coulomb interactions. Multiple factors like scattering probability and angle, distance between scattering events and loss of energy due to inelastic scattering influence the observed image or diffraction pattern. Depending on the thickness of the specimen, one electron can undergo multiple scattering events. Since prediction of the route of an electron that had undergone multiple interactions with the specimen is nearly impossible without exact knowledge of the observed structure, it is assumed that electrons undergo only one scattering event when passing through the specimen. Therefore, thinness of specimen is crucial for TEM imaging.

Information in TEM imaging is gained from the inelastic scattered electrons. Their impact pattern on the screen creates a contrast image that represents different densities of the specimen. Since heavier atoms cause stronger scattering, chemical compositions can be derived from the observed scattering patterns.[41, 42]

3 Results and Discussion

The aim of the project was to synthesise a photoresponsive depsipeptide and analyse its morphology and kinetics of a photoresponsive deprotection. The synthesis of the protective groups as well as the peptide itself and the subsequent analyses will be discussed in the following. Scheme 16 shows the planned synthetic route for photoresponsive depsipeptide **1**. Due to the fibrillation bahaviour of the KIKISQINM sequence observed in previous research of the group of Prof. Dr. T. Weil, the same sequence was chosen as base peptide for protection. Photolinker **PhotoSG6a** was chosen due to previous work by Wegner *et al.* proving that the compound can be used to protect amino groups and will cleave upon irradiation at 365 nm.

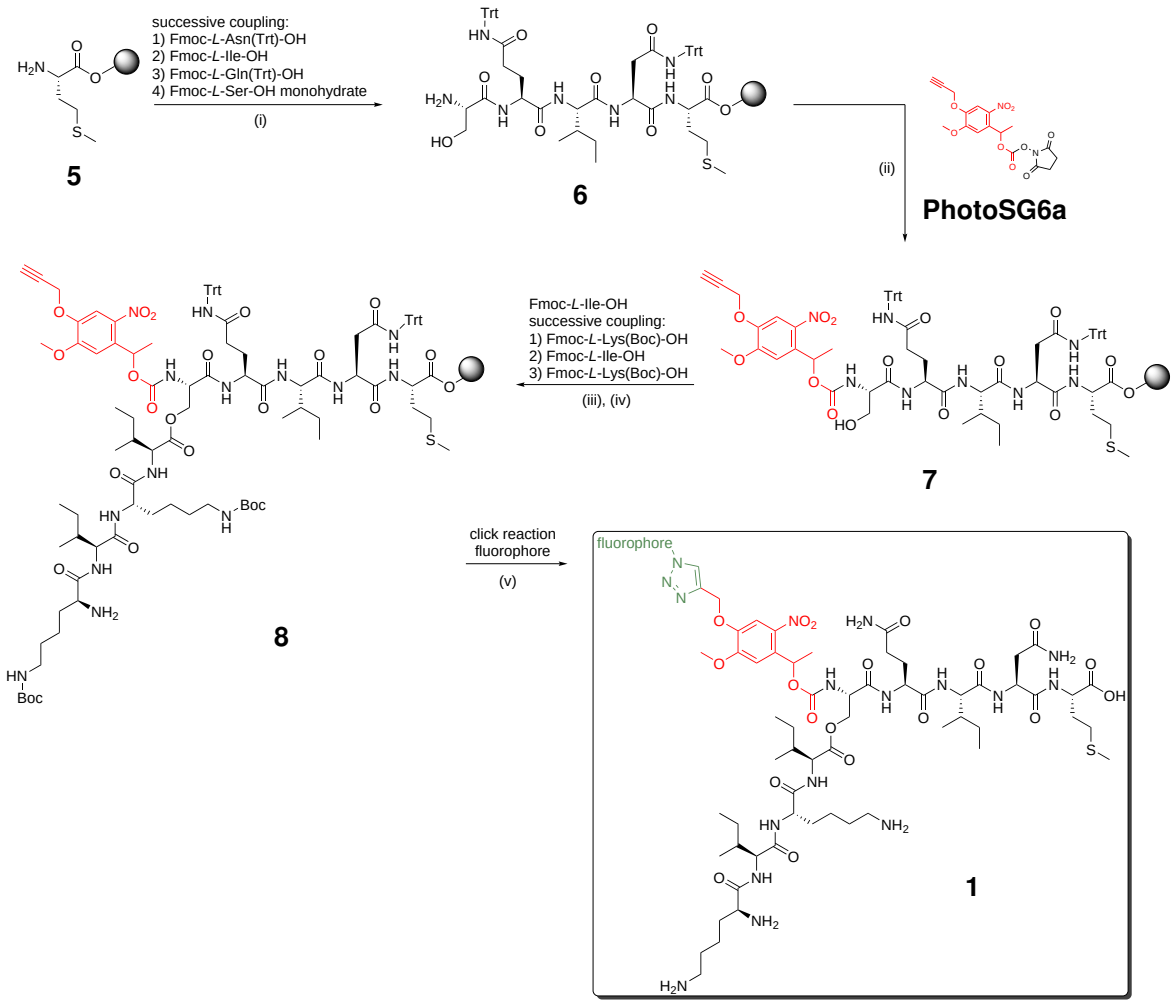

Scheme 16: Planned synthesis of a fluorescence-labelled photosensitive depsipeptide. (i) Successive coupling of Fmoc-*L*-Asn(Trt)-OH, Fmoc-*L*-Ile-OH, Fmoc-*L*-Gln(Trt)-OH and Fmoc-*L*-Ser-OH monohydrate (5 equiv.) in an automated microwave-assisted peptide synthesiser. In every coupling step: PyBOP (5 equiv.), DIPEA (10 equiv.), single coupling, 75 °C, 10 min; Fmoc-deprotection: 20 % piperidine in DMF, 75 °C, 2x 3 min. (ii) **PhotoSG6a** (1 equiv.), DIPEA (10 equiv.), DMF, room temperature, 24 h. (iii) Fmoc-*L*-Ile-OH (10 equiv.), DMAP (1 equiv.), DIC (2 equiv.), DMF, room temperature, double coupling (2 h, 24 h). (iv) Successive coupling of Fmoc-*L*-Lys(Boc)-OH, Fmoc-*L*-Ile-OH, Fmoc-*L*-Lys(Boc)-OH (5 equiv.) in an automated microwave-assisted peptide synthesiser. In every coupling step: PyBOP (5 equiv.), DIPEA (10 equiv.), single coupling, 75 °C, 10 min; Fmoc-deprotection: 20 % piperidine in DMF, 75 °C, 2x 3 min. (v) Addition of a fluorophore was not conducted during the given timeframe.

3.1 Synthesis of the Protective Groups

For this work, photolabile (**PhotoSG6a**,**b**) and non-photolabile (**NSG3**) protective groups were synthesised. The procedures will be described in the following.

The photolabile protective groups **PhotoSG6a** and **PhotoSG6b** were synthesised following the procedures by Mizuta *et al.* [8] (steps 1 to 3), Kaneko *et al.* [9] (steps 4 to 6a) and Pieszka *et al.* (step 6b) [4] as shown in Scheme 17.

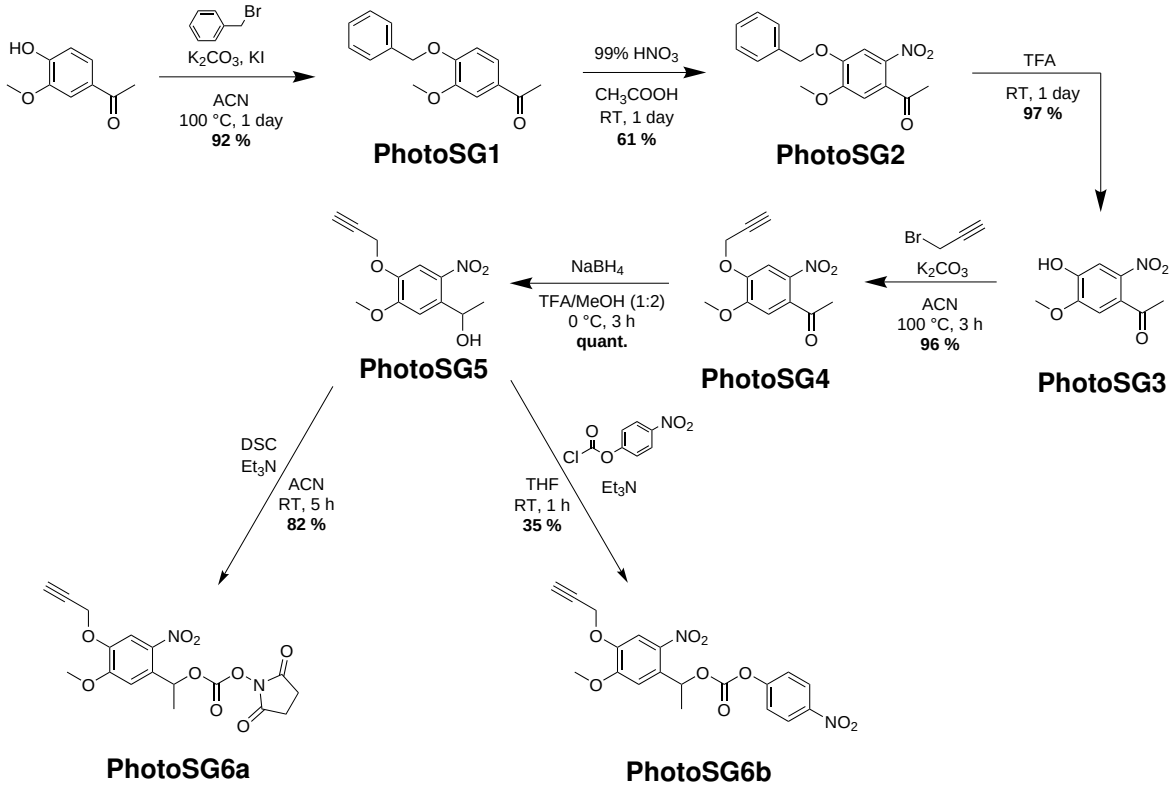

Scheme 17: Synthetic route for the two photolabile protective groups **PhotoSG6a** and **PhotoSG6b** [4, 8, 9]

For all synthesis steps except for nitration of **PhotoSG1** and reaction of **PhotoSG5** with 4-nitrophenyl chloroformate, yields of more than 80 or 90 % or even quantitative yields were obtained, as described by literature. [8, 9] A yield of 61 % for the nitration of **PhotoSG1** is also in compliance with literature values (67 %) and might be a result of the formation of different nitration products. However, the appearance of only 2 aromatic signals in the NMR spectrum of **PhotoSG3** (Figure 13) where the benzyl group is cleaved from the compound verifies nitation on the center aromat. Additionally, the observed singlett multiplicity of the two aromatic proton peaks in the NMR spectrum of **PhotoSG2** verify that nitration did not occur at position 2 (see Figure 11).

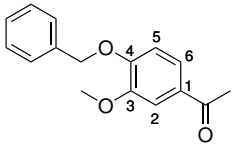

Figure 11: Structure of **PhotoSG1**

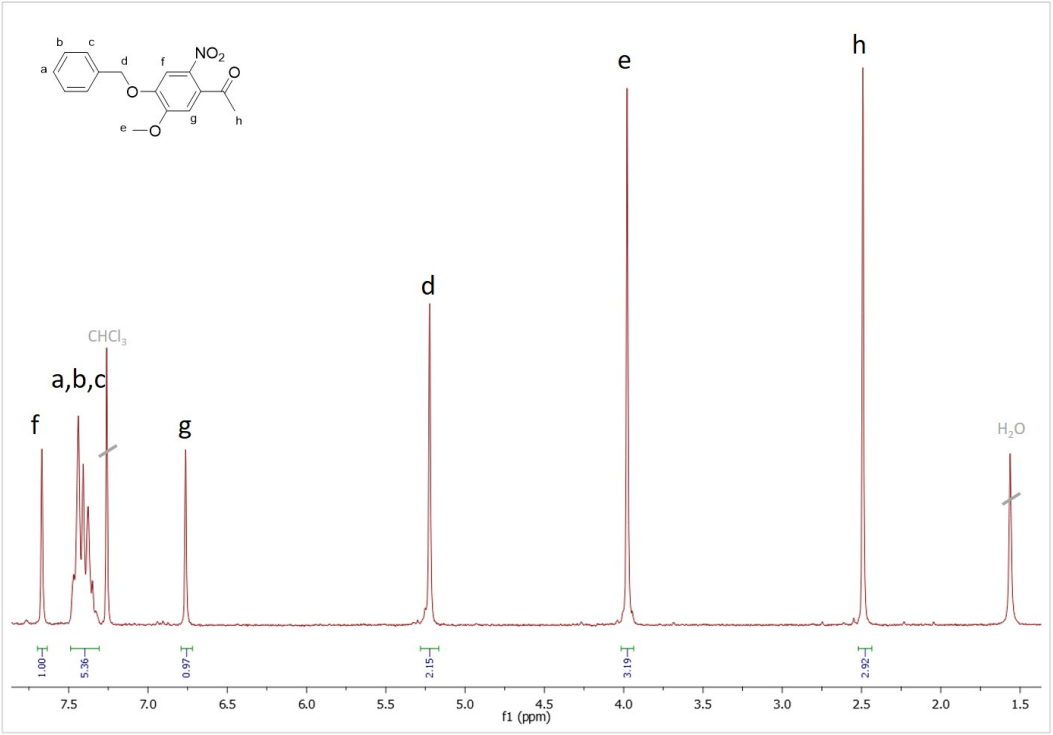

Figure 12: ^{1}H-NMR of **PhotoSG2** (250 MHz, $CDCl_3$): δ [ppm] 7.69 (s, 1 H; f), 7.53 to 7.32 (m, 5 H; a, b, c), 6.79 (s, 1 H; g), 5.25 (s, 2 H; d), 4.00 (s, 3 H; e), 2.52 (s, 3 H; h).

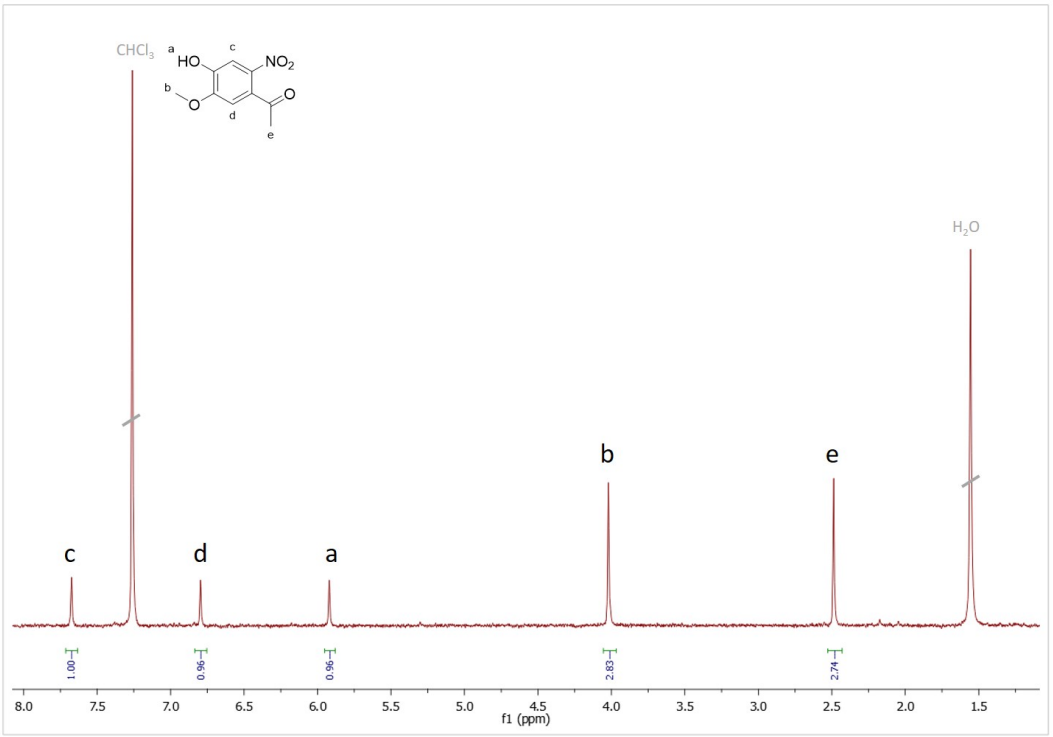

Figure 13: ^{1}H-NMR of **PhotoSG3** (250 MHz, $CDCl_3$): δ [ppm] 7.67 (s, 1 H; c), 6.80 (s, 1 H; d), 5.92 (s, 1 H; a), 4.02 (s, 3 H; b), 2.49 (s, 3 H; e).

PhotoSG6b was prepared in an attempt to optimise the synthesis of protected photo-depsi **10** and will therefore be discussed in section 3.2 in more detail. The synthesis of **PhotoSG6b** itself yielded

only 115 mg (35 %) of the product and was therefore not further explored.

To obtain additional information on the morphology and cleavage kinetics of a photoresponsive depsipeptide, synthesis of a non-photolabile protective group **NSG3** was conducted. **NSG3** was synthesised following the procedure by S. Kaneko *et al.* [9] as shown in Scheme 18.

In contrast to the synthesis of **PhotoSG6**, the intermediates and endproducts of the synthesis of the non-photolabile linker were not solids, but oils and the yields were generally lower. Since the focus of this work laid on the synthesis of a photoresponsive depsipeptide, this route was not further explored but might offer further insight into the peptide's kinetics.

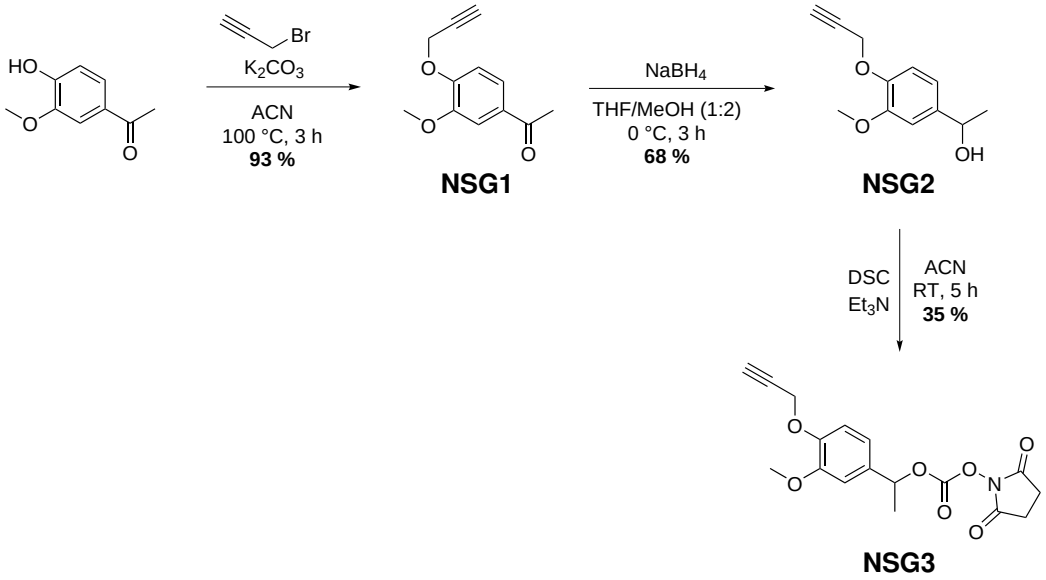

Scheme 18: Synthetic route for the non-photolabile protective group **NSG3** [9]

3.2 Synthesis of the Protected Depsipeptide

The main objective of the project was to synthesise a photoresponsive depsipeptide. The first synthesis route involved usage of PyBOP and DIPEA during SPPS, following the procedure by J. Gačanin *et al.* [6] as shown in Scheme 19. This first setup yielded only trace amounts of the protected depsipeptide (<1 %).

All intermediates except for esterification product **11** (structure in Scheme 20) were found in matrix-assisted laser desorption ionisation – time of flight mass spectrometry (MALDI-TOF-MS) analysis. Since intermediate **11** was neither found in any of the following setups, it was assumed that the intermediate will not ionise in MALDI-TOF-MS analysis and can therefore not be detected. However, the desired protected depsipeptide **10** was still found after continuation of the synthesis.

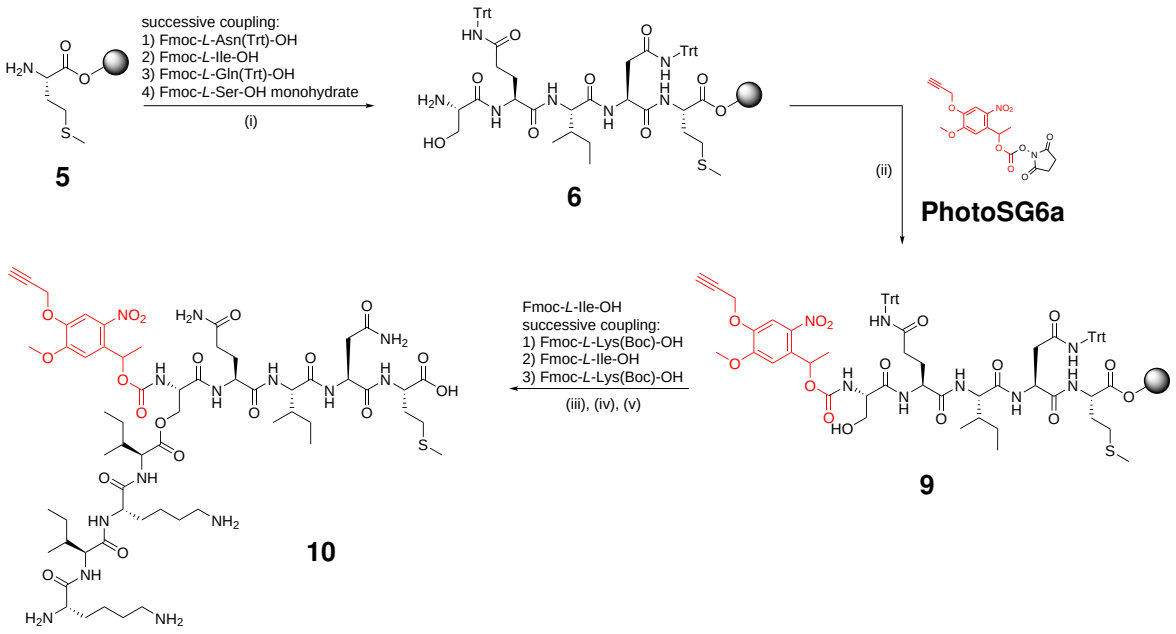

Scheme 19: Synthesis of photosensitive depsipeptide **10**. (i) Successive coupling of Fmoc-*L*-Asn(Trt)-OH, Fmoc-*L*-Ile-OH, Fmoc-*L*-Gln(Trt)-OH and Fmoc-*L*-Ser-OH monohydrate (5 equiv.) in an automated microwave-assisted peptide synthesiser. In every coupling step: PyBOP (5 equiv.), DIPEA (10 equiv.), single coupling, 75 °C, 10 min; Fmoc-deprotection: 20 % piperidine in DMF, 75 °C, 2x 3 min. (ii) **PhotoSG6a** (1 equiv.), DIPEA (10 equiv.), DMF, room temperature, 24 h. (iii) Fmoc-*L*-Ile-OH (10 equiv.), DMAP (1 equiv.), DIC (2 equiv.), DMF, room temperature, double coupling (2 h, 24 h). (iv) Successive coupling of Fmoc-*L*-Lys(Boc)-OH, Fmoc-*L*-Ile-OH, Fmoc-*L*-Lys(Boc)-OH (5 equiv.) in an automated microwave-assisted peptide synthesiser. In every coupling step: PyBOP (5 equiv.), DIPEA (10 equiv.), single coupling, 75 °C, 10 min; Fmoc-deprotection: 20 % piperidine in DMF, 75 °C, 2x 3 min. (v) TFA (95.0 %), TIPS (2.5 %), H_2O (2.5 %), room temperature, 2 h.

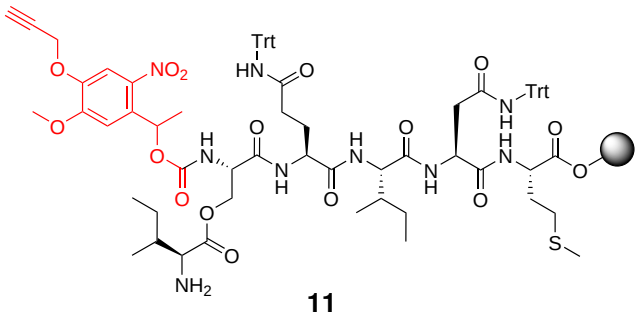

Scheme 20: Structure of esterification product **11**

Purification *via* HPLC showed two seperate peaks for product **10** at 34.3 min and 34.8 min elution time. In liquid chromatography – mass spectrometry (LC-MS) the elution times differed only by approximately 0.2 min, because a different gradient and acid was used (LC-MS: 5 % to 95 % acetonitrile (ACN), 20 min, formic acid (FA); HPLC: 5 % to 100 % ACN, 15 min, TFA). MALDI-TOF-MS and LC-MS analyses of both peaks showed simliar mass-to-charge ratio (*m/z*) (see Figure 14 and Figure 16), thus indicating formation of an isomer.

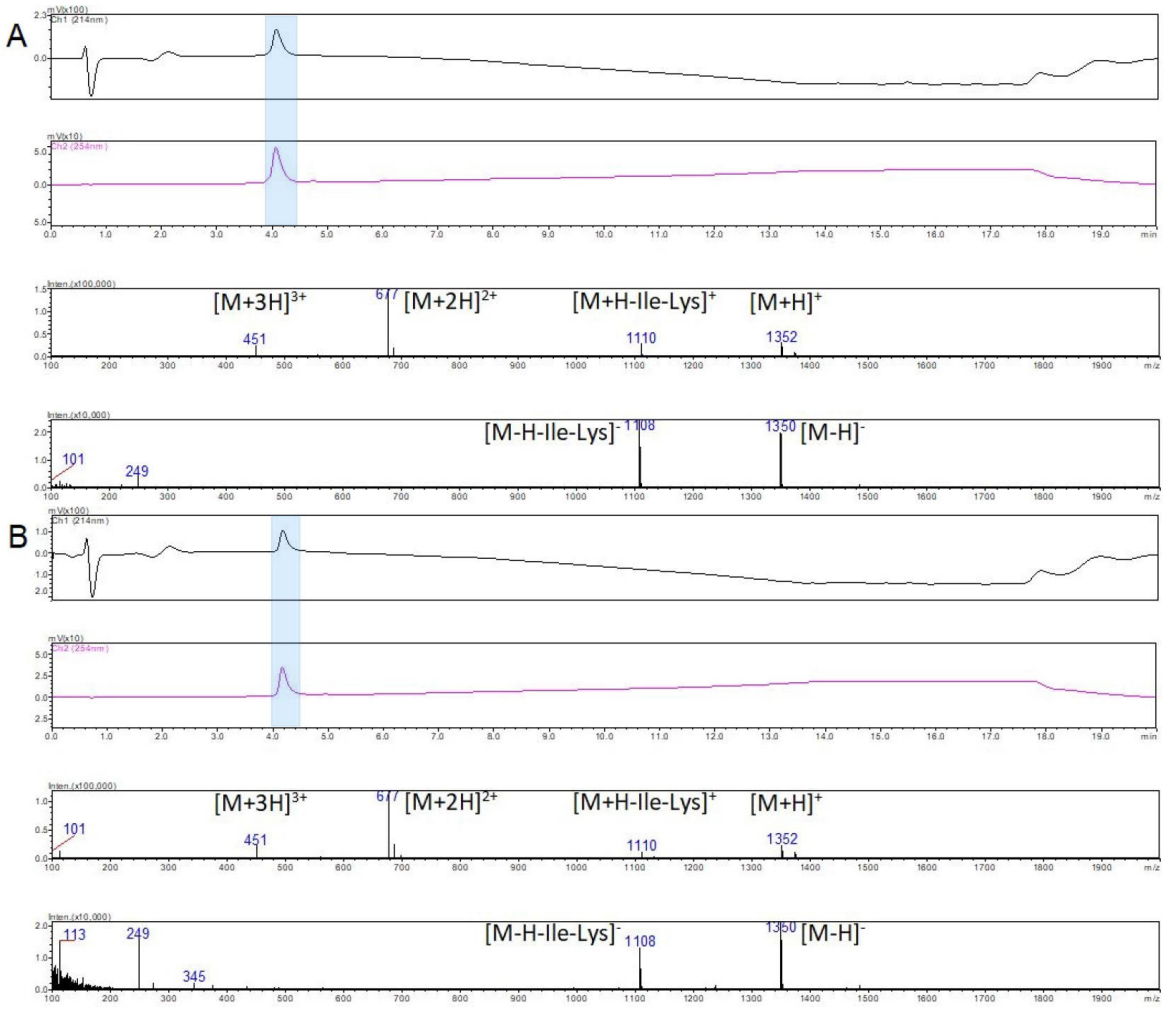

Figure 14: LC-MS analysis of the two product peaks A and B of the first protected depsipeptide setup. The peaks within the blue areas are analysed for *m/z* composition.

Since NHS esters (i. e. **PhotoSG6a**) react not only with amines but nucleophiles in general, it was assumed that the reaction had also taken place at the unprotected hydroxy group of the serine residue (see Figure 15), causing formation of linear isomer **12**. [43]

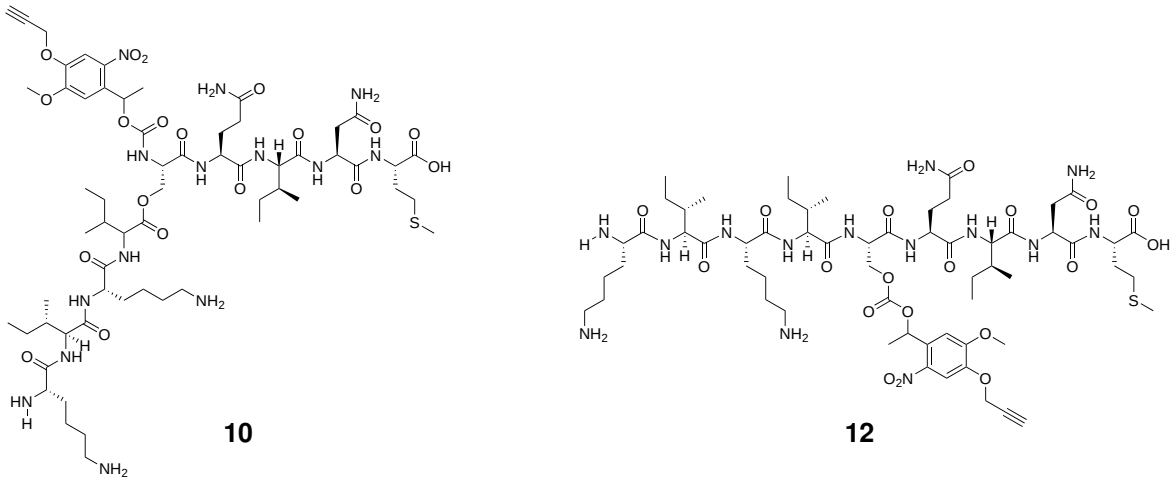

Figure 15: Possible isomers during synthesis of protected depsipeptide **10** due to reaction of the serine residue with NHS ester **PhotoSG6a**

As shown in Figure 16, various peaks for the desired product **10** occur in the mass spectra. Since the photocleavage product KIKISQINM differs significantly in elution time ($\Delta t \approx 10$ min) it can be assumed that the peak at *m/z* = 1074 in the MALDI-TOF-MS spectra is caused by cleavage of the protective group during the measurement. This assumption is supported by the fact that *m/z* = 1074 does not occur in the LC-MS spectra, where another soft ionisation technique (electrospray ionisation–mass spectrometry (ESI-MS)) is used. Sodium and potassium adducts of protected depsipeptide **10** are also visible in MALDI-TOF-MS spectra as well as the sodium adduct of the plain KIKISQINM sequence. LC-MS spectra show multiply protonated species of protected depsipeptide **10**. During both analysis methods a peak at *m/z* = 1110 is observed which can be assigned to a loss of a lysine and an isoleucine residue of protected depsipeptide **10**.

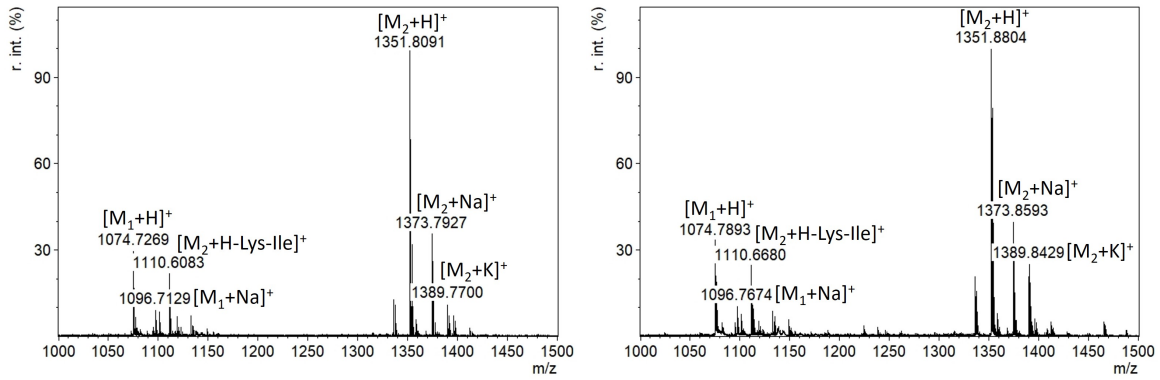

Figure 16: HRMS (MALDI-TOF-MS) analysis comparison between peaks A and B from HPLC of protected depsipeptide **10**. M_1 = 1073.6267 g mol^{-1} (KIKISQINM depsipeptide **2**), M_2 = 1350.6853 g mol^{-1} (protected depsipeptide **10**). Left spectrum: Peak A. Right spectrum: Peak B.

To omit the formation of isomer **12**, *tert*-butyldimethylsilyl (TBDMS)-protected peptide **15** was synthesised and used in a second setup as described in Scheme 21. Even though the desired product **10** was found in MALDI-TOF-MS analysis (**HRMS** (MALDI-TOF-MS, 1350.6853 g mol^{-1}): *m/z* = 1351.5727 $[M+H]^+$), only trace amounts of product **10** could be obtained after HPLC purification. After the coupling with the TBDMS-protected serine **14** the resin took up noticeable less volume in the solution than before the reaction. This indicated collapse of the resin, leading to reduced availability of the binding sites and therefore low yields. Whether the resin collapsed due to the altered reaction steps (introduction of Fmoc-*O*-(2-(trimethylsilyl)propan-2-yl)-*L*-serine and deprotection with tetra-*n*-butylammonium fluoride (TBAF)) or other unknown influences was not further explored. Synthesis of protected depsipeptide **10** utilising TBDMS protected serine was therefore not repeated during the given time-frame.

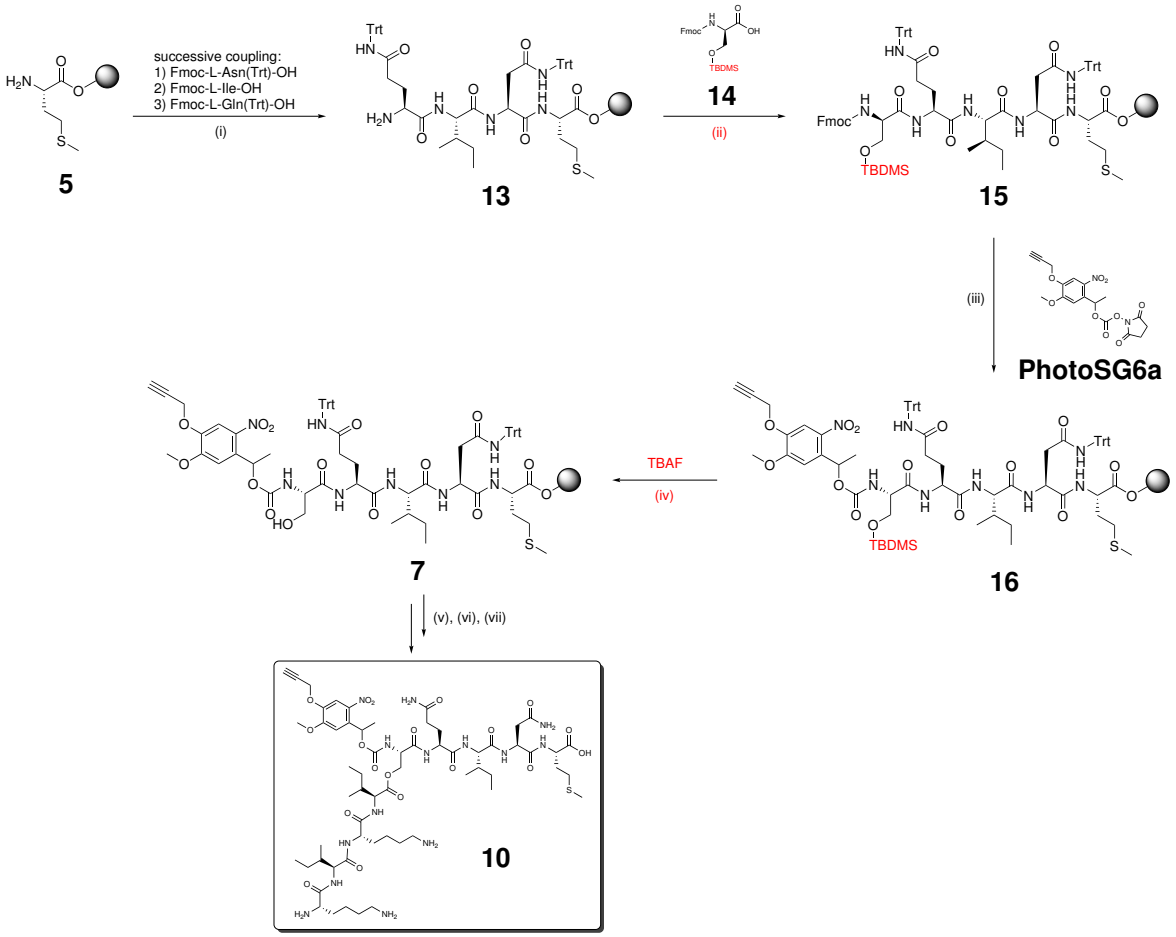

Scheme 21: Synthesis route of protected depsipeptide **10** utilising TBDMS-protected serine. The steps differing from previous syntheses are highlighted in red. (i) Successive coupling of Fmoc-*L*-Asn(Trt)-OH, Fmoc-*L*-Ile-OH and Fmoc-*L*-Gln(Trt)-OH (5 equiv.) in an automated microwave-assisted peptide synthesiser. In every coupling step: PyBOP (5 equiv.), DIPEA (10 equiv.), single coupling, 75 °C, 10 min; Fmoc-deprotection: 20 % piperidine in DMF, 75 °C, 2x 3 min. (ii) Fmoc-*O*-(2-(trimethylsilyl)propan-2-yl)-*L*-serine (5 equiv.), PyBOP (5 equiv.), DIPEA (10 equiv.), DMF, room temperature, 48 h; Fmoc-deprotection: 20 % piperidine in DMF, room temperature, 24 h. (iii) **PhotoSG6a** (1 equiv.), DIPEA (10 equiv.), DMF, room temperature, 24 h. (iv) TBAF (2 eq), room temperature, 24 h. (v) Fmoc-*L*-Ile-OH (10 equiv.), DMAP (1 equiv.), DIC (2 equiv.), DMF, room temperature, double coupling (2 h, 24 h). (vi) Successive coupling of Fmoc-*L*-Lys(Boc)-OH, Fmoc-*L*-Ile-OH, Fmoc-*L*-Lys(Boc)-OH (5 equiv.) in an automated microwave-assisted peptide synthesiser. In every coupling step: PyBOP (5 equiv.), DIPEA (10 equiv.), single coupling, 75 °C, 10 min; Fmoc-deprotection: 20 % piperidine in DMF, 75 °C, 2x 3 min. (vii) TFA (95.0 %), TIPS (2.5 %), H_2O (2.5 %), room temperature, 2 h.

Another idea was to prepare a serine building block already functionalised with the photolabile protective group (compound **17** shown in Figure 17). However, this idea was not further explored since the protective group **PhotoSG6a** had not yet been synthesised in sufficient amounts. Coupling of an amino acid residue to the resin involved usage of five equivalents of the respective amino acid, meaning that compared to the established synthesis a five times higher amount of **PhotoSG6a** would have been needed. Experiments concerning reduction of the used equivalents of amino acids were not conducted during the given timeframe. Reaction of QINM-resin **13** with the suggested building block **17** could still be further explored in the future as well as the need for TBDMS protection in the building block.

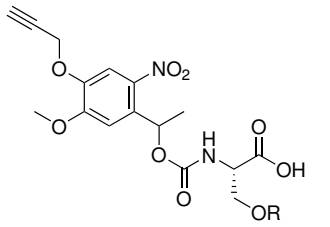

R = H, TBDMS

17

Figure 17: Suggested serine building block with photoresponsively protected amino group

Even though desired protected depsipeptide **10** was found in MALDI-TOF-MS analysis for both of the conducted synthesis routes (with and without TBDMS protection), yields were very low ($< 1\,\%$). The followed procedure for both routes (DIPEA/PyBOP protocol) was taken from previous work of the group (J. Gačanin *et al.* [6]). The procedure described the fully automated synthesis of the plain (KIKI)SQINM depsipeptide **2**. Esterification of SQINM resin **6** was conducted in the automated peptide synthesiser as well, but even in this setup the reported yields were very low (7 %). Following work by A. Sobota showed improved yields when the esterification with isoleucine was conducted manually. As a first test, a new synthesis route utilising *CEM* standard methods with DIC and Oxyma as activator and base was tested for the (KIKI)SQINM depsipeptide **2**. The SQINM sequence was synthesised starting from the Fmoc-*L*-Met-Wang resin (0.1 mmol). Successive coupling of Fmoc-*L*-Asn(Trt)-OH, Fmoc-*L*-Ile-OH, Fmoc-*L*-Gln(Trt)-OH and Fmoc-*L*-Ser(Boc)-OH (5 equiv.) was achieved in single coupling using DIC (5 equiv.) and Oxyma (5 equiv.) at 75 °C for 15 s and subsequently 90 °C for 110 s. Deprotection of the Fmoc protective group was achieved with 20 % piperidine in DMF at 75 °C for 15 s and 90 °C for 50 s. Esterification with isoleucine was conducted in double coupling using Fmoc-*L*-Ile-OH (10 equiv.), 4-(dimethylamino)pyridine (DMAP) (1 equiv.) and DIC (2 equiv.) at room temperature. After 2 h the solution was refreshed with the same amount of reagents and shaken for another 24 h. Successive coupling of Fmoc-*L*-Lys(Boc)-OH, Fmoc-*L*-Ile-OH and Fmoc-*L*-Lys(Boc)-OH was achieved using the same reaction conditions as before during synthesis of the SQINM sequence. Improved yields of (KIKI)SQINM depsipeptide **2** (25.1 mg, 19 %) compared to previous work of the group (7 %) and shorter reaction times for the automated synthesis (DIPEA/PyBOP: 2.6 h; DIC/Oxyma: 1.2 h) resulted (not including reaction times outside of the peptide synthesiser). Additionally, the MALDI-TOF-MS spectra of the (KIKI)SQINM depsipeptide synthesised following the DIC/Oxyma method indicated significantly less side-products prior to HPLC purification in MALDI-TOF-MS analysis (see Figure 18). Based on these findings, all further reactions were carried out with DIC and Oxyma.

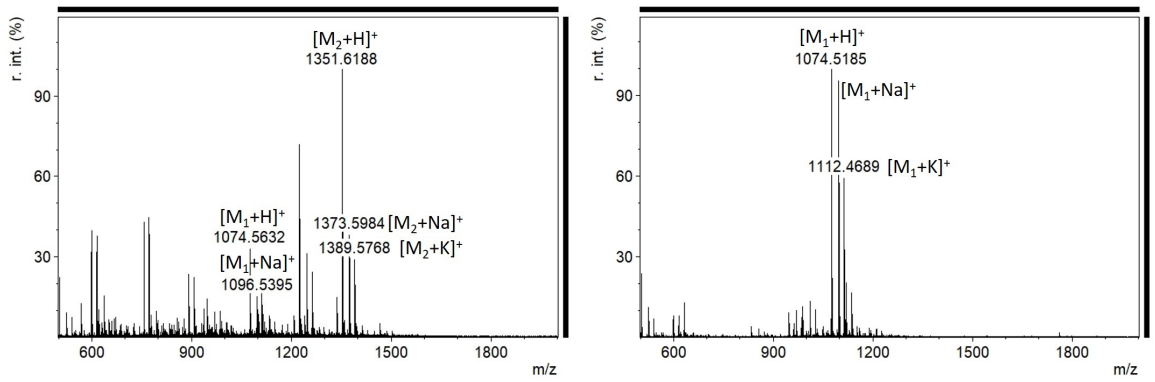

Figure 18: HRMS (MALDI-TOF-MS) analysis comparison between DIPEA/PyBOP and DIC/Oxyma protocol before HPLC purification. M_1 = 1073.6267 g mol^{-1} (KIKISQINM depsipeptide **2**), M_2 = 1350.6853 g mol^{-1} (protected depsipeptide **10**). Left spectrum: DIPEA/PyBOP protocol protected depsipeptide **10** before HPLC purification. Right spectrum: DIC/Oxyma protocol (KIKI)SQINM depsi **2** before HPLC purification.

Aside from SPPS methods, there also arose concern that the reaction conditions of the coupling of NHS ester **PhotoSG6a** to the serine residue were not optimal. The procedure was adapted from previous work by Pieszka *et al.* [4] in which a similar compound was synthesised (see Scheme 13) using 4-nitrophenyl (4-(4,4,5,5-tetramethyl-1,3,2-dioxaborolan-2- yl)benzyl) carbonate (10 equiv.) and DIPEA (20 equiv.) in DMF. The leaving group in their procedure was *p*-nitrophenyl instead of NHS. According to literature, the usual conditions for NHS ester labeling of amino biomolecules involves usage of a buffer in a pH range of 7.0 to 9.0. If the reaction is conducted at lower pH, the protonated form of the peptide's amino group might be the predominant species thus preventing modification. At higher pH, rapid hydrolysis of the NHS ester can occur and lead to decreased yields. [44] Since the reaction had to be conducted on the resin, utilisation of a buffer was not attempted. In presence of the buffer the resin can collapse and therefore hinder spacial availability of the amino groups. Aside from pH control, amine-free solvents are preferred during NHS ester labeling. Since the previously followed procedure involved use of DIPEA – a base and tertiary amine – this compound was omitted as a test (see Scheme 22). This third setup (DIC/Oxyma protocol in SPPS as described for (KIKI)SQINM depsipeptide **2** and no use of DIPEA during esterification) gave a yield of 5 % (6.7 mg) of protected depsipeptide **10**. Purity of the product was verified *via* LC-MS (see Figure 19). The product obtained from this setup was used during following analytic studies (see section 3.3).

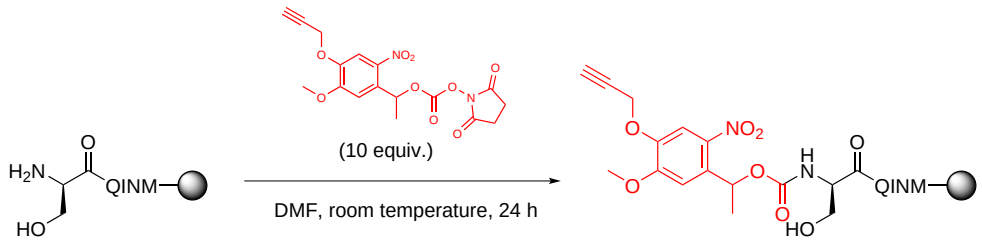

6 **7**

Scheme 22: Adapted procedure for coupling of NHS ester **PhotoSG6a** to SQINM resin **6**

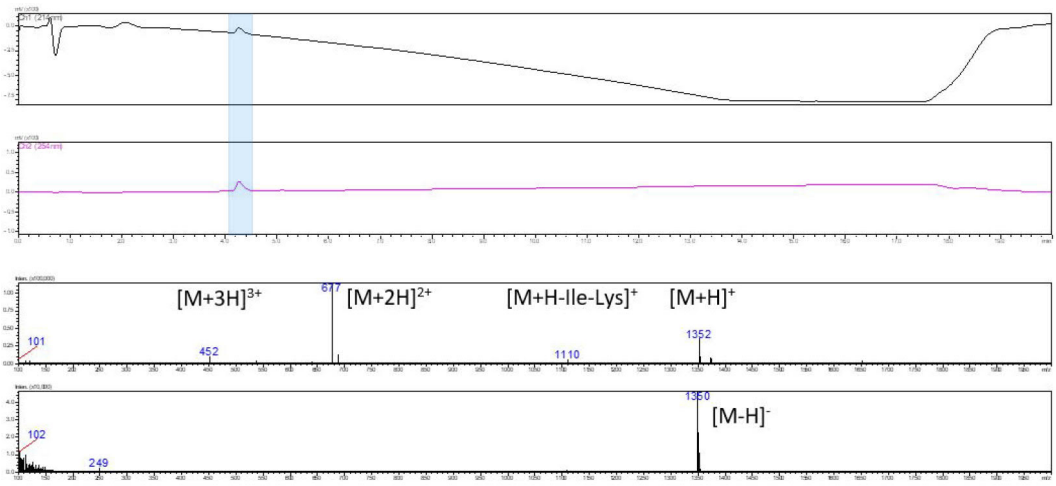

Figure 19: LC-MS analysis of the third protected depsipeptide setup (DIC and Oxyma during SPPS and omission of DIPEA during coupling of SQINM resin **6** with photocleaveable NHS ester **PhotoSG6a**). The peak within the blue area is analysed for *m/z* composition.

A second approach in making the coupling of the photolabile protective group more efficient was to exchange the leaving group to *p*-nitrophenyl as already reported by Pieszka *et al.* and continue utilising similar reaction conditions (no omission of DIPEA). However, incorporation of the different leaving group did not improve yield of protected depsipeptide **10** (1 %).

In an attempt to synthesise a comparable non-photoresponsive depsipeptide **18**, a setup utilising **NSG3** as the protective group was conducted. Unfortunately, the desired product could not be recovered from HPLC since the product fraction of non-photoresponsive depsipeptide **18** could not be identified. During the given timeframe, this route was not explored further. The main focus still laid on synthesis and analysis of photoresponsive depsipeptide **10**.

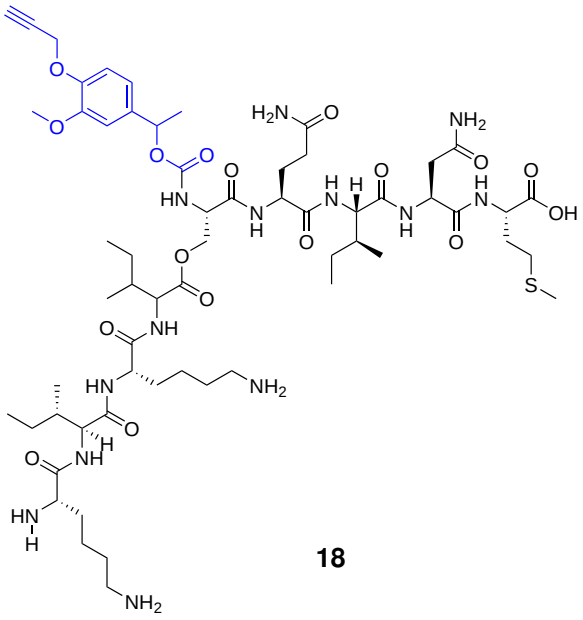

Figure 20: Structure of a comparable non-photoresponsive depsipeptide

Table 2 summarises the different setups with optimisations conducted for the synthesis of protected

depsipeptide **10**. The occurence of two distinct peaks in HPLC which were assumed to be isomers could not be prevented in any of the syntheses.

Table 2: Optimisation of the synthesis of the protected depsipeptide

No.	Act/ActB	Photoprotection Method	Leaving Group	Additional Remarks	Yield
1	PyBOP/DIPEA	1 (DIPEA)	NHS (PhotoSG6a)	–	< 1 %
2	PyBOP/DIPEA	1 (DIPEA)	NHS (PhotoSG6a)	TBDMS-protected	–
3	DIC/Oxyma	2 (no DIPEA)	NHS (PhotoSG6a)	–	5%
4	DIC/Oxyma	1 (DIPEA)	Nitrophenyl (PhotoSG6b)	–	1 %
5	DIC/Oxyma	2 (no DIPEA)	NHS (NSG3a)	–	–

3.3 Analyses of the Photoprotected Depsipeptide

After synthesis of a sufficient amount of protected depsipeptide **10**, different analyses involving TEM imaging, HPLC and NMR spectroscopy followed.

3.3.1 Morphology

As already discussed in section 3.2, HPLC purification of protected depsipeptide **10** showed 2 peaks with similar mass in the chromatogram, thus indicating isomer formation. To verify this conclusion, TEM images of both peak fractions were recorded by Adriana Sobota (see Figure 21). It was assumed that peak A (the linear isomer) would form fibrils, while peak B (the depsipeptide isomer) would not exhibit any kind of self-assembly. Instead, the measurements showed aggregates for peak A and aggregates as well as fibril formation for peak B. Since during TEM imaging only a tiny area of the prepared grid is exmined it should be noted that the absence of fibrils for peak A in the TEM image does not necessarily imply that the structure does not produce such. Since both molecules seemed to exhibit some kind of self-assembly in TEM imaging and literature suggested elution of linear peptides prior to depsipeptides in HPLC, the previous assumption of B being the depsipeptide peak was maintained. Therefore, further studies were conducted with peak B fractions.

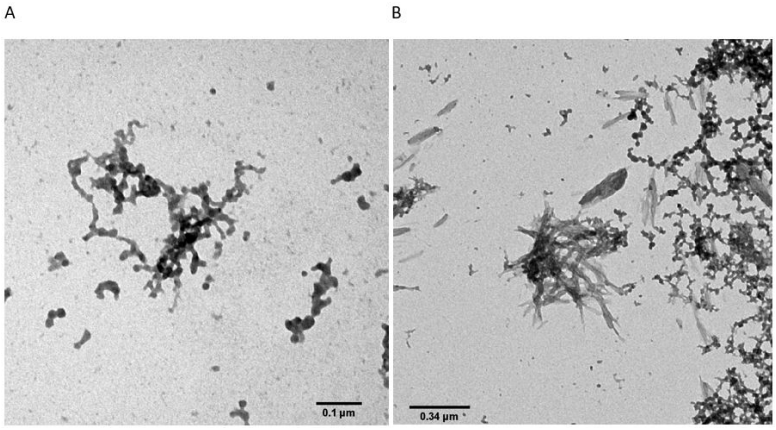

Figure 21: TEM images of protected depsipeptide isomers A and B

3.3.2 Kinetics

Previous work of the group of Prof. Dr. T. Weil showed that the conversion from depsipeptide into its linear isomer causes a change in elution times in HPLC. Gačanin *et al.* reported a shift in elution times from 10.18 min for (KIKI)SQINM depsipeptide **2** to 9.90 min for linear KIKISQINM peptide **3** in reversed-phase HPLC utilising a 0.1 % TFA water and ACN eluant (gradient: 5-10 % ACN, 4 min; 10-40 % ACN, 5 min; 40-100 % ACN, 8 min). [6] Hence, an HPLC study was conducted to observe cleavage and fibrillation behaviour of the synthesised protected depsipeptide **10**. A stock solution of protected depsipeptide **10** (10 mg/mL in dimethyl sulfoxide (DMSO)) was prepared. The stock solution was further diluted to 1 mg/mL with *Gibco®* Dulbecco's phosphate buffered saline (DPBS) (pH range 7.0 to 7.3) for each sample. The samples were further diluted, incubated and irradiated at 365 nm as shown in Table 3. The irradiation times apply for the stock solution, all dilution was performed outside of the irradiation area immediately before injection.

Table 3: Samples, irradiation time, concentration and injection volume of the HPLC study

Sample	Irradiation Time h	Concentration mg/mL	Injection Volume µL	Additional Remarks
Protected Depsipeptide **10**	0	0.5	100	t_0, solution slightly yellow, slight gelation at 1 mg/mL
		0.5	100	24 h incubation in PBS
	1	0.5	100	solution yellow, less viscous at 1 mg/mL
	5	0.5	100	
	24	0.5	100	solution colourless
Depsipeptide **2**	0	0.5	100	in *Milli-Q* H_2O + 0.1 % TFA
Linear peptide **3**	0	0.25	200	gelation at higher concentration

The t_0 protected depsipeptide **10** sample had to be further diluted with *Gibco®* DPBS to a concentration of 0.5 mg/mL due to slight gelation of the 1 mg/mL sample. All following samples were treated likewise except for the linear KIKISQINM peptide **3** (compound provided by Sarah Backfisch). Due to its linearity, fibrillisation and gelation of the sample was more pronounced which is why the sample was diluted to a concentration of 0.25 mg/mL. 100 µL of the 0.5 mg/mL solutions were injected (200 µL of 0.25 mg/mL respectively).

Depsipeptide **2** (compound provided by Adriana Sobota) was prepared in *Milli-Q* H_2O + 0.1 % TFA to suppress the *O,N*-acyl shift on the unprotected amino group during HPLC. Another sample of depsipeptide **2** in *Gibco®* DPBS was prepared equal to the other samples to observe gelation behaviour. No initial gelation was observed during injection of the 10 mg mL^{-1} (in DMSO) into the buffer solution. However, after short incubation (1 h), the sample had turned into a gel. In comparison, the protected depsipeptide **10** sample showed strong gelation behaviour immediately during injection into the buffer solution during sample preparation. Presumably, the gelation in protected depsipeptide **10** occured due to π-π-stacking of the protective group. After one hour of irradiation time, the sample of protected depsipeptide **10** showed decreased viscosity.

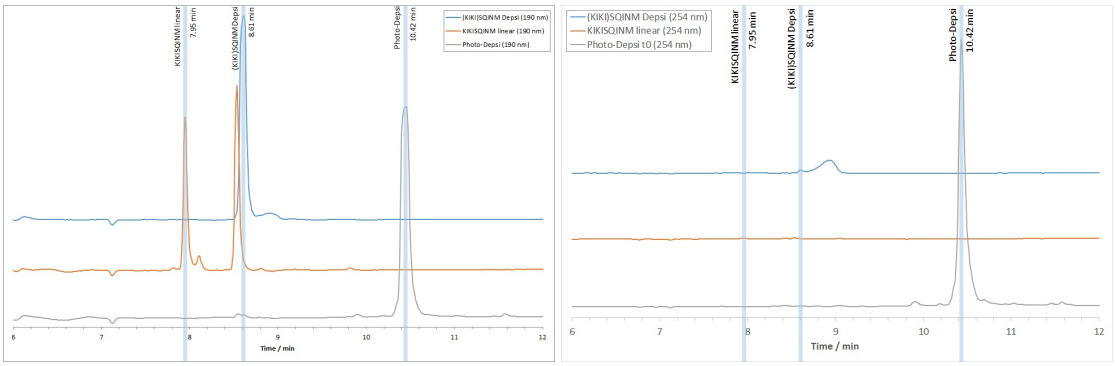

Figure 22: t_0 chromatogram recorded during HPLC study at 190 nm and 254 nm of linear KIKISQINM, kinked (KIKI)SQINM depsipeptide and the protected depsipeptide. Elution times of the three molecules are marked by blue vertical bars at 7.95 min, 8.61 min and 10.42 min.

Figure 22 shows the stacked chromatograms of (KIKI)SQINM depsipeptide **2**, the linear KIKISQINM peptide **3** and the protected depsipeptide **10** at 190 nm and 254 nm. Peaks for all peptides were observed in the 190 nm chromatogram, protected depsipeptide **10** absorbs at 254 nm, presumably due to the aromatic system in the protective group. Additionally, a very broad peak at 8.94 min in the 254 min chromatogram of (KIKI)SQINM depsipeptide **2** is observed. This might indicate contamination of the sample. However, since this sample was only used to determine the elution time of (KIKI)SQINM depsipeptide **2** in the HPLC study, the sample was not purified further.

As expected, the depsipeptide **2** eluted later (8.61 min) than the native peptide **3** (7.95 min) while protected depsipeptide **10** with the rather unpolar photolabile protective group eluted at 10.42 min. Surprisingly, the chromatogram of linear KIKISQINM peptide **3** exhibits a second peak at 8.53 min as well, suggesting the presence of (KIKI)SQINM depsipeptide **2**. The occurence of an *N,O*-acyl shift is a known side reaction of serine and threonine residues during resin cleavage in TFA. [45] However, since the peptide had already been purified *via* HPLC these isomers should have been separated. Therefore, (KIKI)SQINM depsipeptide **2** should not be present in the linear KIKISQINM peptide's sample. Contamination with the depsipeptide could have occured during sample preparation.
The slight shift between the peak from the depsipeptide sample (8.61 min) and the depsipeptide peak in the linear sample (8.53 min) can be a result of the differing concentrations (depsi: 0.5 mg/mL, linear: 0.25 mg/mL), but might as well not be significant. Assuming an error of 1 % for the method would make the shift insignificant.

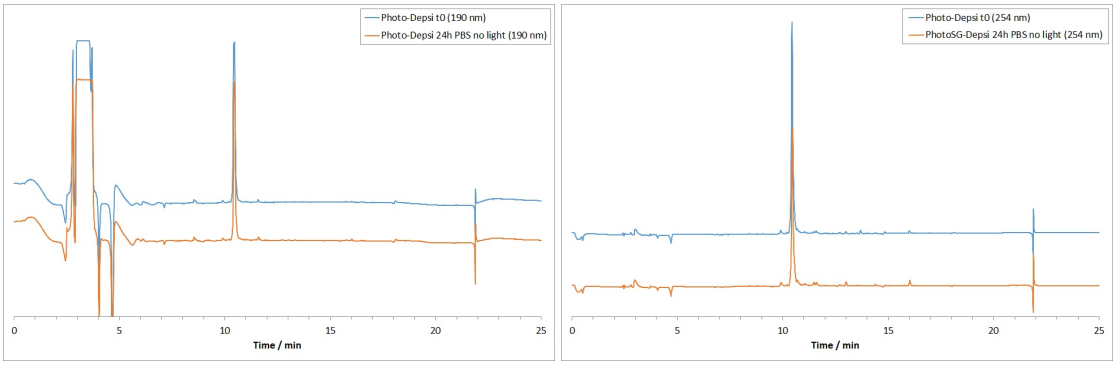

Figure 23: Chromatogram of the t_0 sample after 0 h and 24 h incubation in phosphate buffered saline recorded during HPLC study at 190 nm and 254 nm.

Since the plain KIKISQINM depsipeptide **2** performs an *O,N*-acyl shift at physiological pH, another vital information for the study was whether the synthesised protected depsipeptide **10** is stable in the buffer solution. To verify the peptide's stability the t_0 sample solution was incubated for 24 hours after the first injection. After the incubation period a second injection of 100 µL was conducted. The resulting chromatograms recorded at 190 nm and 254 nm are displayed in Figure 23. Since no visible change occured it can be assumed that the protected depsipeptide is stable in the buffer. Located in the region from 0 min to 6 min are signals of the phosphate buffer.

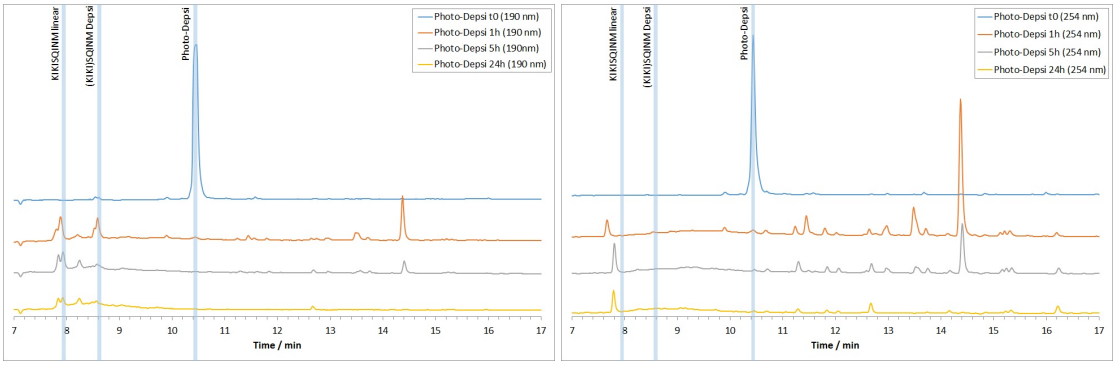

Figure 24: Chromatogram recorded during HPLC study at 190 nm and 254 nm after 0 h, 1 h, 5 h and 24 h of irradiation. Elution times of linear KIKISQINM, depsipeptide (KIKI)SQINM and the protected depsipeptide are marked by blue vertical bars at 7.95 min, 8.61 min and 10.42 min.

Figure 24 shows the chromatograms after 0 h, 1 h, 5 h and 24 h irridiation at 365 nm (recorded at 190 nm and 254 nm). The peak of the protected depsipeptide visible in the t_0 chromatogram at 10.42 min is no longer present in the chromatogram after 1 h irradiation. This implies that the photolinker is cleaved from the peptide in less than an hour. This is in accordance with observations by Wegner *et al.* [7] where dissociation was completed after 20 min of irradiation at 365 nm. Nevertheless, slight changes were observed in the chromatograms up to 24 h irradiation time. After 1 h a peak of almost similar intensity as the initial protected depsipeptide peak at t_0 is observed in the 254 nm chromatogram and with less intensity at 190 nm. Since the photocleavage product (KIKISQINM peptides **3** or **2**) is expected to elute at 7.95 or 8.61 nm, it was assumed that this was an intermediate or side product of the photoinduced cleavage that would undergo further decomposition upon irradiation. The peak shows a lower intensity after 5 h of irradiation and is not observed in the 24 h irradiation chromatograms which agrees with the aforementioned assumption of intermediate or side-product formation. Repetition of the study to further analyse this compound and its behaviour without further irradiation can provide additional information on the cleavage mechanism.
MALDI-TOF-MS analysis of the 10.42 min peak showed the mass of the protected depsipeptide as expected (*m/z* = calcd. 1350.6853; found 1351.6372 $[M+H]^+$). Various smaller peaks in the area of 10 min to 17 min appear to be additional intermediates and side products of the reaction since the intensity of the respective peaks decreased upon further irradiation. MALDI-TOF-MS and ESI-MS analysis of these fractions did not show the mass of protected depsipeptide (1351.58 g/mol) or depsi-/linear peptide (1074.35 g/mol). The expected peaks of (KIKI)SQINM depsipeptide **2** (1 h irradiation, 8.61 min) and linear KIKISQINM peptide **3** (1 h irradiation, 7.95 min) were collected and analysed as well, but the expected product mass (1074.35 g/mol) was not found. Only the protected depsipeptide

10 sample was a pure fraction of which 100 µL (50 µg peptide) were injected, while other samples contained multiple compounds in the same injection volume. Presumably, the amounts of other compounds in the collected fractions were below the detection limit.

After 1 h irradiation time the peaks of the linear KIKISQINM **3** and (KIKI)SQINM depsipeptide **2** are visible in the 190 nm chromatogram, indicating that the photolinker was cleaved from the peptide as expected as well as the transformation of the depsipeptide into its linear form *via* an *O,N*-acyl shift. The depsipeptide-peak decreases over time, but the peak of the linear peptide does not seem to increase in intensity. Instead, the linear peptide's peak seems to split with the slightly earlier peak also appearing in the 254 nm chromatogram. This might indicate another aromatic system of a side product.

3.3.2.1 TEM Imaging of HPLC study samples

The initial gelation and later decrease of viscosity of protected depsipeptide **10** raised further interest in the morphology of the photoproducts and the changes in self-assembly. Therefore, TEM images of the following HPLC study samples were recorded by Adriana Sobota: t_0, 24 h without irratiation and 1 h and 24 h of irradiation. An additional sample of depsipeptide **2** of 1 mg mL^{-1} in *Gibco®* DPBS was freshly prepared from the 10 mg/mL stock solution (in DMSO) and analysed for comparison. It should be noted that the samples were prepared following the usual TEM sample preparation protocol, meaning that all samples were incubated for an additional 24 h in phosphate-buffered saline (PBS).

Comparison of t_0 and 24 h without irradiation samples showed fibrils for both (see Figure 25), as already indicated during the initial comparison of HPLC peaks A and B. While the t_0 sample assembled into a much more dense "rug-like" network of fine and short fibrils, the additional 24 h incubation seemed to allow for formation of thicker and longer strands.
Various peaks are visible in the HPLC chromatogram of the protected depsipeptide after 1 h irradiation time. This and the visible decrease in viscosity of the sample made TEM imaging of the respective HPLC sample especially intriguing. While the latter suggested a disturbance of fibrillation, TEM imaging still showed formation of fibrils. Additionally, aggregates and larger dark spots are visible. The dark spots can indicate salt crystals of the buffer or uranyl acetate from sample preparation or respective salts of side-products, while the aggregate clusters (magnificated in Figure 26) might indicate a photocleavage product. This assumption is further strengthened by the images after 24 h irradiation time. In these, mostly clusters of aggregates are visible and only slight fibrillation is observed. The expected product of the photocleavage ((KIKI)SQINM depsipeptide **2**) as well as its linear KIKISQINM analogue **3** self-assemble into fibrils after the 24 h incubation period of TEM sample preparation. The fibrils for (KIKI)SQINM depsipeptide **2** occur due to linearisation in the buffer at pH $\approx$ 7. As already assumed, the photocleavage product observed in the 254 nm chromatogram at about 7.8 min in Figure 24 might therefore not be the desired KIKISQINM peptide **3**, but another molecule that disrupts fibrillation. There is also the chance that the peptide itself decomposes upon long irradiation times.

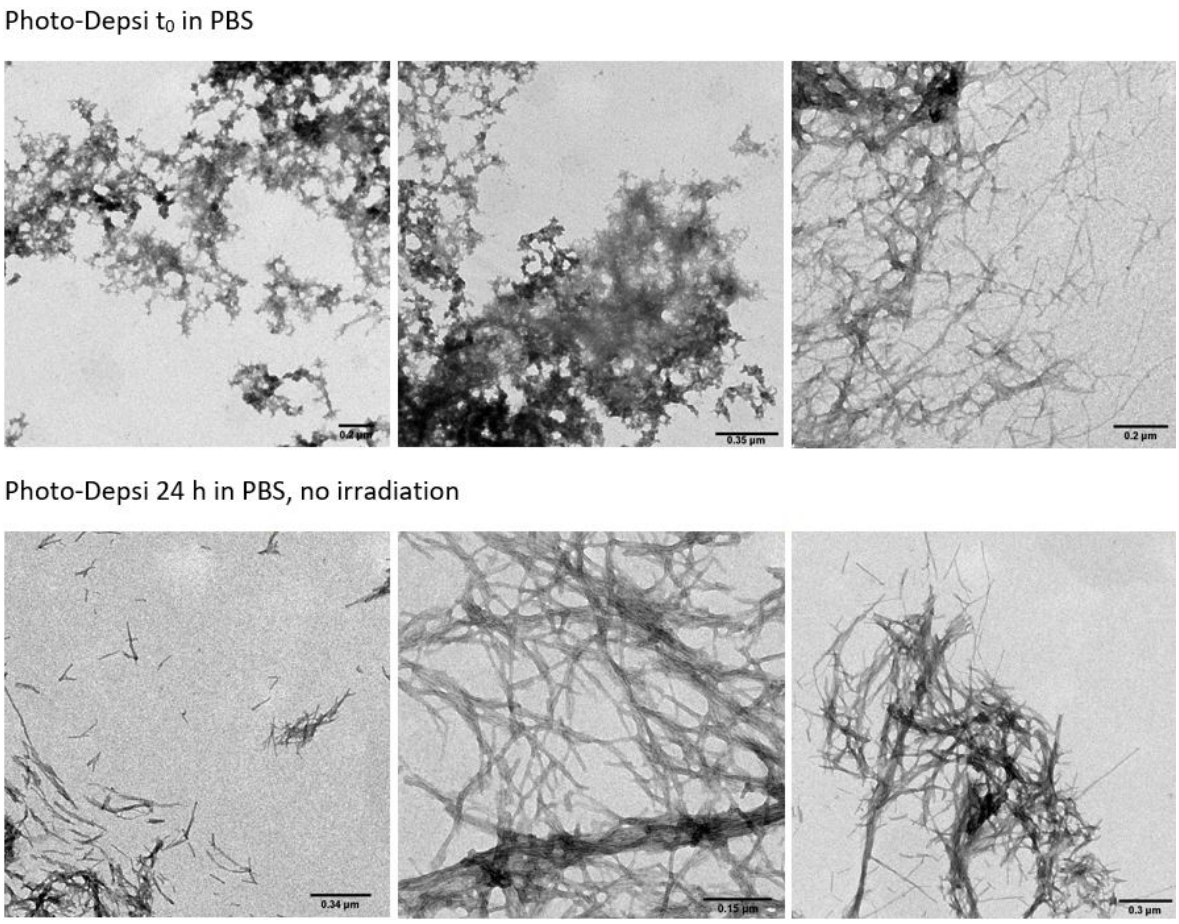

Figure 25: TEM Images of the protected depsipeptide **10** sample in PBS at t_0 and after 24 h without irradiation

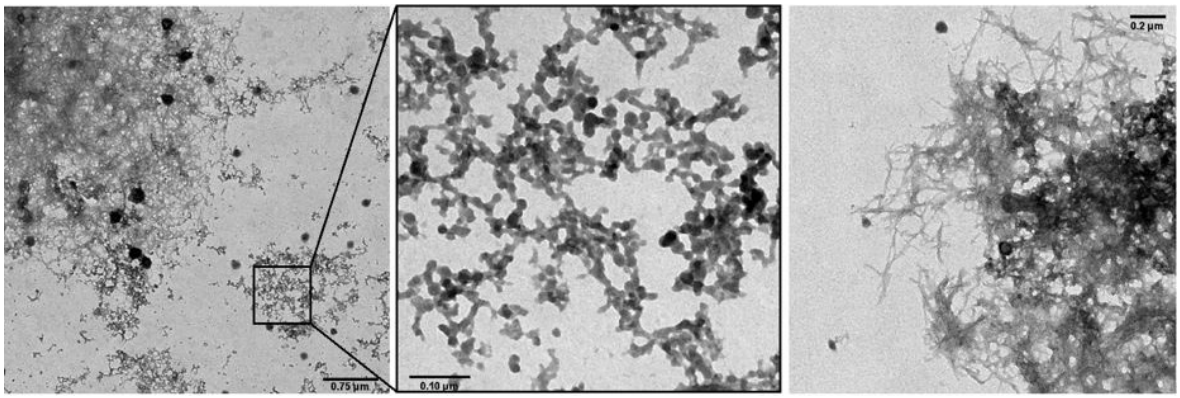

Figure 26: TEM Images of the protected depsipeptide **10** sample in PBS after 1 h of irradiation at 365 nm

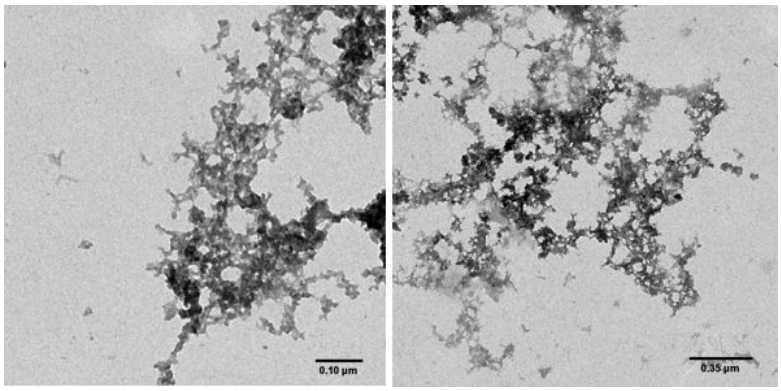

Figure 27: TEM Images of the protected depsipeptide **10** sample in PBS after 24 h of irradiation at 365 nm

3.3.2.2 NMR Study of Photocleavage Kinetics

In addition to the conducted HPLC study, photocleaveable depsipeptide **10** was analysed by Sarah Backfisch utilising NMR spectroscopy. The stacked spectra after 0 min, 5 min, 10 min, 15 min, 20 min, 30 min and 60 min of irradiation at 365 nm are displayed in Figure 28. The sample was analysed in a mixture of 90 % *Gibco®* DPBS buffer and 10 % D_2O with a concentration of 1 mg mL^{-1}. No previous preparation in DMSO was conducted due to the gelation at concentrations of 1 mg/mL already observed during the HPLC study. Additionally, it was unknown whether the signals of DMSO would overlap with the peptide's signals. Unfortunately, due to gelation and solubility issues, the spectra represent differing unknown concentrations of the sample, which is why peaks generally increase in area with longer irradiation time. Upon longer irradiation, the sample also showed reduced viscosity.

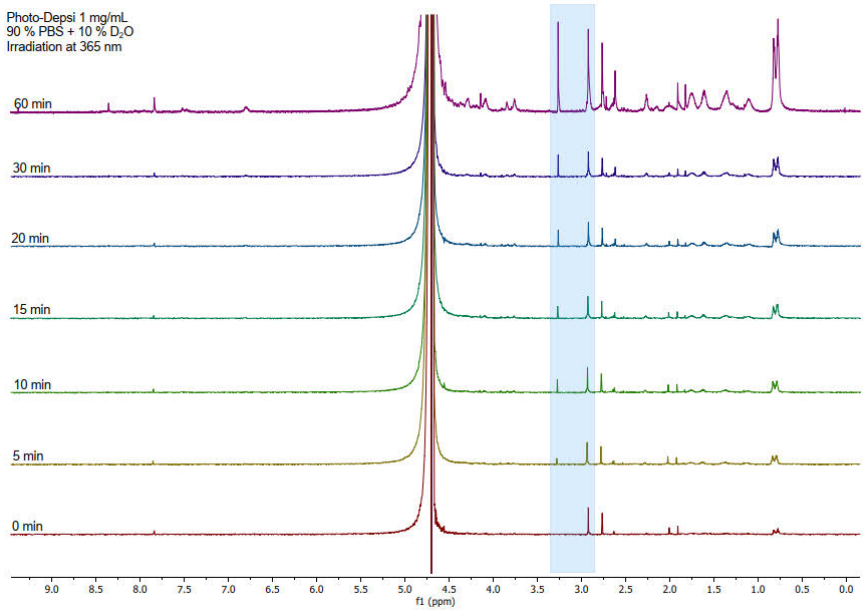

Figure 28: Stacked NMR spectra of the NMR study on cleavage kinetics of protected depsipeptide **10**. The peaks in the blue area were assumed to belong to two different compounds.

While the speactra cannot be compared directly with one another due to differing concentrations, the peaks within one spectrum can be set in relation. A peak arising in the spectra at 3.28 ppm was set in relation to another at 2.94 ppm (blue area in Figure 28) that had already been observed in

the t_0 spectrum (see Figure 29). When integrated, the peak at 3.28 ppm increases in relation to the one at 2.94 ppm. This suggests that the peaks do not belong to the same molecule, thus proving a cleavage.

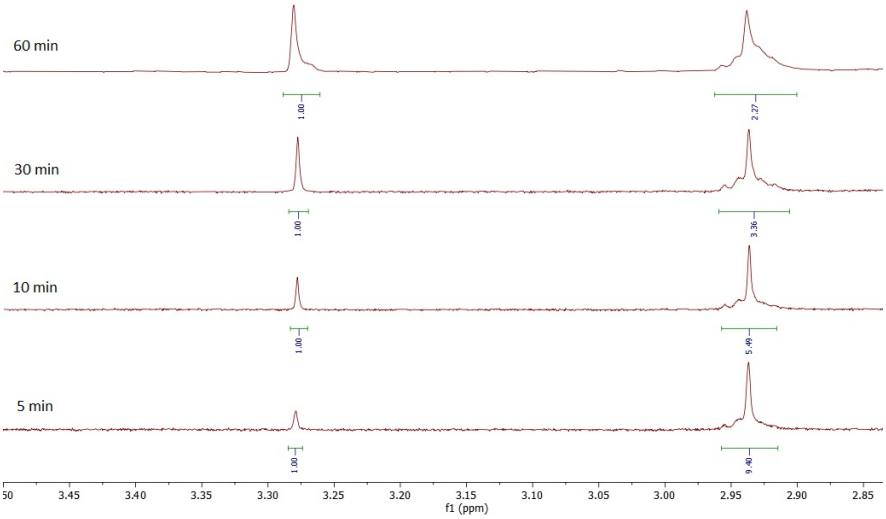

Figure 29: Integration of the peaks at 3.28 ppm and 2.94 ppm from the NMR study

The peak areas obtained within the NMR spectra have been set in relation ($\frac{(Peak at 3.28 ppm)}{(Peak at 2.94 ppm)}$) and were plotted against the irradiation time to obtain additional information on the reaction kinetics (see Figure 30). The curve plotted along the datapoints shows a saturation trend which is in accordance with experiments by Sezer *et al.* concerning Norrish type II photodissociation in solution and vacuum. [46] However, it has to be noted that the data obtained during the study might not be reliable due to effects of the precipitate in the sample. Fine dispersed particles in the solution can cause diffraction which can influence the photoinduced cleavage. Additionally, it is not known at which wavelengths the photocleavage products absorb. Absorbance of surrounding molecules can also cause alteration in energy availablity.

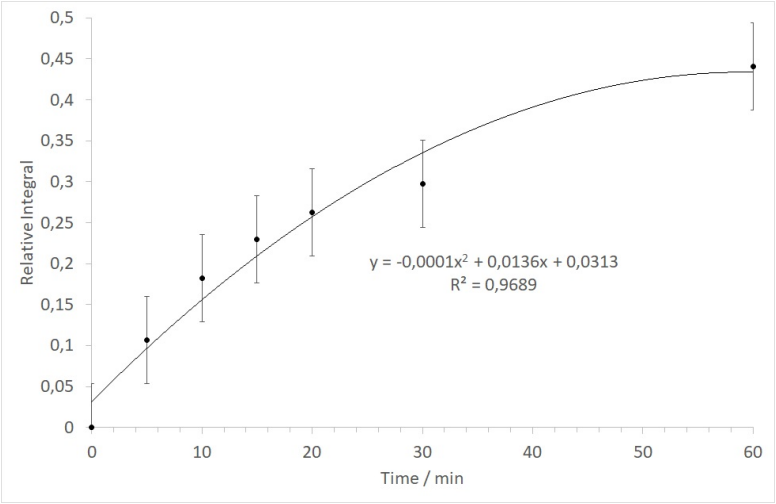

Figure 30: Relative peak areas from the NMR kinetic study plotted against the irradiation time

Furthermore, photos of the NMR samples were taken during the study (see Figure 31). The most

noticeable change in the pictures is the color change of the precipitate and the solution. Prior to irradiation, the solution was colourless with a white precipitate. Additionally, the sample gelated in the NMR tube. After 5 min of irradiation the solution turns slightly yellow, while the colour of the precipitate turns to a bright yellow. This change in colour as well as a reduced viscosity after only 5 min irradiation time indicated that cleavage of the protective group had already happened to an unknown extent. Upon further irradiation the solution loses colour while the precipitate darkens to orange (20 min and 30 min) and later light brown (60 min). Since the sample was prepared in an aqueous buffer solution, the change in color of the precipitate might indicate the rather hydrophobic cleaved photolinker not dissolving in the solution. The further darkening of the precipitate might indicate decomposition of the cleaved photolinker either caused by continued irradiation or general instability of cleavage products in the solution. After 24 h of irradiation at 365 nm, the solution is colourless and the precipitate almost white. This strengthens the assumption that initial cleavage products will further decompose or react with one another.

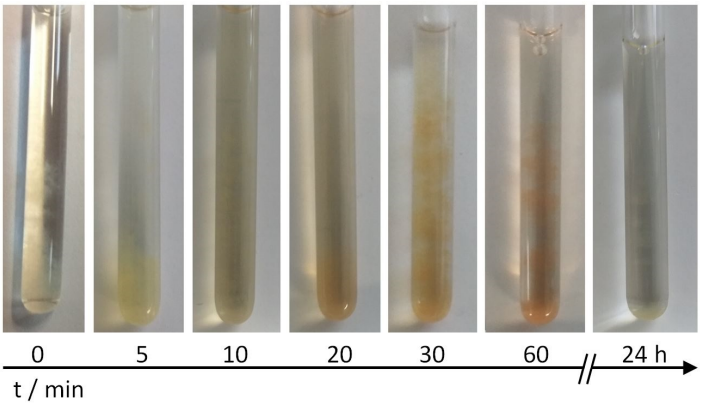

Figure 31: Photos taken of the photoresponsive depsipeptide **10** sample during the NMR study

3.4 Conclusion and Outlook

Protected depsipeptide **10** was synthesised under differing conditions for optimisation. However, the amount of synthesised product still did not allow for a wide variety of analyses or multiple runs. The first obstacle to overcome would therefore still be to find a route providing improved yields. The only analysis method for SPPS intermediates used in this work was MALDI-TOF-MS where qualification but not quantification was possible. To determine the "bottleneck" of the synthesis route, "Kaiser Tests" of the reaction steps in SPPS could be performed to detect free amino groups, i. e. monitor the completion of the reaction. This can provide vital information for optimisations.
In the case that the coupling of the photolabile protective group to the resin is the yield determining step, synthesis of PhotoSG-Ser building block **17** can provide another optimisation method that has not been explored yet due to insufficient reagents. An advantage of this building block would be that purification of the amino acid prior to the coupling is possible, therefore possibly omitting the formation of the assumed linear isomer of protected depsipeptide **10**.
With sufficient protected depsipeptide **10**, kinetic studies and analyses of morphology involving HPLC, NMR and TEM can be explored further. Especially the NMR study was merely a test run

and is still far from optimisation. Both HPLC and NMR study need to be attuned to one another. This involves adjustment of irradiation times and sample preparation among other things. Additionally, not much is yet known about the differences between linear peptides and their depsipeptide analogues concerning NMR spectroscopy. The *O,N*-acyl shift in the KIKISQINM sequence in NMR spectra is currently investigated by Sarah Backfisch from the group of Prof. Dr. T. Weil and might in the future provide references for the study of trigger-responsive depsipeptides. In the meantime, another HPLC study with shorter irradiation times fit to the cleavage kinetics of the photoresponsive depsipeptide (steps up to 60 min) can be conducted to observe the cleavage rather than formation of side-products. Furthermore, potential decomposition of the peptide itself upon irradiation (i. e. a triggered disruption of a hydrogel) might as well be an interesting topic to be explored. This approach would reverse the initial path of the project from triggered self-assembly and gelation to triggered disassembly and decomposition of an existing hydrogel.

Comparative experiments with the non-photolabile linker **NSG3** could provide more insight into fibrillation behaviour and morphology of the peptide. During the given timeframe a further exploration of non-photocleaveable analogues of protected depsipeptide **10** was not possible. Since the non-photocleaveable linker **NSG3** can be synthesised in 3 steps instead of 6 it might provide an easier accessible compound for further synthesis optimisation of protected depsipeptides. However, a disadvantage of this compound are the lower yields over the entire synthesis compared to **PhotoSG6a** (**NSG3**: 22 %, **PhotoSG6a**: 43 %) as well as the more complicated handling due to **NSG3** being an oil.

Unfortunately, labelling of protected depsipeptide **10** was not attempted during the project. A further look into the kinetics and especially morphology of the peptide as well as synthesis of sufficient amount for such studies is needed before experimenting with dye labelling. With sufficient amounts of protected depsipeptide **10** available, future work could focus on these analyses. An examplary Cyanine5-labelled depsipeptide that might be synthesised in the future is shown in Figure 32. The dye absorbs at 646 nm and emits at 662 nm, making it a suitable fluorophore to observe morphology of the peptide without disturbing the photocleavage reaction. However, it is not known how the dye itself influences the properties of the peptide, which creates another possible field to be explored.

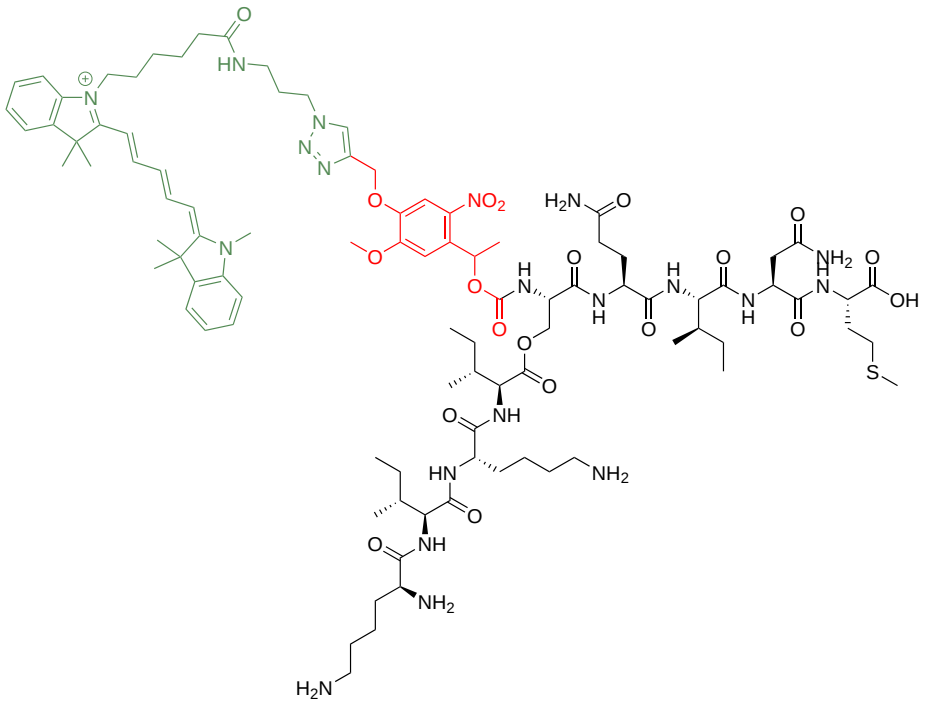

Figure 32: Structure of a Cyanine5-labelled photoresponsive depsipeptide. The photoceaveable linker is highlighted in red, the fluorophore bound to the linker is highlighted in green.

Studies considering the biocompatibility of protected depsipeptide **10** and the ability to form hydrogels and other scaffolds in bioorganic systems might pave the way for applications in biomedicine. Such compounds might be used to mimic extracellular matrices with additional photoresponsive characteristics.

4 Experimental Part

4.1 General Methods and Materials

Unless stated otherwise, all chemical compounds used for synthesis were acquired commercially (*Sigma Aldrich, Thermo Fisher Scientific, Merck*) and used without further purification.

4.1.1 Thin Layer Chromatography

Purity and reaction progress were checked by thin layer chromatography (TLC) using ALUGRAM® Xtra SIL G/UV_{254} plates from *Macherey-Nagel GmbH & Co. KG* (detection at λ = 254 nm and 365 nm).

4.1.2 Column Chromatography

The synthesised compounds were purified *via* column chromatography using Silica 60 M (particle size 0.04 mm to 0.063 mm) from *Machery-Nagel GmbH & Co. KG*. Solvents were acquired commercially in analytical reagent grade purity. The composition of the mobile phase is stated in volume shares (v:v) in the following.

4.1.3 High Performance Liquid Chromatography

HPLC was run with *Milli-Q*-water and ACN each with 0.1 vol% TFA. Gradients were applied according to the used device (see below). Solvents in HPLC grade purity were used.

Sample Preparation (Semipreparative HPLC): A stock solution of 10 mg/mL peptide in DMSO was prepared. The stock slution was diluted to a concentration of 1 mg/mL with *Gibco®* DPBS (ph range 7.0 to 7.3). Further dilution, incubation and irradiation of the samples was varied as required.

Semipreparative HPLC: Device by *Shimadzu* equipped with DGU-$20A_{5R}$, LC-20AP (2x), CBM-20A, SPD-M20A, SIL-10AP, FRC-10A.
Column: Agilent ZORBAX Eclipse XDB-C18, 80 Å, 5 µm, 9.4 x 250 mm; Agilent Safety Guard Kit
Flow rate: 4 mL/min

Sample Preparation (Preparative HPLC): The peptide was dissolved in *Milli-Q* H_2O + 0.1 % TFA and filtered through a syringe filter (VWR®, ∅ 25 mm, 0.2 µm nylon membrane, non-sterile, or Whatman® GD/X, ∅ 13 mm, 0.2 µm polyether sulfone (PES) membrane, non-sterile).

Preparative HPLC: Device by *Shimadzu* equipped with DGU-$20A_{5R}$, LC-20AT, CBM-20A, CTO-20AC, SPD-M20A, SIL-20AC, FRC-10A.
Column: Phenomenex Gemini® 5 µm NX-C18, 110 Å, 150 x 30 mm; Phenomenex® AJ0-8277 precolumn
Flow rate: 10 mL/min

Table 4: Gradients used during HPLC

Semipreparative		Preparative	
Time / min	**% ACN**	**Time / min**	**% ACN**
1.00	5	5.00	0
16.00	100	35.00	40
18.00	100	40.00	100
22.00	5	45.00	100
25.00	5	50.00	0
		55.01	0

4.1.4 Nuclear Magnetic Resonance Spectroscopy

The spectra were acquired using *Bruker Avance III 250*, *Bruker Avance 300*, *Bruker Avance III 700* and *Bruker Avance 850*. Deuterated solvents ($CDCl_3$, MeOD, $DMSO-d_6$) were acquired commercially from *Sigma Aldrich*.

4.1.5 Mass Spectrometry

Progress of the reaction (especially during peptide synthesis) was analysed with MALDI-TOF-MS using a *Waters MALDI SYNAPT G2-Si HDMS*.

Levels of purity were analysed by LC-MS using a *Shimadzu LCMS-2020 Single Quadrupole MS* equipped with a *Kinetex® EVO C18* column (2.6 µm, 100 Å) run with *Milli-Q*-water and ACN each with 0.1 vol% FA (5 % to 95 % ACN, 20 min).

4.1.6 Transmission Electron Microscopy

Device: *JEOL 1400*

Sample preparation: A stock solution of 10 mg mL^{-1} peptide in DMSO was prepared. The stock solution was diluted to a concentration of 1 mg/mL with *Gibco®* DPBS (ph range 7.0 to 7.3) and incubated at room temperature for 24 h while shaking.

TEM grid preparation: The TEM grids (*plano* GmbH, art. no. S162-3, Formvar/coal film on 3.05 mm Cu grids, 300 mesh) were plasma cleaned prior to sample application. 4 µL of the prepared 1 mg/mL DPBS sample solution was pipetted onto the grid, incubated for 5 min and the exess liquid removed using a filterpaper. The grid was then placed on a drop of 1 % uranyl acetate solution, incubated for 2.5 min and subsequently washed with water (3x). The dried TEM grids were then analysed.

4.1.7 Solid Phase Peptide Synthesis

The peptides were synthesised in a microwave-equipped *Liberty Blue Automated Peptide Synthesizer* by *CEM* from C to N terminus according to Fmoc SPPS strategy by Merrifield. Either PyBOP

and DIPEA or DIC and Oxyma were used as activator and base. Both protocols involved piperidine solution (20 vol% in DMF) for deprotection and DMF as the main washing agent (see Table 5). The preloaded PS based Fmoc-*L*-Met-Wang resin (*Novabiochem*®, loading: 0.68 mmol/g, 100–200 mesh) and *L*-amino acids were used for coupling.

Table 5: Concentrations of reagents used during automated peptide synthesis depending on the synthesis scale.

Reagents	**Concentration in DMF**	
Resin	0.05 mmol	0.1 mmol
Fmoc-amino acid	0.2 M	0.2 M
Activator	0.25 M	0.5 M
Activator-Base (DIPEA)	1.0 M	2.0 M
Activator-Base (Oxyma)	0.5 M	1.0 M
Piperidine solution	20 vol%	20 vol%

Sample cleavage: To test progress of the reaction, a few resin beads were placed in TFA and shaken for 30 min. A few drops of *Milli-Q* H_2O were added until the solution turned colourless. The sample was then analysed *via* MALDI-TOF-MS.

Final cleavage: The peptide was cleaved from the resin following the protocol provided by *Iris Biotech GmbH*: The resin was shaken for 2 h in a solution of TFA (95.0 %), TIPS (2.5 %) and *Milli-Q* H_2O (2.5 %). Deprotection of the side-chains occured simultaneously.

4.1.8 Irradiation During Kinetic Studies

The samples were irradiated utilising a lamp by *Opulent Americas* at 365 nm (intensity: 309 mW cm^{-2}).

4.2 Synthesis of the Photolabile Protective Group

The compounds were synthesised following routes by Mizuta *et al.* [8], Kaneko *et al.* [9] and Sobota [47].

4.2.1 4-Benzyloxy-3-methoxyacetophenone (PhotoSG1)

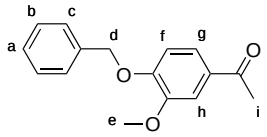

1-(4-Hydroxy-3-methoxyphenyl)ethan-1-one (4.70 g, 28.3 mmol), K_2CO_3, 1 equiv. (8.05 g, 58.3 mmol, 2.1 equiv.) and KI (200 mg, 1.2 mmol, 0.04 equiv.) were dissolved in ACN (60 mL) under argon. Benzyl bromide (4.0 mL, 34 mmol, 1.2 equiv.) was added slowly and the reaction mixture was refluxed overnight. The heat source was removed and the mixture cooled to room temperature. After filtration, the solvent of the remaining liquid was removed under reduced pressure. Purification *via* column chromatography (hexane/ethyl acetate (EtOAc) 20 %) yielded 6.7 g (26.0 mmol, 92 %) of **PhotoSG1** as slightly yellow-ish needles.

^{1}H-NMR (250 MHz, $CDCl_3$): δ 7.57 to 7.29 (m, 7 H; a, b, c, g, h), 6.89 (d, J = 8.2 Hz, 1 H; f), 5.25 (s, 2 H; d), 3.95 (s, 3 H; e), 2.55 ppm (s, 3 H; i).

4.2.2 4-Benzyloxy-5-methoxy-2-nitroacetophenone (PhotoSG2)

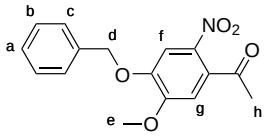

PhotoSG1 (3.00 g, 11.70 mmol) was dissolved in acetic acid (35 mL) and put on an ice bath. Fuming nitric acid (3.6 mL, 87.75 mmol, 7.5 equiv.) was added dropwise and the mixture was left to stir overnight on the ice bath. The reaction mixture was poured into ice-water and filtered. The precipitate was purified *via* column chromatography (hexane/EtOAc 20 %) to yield 2.15 g (7.14 mmol, 61 %) of **PhotoSG2** as a yellow solid.

^{1}H-NMR (250 MHz, $CDCl_3$): δ 7.69 (s, 1 H; f), 7.53 to 7.32 (m, 5 H; a, b, c), 6.79 (s, 1 H; g), 5.25 (s, 2 H; d), 4.00 (s, 3 H; e), 2.52 ppm (s, 3 H; h).

4.2.3 4-Hydroxy-5-methoxy-2-nitroacetophenone (PhotoSG3)

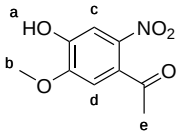

PhotoSG2 (3.00 g, 9.96 mmol) was dissolved in trifluoroacetic acid (25 mL) and stirred overnight at room temperature. The solvent was removed under reduced pressure. Aqueous 1 M NaOH solution and EtOAc were added and the layers separated. The aqueous layer was acidified with aqueous 6 M HCl solution and extracted with EtOAc. The combined organic layers were dried over Na_2SO_4, filtered and the solvent removed under reduced pressure to yield 2.03 g (9.66 mmol, 97 %) of **PhotoSG3** as bright yellow needles.

^{1}H-NMR (250 MHz, $CDCl_3$): δ 7.67 (s, 1 H; c), 6.80 (s, 1 H; d), 5.92 (s, 1 H; a), 4.02 (s, 3 H; b), 2.49 ppm (s, 3 H; e).

4.2.4 5-Methoxy-2-nitro-4-prop-2-ynyloxyacetophenone (PhotoSG4)

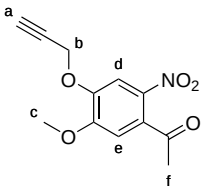

PhotoSG3 (1.68 g, 7.98 mmol) and K_2CO_3 (1.54 g, 11.17 mmol, 1.4 equiv.) were dissolved in dry ACN (60 mL) and put under argon atmosphere. Propargyl bromide (1.15 mL (80 % in toluol), 10.37 mmol, 1.3 equiv.) was added and the solution was refluxed overnight. After completion, the solvent was removed under reduced pressure. Water and aqueous 2 M HCl solution were added and the mixture was extracted with $CHCl_3$. The combined organic layers were dried over $MgSO_4$, filtered and the solvent removed under reduced pressure. Purification *via* column chromatography (hexane/EtOAc 20 %) yielded 1.91 g (7.65 mmol, 96 %) of **PhotoSG4** as bright yellow needles.

^{1}H-NMR (250 MHz, $CDCl_3$): δ 7.80 (s, 1 H; d), 6.78 (s, 1 H; e), 4.87 (d, J = 2.4 Hz, 2 H; b), 3.98 (s, 3 H; c), 2.61 (t, J = 2.5 Hz, 1 H; a), 2.51 ppm (s, 3 H; f).

4.2.5 1-(5-Methoxy-2-nitro-4-prop-2-ynyloxyphenyl)ethanol (PhotoSG5)

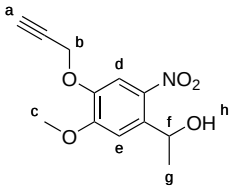

PhotoSG4 (800 mg, 3.20 mmol) was dissolved in THF/MeOH (1:2, 180 mL) and put on an ice bath. $NaBH_4$ (850 mg, 22.46 mmol, 7 equiv.) was added and the reaction mixture was left to stir overnight on the ice bath. After completion, the solvent was removed under reduced pressure. Water and aqueous 2 M HCl solution were added and the mixture was extracted with $CHCl_3$. The combined organic layers were dried over $MgSO_4$, filtered and the solvent removed under reduced pressure. Purification *via* column chromatography (hexane/EtOAc 2:1) yielded 754 mg (2.99 mmol, 94 %) of **PhotoSG5** as bright yellow needles.

^{1}H-NMR (250 MHz, $CDCl_3$): δ 7.75 (s, 1 H; d), 7.34 (s, 1 H; e), 5.59 (q, J = 6.3 Hz, 1 H; f), 4.83 (d, J = 2.4 Hz, 2 H; b), 4.00 (s, 3 H; c), 2.57 (t, J = 2.5 Hz, 1 H; a), 1.57 ppm (d, J = 6.3 Hz, 3 H; g).

4.2.6 1-(5-Methoxy-2-nitro-4-prop-2-ynyloxyphenyl)ethyl *N*-succinimidyl carbonate (PhotoSG6a)

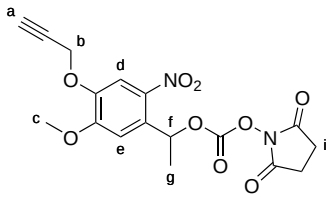

PhotoSG5 (500 mg, 1.99 mmol) and triethylamine (TEA) (0.8 mL, 5.77 mmol, 2.9 equiv.) were dissolved in dry ACN (100 mL). *N,N'*-disuccinimidyl carbonate (DSC) (1.43 g, 5.57 mmol, 2.8 equiv.) was added under argon atmosphere. The reaction mixture was stirred at room temperature for 5 hours. After removal of the solvent under reduced pressure, water and aqueous 2 M HCl solution were added and the mixture was extracted with CH_2Cl_2. The combined organic layers were washed with saturated $NaHCO_3$ solution, dried over $MgSO_4$, filtered and the solvent removed under reduced pressure. Purification *via* column chromatography (hexane/EtOAc 2:1) yielded 639 mg (1.63 mmol, 82 %) of **PhotoSG6a** as bright yellow solid.

^{1}H-NMR (300 MHz, $CDCl_3$): δ 7.83 (s, 1 H; d), 7.11 (s, 1 H; e), 6.52 (q, J = 6.4 Hz, 1 H; f), 4.83 (d, J = 2.0 Hz, 2 H; b), 4.03 (s, 3 H; c), 2.78 (s, 4 H; h), 2.59 (s, 1 H; a), 1.77 ppm (d, J = 6.3 Hz, 3 H; g).

4.2.7 1-(5-Methoxy-2-nitro-4-prop-2-ynyloxyphenyl)ethyl (4-nitrophenyl) carbonate (PhotoSG6b)

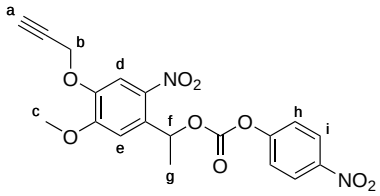

PhotoSG5 (200 mg, 796 µmol) was dissolved in dry THF (2 mL) and placed in an ice bath. Triethylamine (0.22 mL, 1.59 mmol, 2 equiv.) and 4-nitrophenyl chloroformate (176.5 mg, 876 µmol, 1.1 equiv.; predissolved in 2 mL dry THF) were added slowly while cooling. After addition of the reactant, the solution was left to stir overnight at room temperature. The solvent was removed under reduced pressure and the residue was redissolved in EtOAc and washed with aqueous 1 M HCl solution, saturated $NaHCO_3$ solution and brine. The organic layer was dried over $MgSO_4$ and the solvent was evaporated. The crude product was purified *via* column chromatography (hexane/EtOAc 4:1) to yield 115 mg (277 µmol, 35 %) of **PhotoSG6b** as bright yellow powder.

^{1}H-NMR (300 MHz, $CDCl_3$): δ 8.26 (d, J = 8.8 Hz, 2 H; i), 7.80 (s, 1 H; d), 7.35 (d, J = 9.1 Hz, 2 H; h), 7.15 (s, 1 H; e), 6.56 (q, J = 6.4 Hz, 1 H; f), 4.84 (d, J = 2.4 Hz, 2 H; b), 4.02 (s, 3 H; c), 2.59 (d, J = 2.6 Hz, 1 H; a), 1.78 ppm (d, J = 6.4 Hz, 3 H; g).

4.3 Synthesis of the Non-Photolabile Protective Group

4.3.1 1-(3-Methoxy-4-prop-2-ynyloxyphenyl)ethan-1-one (NSG1)

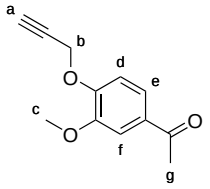

NSG1 was prepared following the procedure of **PhotoSG4** using the following equivalents: 1-(4-Hydroxy-3-methoxyphenyl)ethan-1-one (1.00 g, 6.02 mmol), propargyl bromide (0.87 mL (80 % in toluol), 7.82 mmol, 1.3 equiv.), K_2CO_3 (1.164 g, 8.43 mmol, 1.4 equiv.), ACN (60 mL). **NSG1** was obtained as a colourless oil in 93 % yield (1.14 g).

^{1}H-NMR (250 MHz, $CDCl_3$): δ 7.57 (d, J = 8.9 Hz, 2 H; e, f), 7.05 (d, J = 8.2 Hz, 1 H; d), 4.84 (d, J = 2.4 Hz, 2 H; b), 3.94 (s, 3 H; c), 2.58 (s, 3 H; g), 2.55 ppm (d, J = 3.3 Hz, 1 H; a).

4.3.2 1-(3-Methoxy-4-prop-2-ynyloxyphenyl)ethan-1-ol (NSG2)

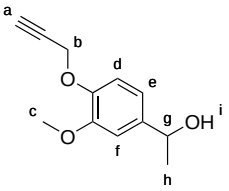

NSG2 was prepared following the procedure of **PhotoSG5** using the following equivalents: **NSG1** (500 mg, 2.45 mmol), $NaBH_4$ (648.4 mg, 17.14 mmol, 7.0 equiv.), tetrahydrofuran (THF)/MeOH (1:2, 120 mL). **NSG2** was obtained as a yellowish oil in 68 % yield (345 mg).

^{1}H-NMR (250 MHz, $CDCl_3$): δ 7.00 (d, J = 8.3 Hz, 1 H; d), 6.96 (d, J = 1.9 Hz, 1 H; f), 6.88 (dd, J = 8.2, 2.0 Hz, 1 H; e), 4.86 (q, J = 6.4 Hz, 1 H; g), 4.75 (d, J = 1.6 Hz, 2 H; b), 3.89 (s, 3 H; c), 2.53 to 2.46 (m, 1 H; a), 1.80 (s, 1 H; i), 1.48 ppm (d, J = 6.4 Hz, 3 H; h).

4.3.3 1-(3-Methoxy-4-prop-2-ynyloxyphenyl)ethyl *N*-succinimidyl carbonate (NSG3)

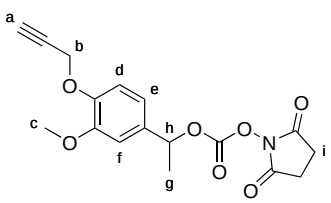

NSG3 was prepared following the procedure of **PhotoSG6a** using the following equivalents: **NSG2** (200 mg, 970 µmol), DSC (696 mg, 2.72 µmol, 2.8 equiv.), TEA (0.4 mL, 2.81 µmol). **NSG3** was obtained as a colourless oil in 35 % yield (118 mg).

^{1}H-NMR (250 MHz, $CDCl_3$): δ 7.11 (d, J = 1.9 Hz, 1 H; f), 6.95 (d, J = 8.2 Hz, 1 H; d), 6.87 (dd, J = 8.2, 1.9 Hz, 1 H; e), 5.51 (q, J = 6.5 Hz, 1 H; h), 4.75 (d, J = 2.4 Hz, 2 H; b), 3.91 (s, 3 H; c), 2.51 (h, J = 2.7, 2.1 Hz, 5 H; a, i), 1.63 ppm (d, J = 6.5 Hz, 3 H; g).

4.4 Synthesis of the Protected Depsipeptide

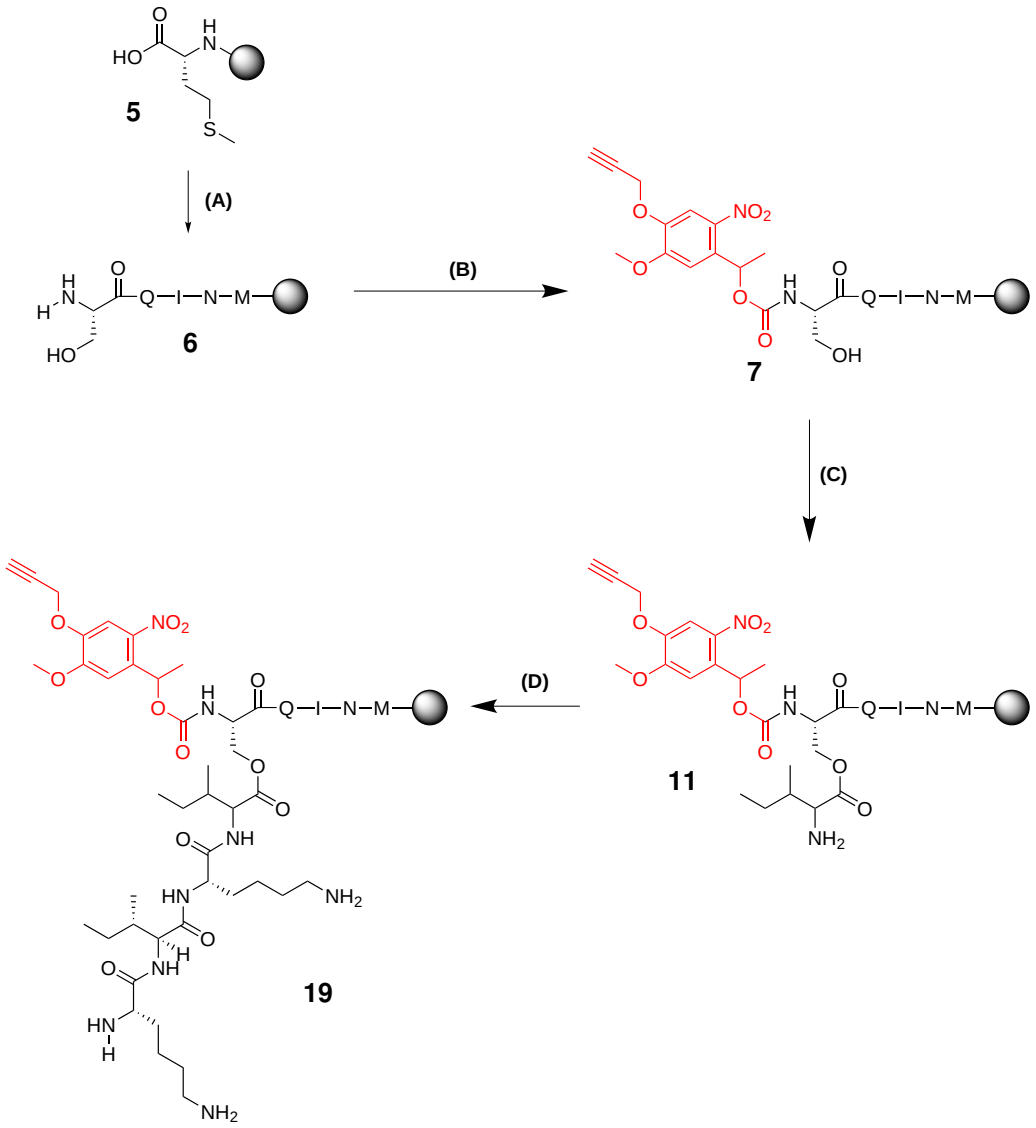

4.4.1 Synthesis of SQINM Sequence (A)

The synthesis was conducted in an automated peptide synthesiser. Reagent usage is summarised in Table 6.

Table 6: Reagent usage during successive coupling of SQIN sequence in automated SPPS

Reagent	Mass / mg	Volume / mL	DMF / mL
Fmoc-*L*-Asn(Trt)-OH	360	–	3
Fmoc-*L*-Ile-OH	220	–	3
Fmoc-*L*-Gln(Trt)-OH	370	–	3
Fmoc-*L*-Ser-OH Monohydrate	210	–	3
PyBOP	1800	–	7
DIPEA	–	1.7	5
DIC	–	0.5	7
Oxyma	711	–	5

Method 1: Fmoc-*L*-Methionine-Wang resin (147 mg, 0.1 mmol) was swelled in DMF for 1 h at room temperature. Another swelling step was done in the peptide synthesiser with 10 mL DMF for 5 s. Deprotection of the Fmoc protective group was carried out in two steps utilising 3 mL of a 20 % piperidine solution in DMF at 75 °C for 3 min. Four subsequent washes with 3 mL DMF for 7 s were followed by single coupling with 2.5 mL of the Fmoc-protected amino acid (5 equiv., 0.2 M in DMF) at 75 °C for 10 min. PyBOP (5 equiv., 1 mL 0.5 M in DMF) and DIPEA (10 equiv., 0.5 mL 2.0 M in DMF) were added in the coupling step. Deprotection, wash and coupling were repeated for each successively coupled amino acid (reagent masses listed in Table 6). Final deprotection of the Fmoc-protected main chain amino group was conducted using 3 mL of a 20 % piperidine solution in DMF at 75 °C in two steps for 0.5 min and 3 min. Finally, the resin was washed two times with 2 mL DMF and once with 3 mL DMF for 5 s.

A sample cleavage was conducted.
HRMS (MALDI-TOF-MS, 591.2686 g mol^{-1}): *m/z* = 614.1881 $[M+Na]^+$, 630.1588 $[M+K]^+$, 655.9880 $[M+ACN+Na]^+$

Method 2: Fmoc-*L*-Methionine-Wang resin (147 mg, 0.1 mmol) was swelled in DMF for 1 h at room temperature. Another swelling step was done in the peptide synthesiser with 10 mL DMF for 5 s. Deprotection of the Fmoc protective group was carried out in two steps utilising 3 mL of a 20 % piperidine solution in DMF at 75 °C for 15 s and 90 °C for 50 s. Three subsequent washes with 2 mL, 2 mL and 3 mL DMF for 5 s were followed by single coupling with 2.5 mL of the Fmoc-protected amino acid (5 equiv., 0.2 M in DMF) at 75 °C for 15 s and 90 °C for 110 s. DIC (5 equiv., 1 mL 0.5 M in DMF) and Oxyma (5 equiv., 0.5 mL 1.0 M in DMF) were added in the coupling step. Deprotection, wash and coupling were repeated for each successively coupled amino acid (reagent masses listed in Table 6). Final deprotection of the Fmoc-protected main chain amino group was conducted using 3 mL of a 20 % piperidine solution in DMF at 25 °C in two steps for 5 min and 10 min. Finally, the resin was washed two times with 2 mL DMF and once with 3 mL DMF for 5 s.

4.4.2 Protection of the Peptide (B)

Method 1: The resin (0.1 mmol) was swelled in DMF (1.5 mL) for an hour. **PhotoSG6a** (39.2 mg, 0.1 mmol, 1 equiv.) and DIPEA (174 µL, 1.0 mmol, 10 equiv.) were added and the mixture was stirred overnight at room temperature. After completion of the reaction, the resin was washed with DMF and DCM multiple times.

A sample cleavage was conducted.
HRMS (MALDI-TOF-MS, 868.3273 g mol^{-1}): *m/z* = 907.6390 $[M+K]^+$

Method 2: The resin (0.1 mmol) was swelled in DMF (1.5 mL) for an hour. **PhotoSG6a** (39.2 mg, 0.1 mmol, 1 equiv.) was added and the mixture was stirred overnight at room temperature. After completion of the reaction, the resin was washed with DMF and DCM multiple times.

A sample cleavage was conducted.
HRMS (MALDI-TOF-MS, 868.3273 g mol^{-1}): *m/z* = 891.5576 $[M+Na]^+$, 907.5464 $[M+K]^+$

4.4.3 Esterification with Isoleucine (C)

The resin (0.1 mmol) was swelled in DMF (1.5 mL) for an hour. Fmoc-L-Ile-OH (353.4 mg, 1 mmol, 10 equiv.; dissolved in 1 mL DMF), DMAP (12.2 mg, 0.1 mmol, 1 equiv.; dissolved in 0.5 mL DMF) and DIC (31 µL, 0.2 mmol, 2 equiv.) were added. After 2 h of stirring at room temperature, the liquid was removed and a fresh solution of Fmoc-L-Ile-OH, DMAP and DIC as described before was added to the resin. The mixture was subsequently stirred overnight at room temperature. After completion of the reaction, the resin was washed with DMF and DCM multiple times.

A sample cleavage was conducted. The product was not found in MALDI-TOF-MS analysis.

4.4.4 Coupling of KIK Sequence (D)

The sequence (Lys–Ile–Lys) was successively coupled to the Ile-esterificated SQINM resin in automated peptide synthesis. Reagent usage is summarised in Table 7

Table 7: Reagent usage during successive coupling of KIK sequence in automated SPPS

Reagent	Mass / mg	Volume / mL	DMF / mL
Fmoc-*L*-Lys(Boc)-OH	562	–	6
Fmoc-*L*-Ile-OH	212	–	3
PyBOP	1560	–	6
DIPEA	–	1.4	4
DIC	–	0.5	6
Oxyma	568	–	4

Method 1: Resin **11** (0.1 mmol) was swelled in DMF for 1 h at room temperature. Another swelling step was done in the peptide synthesiser with 10 mL DMF for 5 min. Deprotection of the Fmoc protective group was carried out in two steps utilising 3 mL of a 20 % piperidine solution in DMF at

75 °C for 3 min. Four subsequent washes with 3 mL DMF for 7 s were followed by single coupling with 2.5 mL of the Fmoc-protected amino acid (5 equiv., 0.2 M in DMF) at 75 °C for 10 min. PyBOP (5 equiv., 1 mL 0.5 M in DMF) and DIPEA (10 equiv., 0.5 mL 2.0 M in DMF) were added in the coupling step. Deprotection, wash and coupling were repeated for each successively coupled amino acid (reagent masses listed in Table 7). Final deprotection of the Fmoc-protected main chain amino group was conducted using 3 mL of a 20 % piperidine solution in DMF at 25 °C in two steps for 5 min and 10 min. Finally, the resin was washed two times with 2 mL DMF and once with 3 mL DMF for 5 s.

The peptide was cleaved from the resin according to final cleavage conditions in subsection 4.1.7. Protected depsipeptide **10** was obtained as a white solid in less than 1 % yield (1.1 mg).

HRMS (MALDI-TOF-MS, 1350.6853 g mol^{-1}): *m/z* = 1351.6211 $[M+H]^+$, 1373.5940 $[M+Na]^+$, 1389.5754 $[M+K]^+$

LC-MS (ESI-MS, 1351 g mol^{-1}): *m/z* = 1352 $[M+H]^+$, 1110 [M-Ile-Lys+H]$^+$, 677 $[M+2H]^{2+}$, 451 $[M+3H]^{3+}$, 1350 $[M-H]^-$, 1108 [M-Ile-Lys-H]$^-$

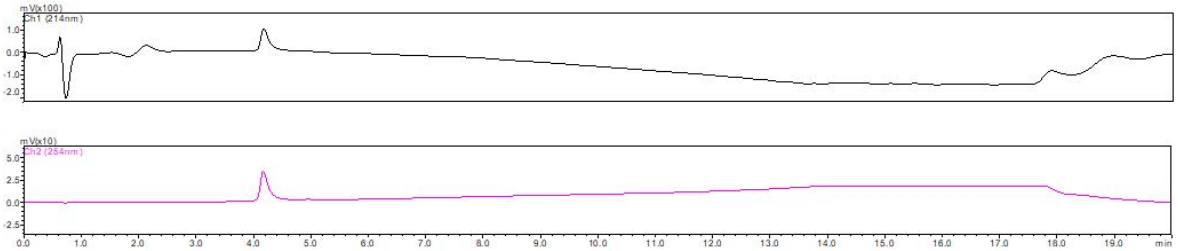

Figure 33: LC-MS spectrum of photoresponsive depsipeptide **10** prepared with PyBOP and DIPEA in SPPS at 214 nm and 254 nm

Method 2: Resin **11** (0.1 mmol) was swelled in DMF for 1 h at room temperature. Another swelling step was done in the peptide synthesiser with 10 mL DMF for 5 min. Deprotection of the Fmoc protective group was carried out in two steps utilising 3 mL of a 20 % piperidine solution in DMF at 75 °C for 15 s and 90 °C for 50 s. Three subsequent washes with 2 mL, 2 mL and 3 mL DMF for 5 s were followed by single coupling with 2.5 mL of the Fmoc-protected amino acid (5 equiv., 0.2 M in DMF) at 75 °C for 15 s and 90 °C for 110 s. DIC (5 equiv., 1 mL 0.5 M in DMF) and Oxyma (5 equiv., 0.5 mL 1.0 M in DMF) were added in the coupling step. Deprotection, wash and coupling were repeated for each successively coupled amino acid (reagent masses listed in Table 7). Final deprotection of the Fmoc-protected main chain amino group was conducted using 3 mL of a 20 % piperidine solution in DMF at 25 °C in two steps for 5 min and 10 min. Finally, the resin was washed two times with 2 mL DMF and once with 3 mL DMF for 5 s.

The peptide was cleaved from the resin according to final cleavage conditions in subsection 4.1.7.

HRMS (MALDI-TOF-MS, 1350.6853 g mol^{-1}): *m/z* = 1351.8244 $[M+H]^+$, 1373.8168 $[M+Na]^+$, 1389.7995 $[M+K]^+$, 1395.7990 $[M+2Na-H]^+$

LC-MS (ESI-MS, 1351 g mol^{-1}): *m/z* = 1352 $[M+H]^+$, 1110 [M-Ile-Lys+H]$^+$, 677 $[M+2H]^{2+}$, 452 $[M+3H]^{3+}$, 1350 $[M-H]^-$

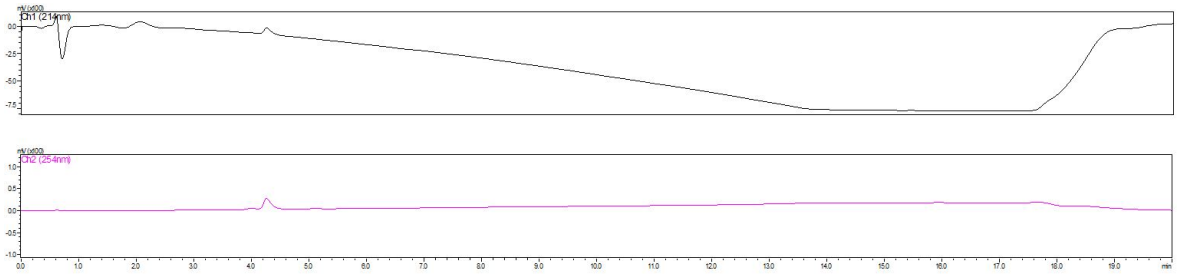

Figure 34: LC-MS spectrum of photoresponsive depsipeptide **10** prepared with DIC and Oxyma in SPPS at 214 nm and 254 nm

Protected depsipeptide **10** was prepared in another setup utilising DIC/Oxyma methods, protection of the serine residue and isoleucine coupling as described above, using **PhotoSG6b** (41.6 mg, 0.1 mmol, 1 equiv.) and DIPEA (174 µL, 1.0 mmol, 10 equiv.) in 1.5 mL DMF in step **B**.

The peptide was cleaved from the resin according to final cleavage conditions in subsection 4.1.7. Protected depsipeptide **10** was obtained as a white solid in 1 % yield (1.4 mg).

LC-MS (ESI-MS, 1351 g mol^{-1}): *m/z* = 1352 $[M+H]^+$, 1110 $[M\text{-Ile-Lys+H}]^+$, 677 $[M+2H]^{2+}$, 451 $[M+3H]^{3+}$, 1350 $[M-H]^-$, 1108 $[M\text{-Ile-Lys-H}]^-$

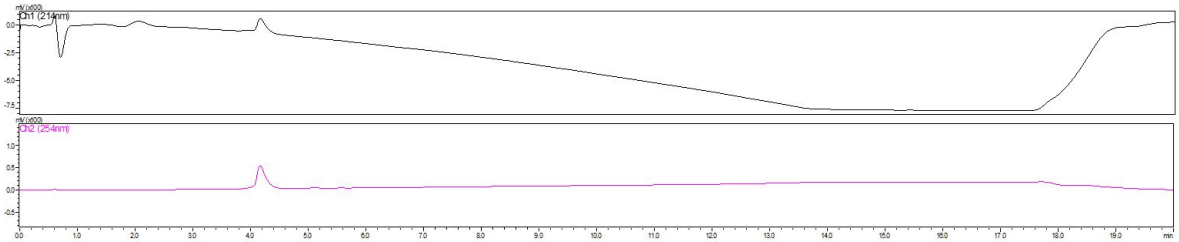

Figure 35: LC-MS spectrum of photoresponsive depsipeptide **10** prepared with **PhotoSG6b** at 214 nm and 254 nm

4.5 Synthesis of the Protected Depsipeptide Using TBDMS-protected Serine

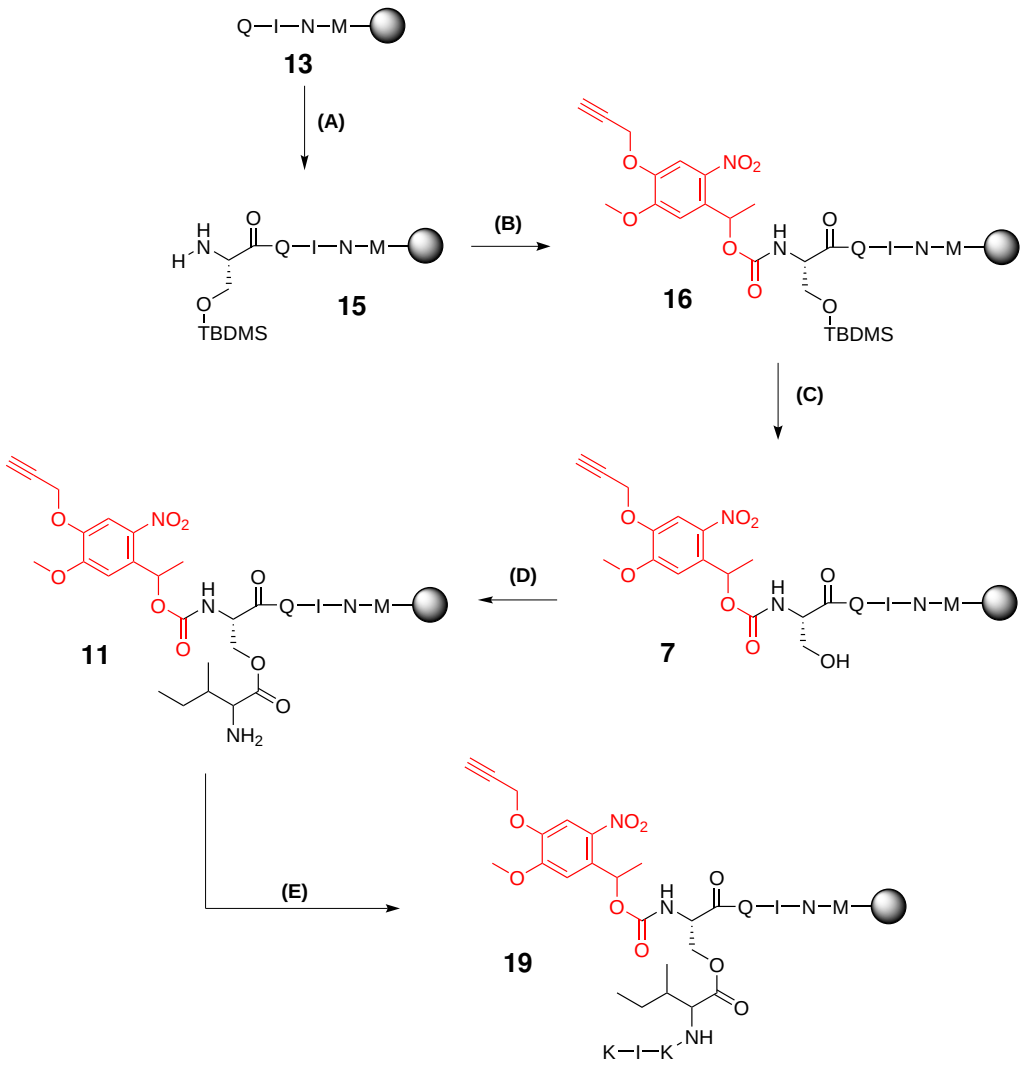

4.5.1 Fmoc-*O*-(2-(Trimethylsilyl)propan-2-yl)-L-serine

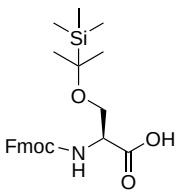

The procedure was adapted from X. J. Wang [48].

Fmoc-*L*-Ser monohydrate (528 mg, 1.53 mmol) and imidazole (520 mg, 7.64 mmol, 5.0 equiv.) were dissolved in DMF (3.2 mL) and cooled to 0 °C. *tert*-Butyldimethylsilyl chloride (576 mg, 3.82 mmol, 2.5 equiv.) was added and the reaction mixture was stirred for 3 h. DCM (50 mL) was added and washed with NH_4Cl (3 x) and H_2O (1 x). The organic layer was dried over Na_2SO_4 and the solvent

was removed under reduced pressure. The crude product was purified *via* column chromatography (hexane/EtOAc 9:1 to remove impurities, 5 % MeOH in $CHCl_3$ to wash down the product) to yield 111 mg (251 µmol, 16 %) Fmoc-*O*-(2-(trimethylsilyl)propan-2-yl)-L-serine.

^{1}H-NMR (300 MHz, $CDCl_3$): δ 7.77 (d, J = 7.5 Hz, 2 H), 7.61 (t, J = 6.4 Hz, 2 H), 7.40 (t, J = 7.5 Hz, 2 H), 7.31 (t, J = 7.2 Hz, 2 H), 5.61 (d, J = 8.0 Hz, 1 H), 4.51 to 4.32 (m, 3 H), 4.25 (t, J = 7.1 Hz, 1 H), 4.19 to 4.07 (m, 1 H), 3.90 to 3.80 (m, 1 H), 0.90 (s, 9 H), 0.12 to 0.03 ppm (m, 6 H).

4.5.2 Synthesis of QINM Sequence

The QINM sequence **13** was prepared on a 0.1 mmol scale following the PyBOP/DIPEA protocol from SQINM synthesis (see subsection 4.4.1). After QINM synthesis only half of the resin ($\approx$ 0.05 mmol) was used in the following steps.

A sample cleavage was conducted.
HRMS (MALDI-TOF-MS, 504.2366 g mol^{-1}): *m/z* = 527.2892 $[M+Na]^+$, 543.2723 $[M+K]^+$, 549.2780 $[M+2Na-H]^+$

4.5.3 Coupling of Protected Serine to QINM (B)

0.05 mmol QINM-resin (sythesised following PyBOP/DIPEA protocol) was swelled in DMF for an hour. Fmoc-*O*-(2-(trimethylsilyl)propan-2-yl)-L-serine (111 mg in 1.5 mL DMF, 251 µmol, 5.0 equiv.), PyBOP (130 mg in 1 mL DMF, 251 µmol, 5 equiv.) and DIPEA (0.09 mL in 0.25 mL DMF, 2.51 mmol, 10.0 equiv.) were added to the resin and stirred for 48 h. Afterwards the resin was washed multiple times with DMF. For Fmoc-deprotection of the N-terminal amino group the resin was swelled in DMF for an hour again. 20 % piperidine in DMF were added to the resin the mixture was stirred overnight. The resin was washed multiple times with DMF after the reaction.

A sample cleavage was conducted. The product was not found in MALDI-TOF-MS analysis.

4.5.4 Photo-protection of TBDMS-protected SQINM (C)

The reaction was carried out as described in subsection 4.4.2 (Method 1) using the following equivalents: TBDMS-protected SQINM-resin (0.05 mmol), **PhotoSG6a** (19.6 mg, 0.05 mmol, 1.0 equiv.), DIPEA (87 µL, 0.5 mmol, 10.0 equiv.), DMF (0.75 mL).

A sample cleavage was conducted.
HRMS (MALDI-TOF-MS, 982.4138 g mol^{-1}): *m/z* = 891.6150 $[M-TBDMS+H+Na]^+$, 907.6043 $[M-TBDMS+H+K]^+$

4.5.5 *tert*-Butyldimethylsilyl Deprotection of SQINM (D)

The resin was swelled in DMF for an hour. The resin was stirred in TBAF (1.0 mL 0.1 M in DMF, 0.1 mmol, 2.0 equiv.) overnight and subsequently waashed multiple times with DMF.
No MALDI-TOF-MS analysis was conducted since the TBDMS protective group is labile to TFA and would therefore not show mass differences to the previous product.

4.5.6 Ile and KIK Coupling (E)

The esterification with isoleucine and coupling of KIK to the resin was conducted as already described in subsection 4.4.3 and subsection 4.4.4.
The peptide was cleaved from the resin according to final cleavage conditions in subsection 4.1.7. Only trace amounts of protected depsipeptide **10** were obtained.

HRMS (MALDI-TOF-MS, 1350.6853 g mol^{-1}): *m/z* = 1351.5795 $[M+H]^+$, 1373.5603 $[M+Na]^+$

4.6 Synthesis of the Unprotected Depsipeptide

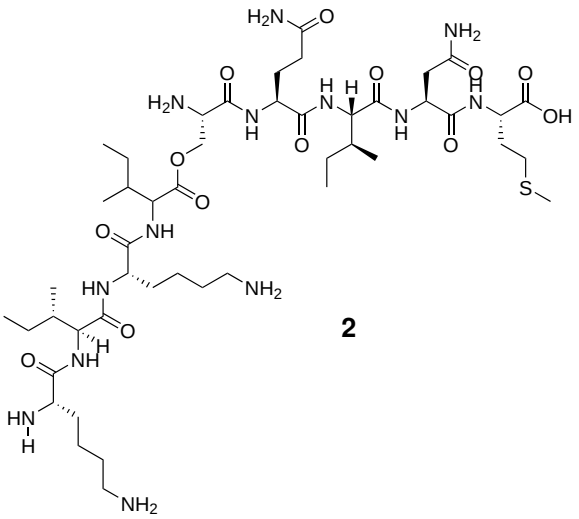

2

The unprotected (KIKI)SQINM depsipeptide was prepared following the DIC/Oxyma protocol for synthesis of SQINM (subsection 4.4.1) and KIK (subsection 4.4.4) sequences. Boc-protected serine (128 mg, 0.6 mmol in 3 mL DMF) was used instead of the unprotected monohydrate. Esterification with isoleucine was carried out as described in subsection 4.4.3 between the automated coupling steps.

The peptide was cleaved from the resin according to final cleavage conditions in subsection 4.1.7. Depsipeptide **2** was obtained as a white solid in 19 % yield (25.1 mg).

HRMS (MALDI-TOF-MS, 1073.6267 g mol^{-1}): *m/z* = 1074.5323 $[M+H]^+$, 1096.5132 $[M+Na]^+$, 1112.4854 $[M+K]^+$

5 Summary

The project during this work consisted of two main objectives: The first objective was the synthesis of a photoresponsive depsipeptide of the base sequence (KIKI)SQINM. This peptide should feature an ester bond in the serine's side-chain to provide a kink in the structure. Photoresponsive properties were achieved *via* protection of the serine's amino group by a photocleaveable protective group. This protective group shall prohibit the pH dependent *O,N*-acyl shift of the depsipeptide upon which it would linearise and self-assemble into fibrils. The second objective was to analyse this protected peptide's morphology and cleavage kinetics upon irradiation.

To synthesise the photoresponsive depsipeptide, the photocleaveable protective group had to be synthesised seperately in 6 steps. Two photolabile protective agents were synthesised in 43 and 18 % over the course of the entire route. Additionally, synthesis of a comparable non-photolabile protective agent was conducted to synthesise a respective non-photoresponsive depsipeptide and gain further insight into morphology of the peptide. The non-photolabile protective agent was obtained in 22 % yield over the course of the synthetic route. The structures and intermediates were confirmed by nuclear magnetic resonance (NMR) spoctroscopy.

Multiple routes for optimisation of the synthesis of a photoresponsive depsipeptide were tested. Utilising *N,N'*-diisopropylcarbodiimide (DIC) and ethyl cyano(hydroxyimino)acetate (Oxyma) in solid phase peptide synthesis (SPPS) with standard procedures from *CEM* as well as coupling of an *N*-hydroxysuccinimid ester functionalised protective group returned the highest yields (5 %). Synthesis of the compounds and purity were verified *via* mass spectrometry. Synthesis of a comparable depsipeptide protected by a non-photolabile compound for further analyses was attempted, but no product could be obtained. Optimisation of the synthesis by identification of the yield-determining step could be subject of future work.

The second objective of the project involved different analyses of synthesised protected depsipeptide. These included studies utilising HPLC and nuclear magnetic resonance (NMR) spectroscopy as well as transmission electron microscopy (TEM) imaging.

Initial TEM images of protected depsipeptide showed formation of fibrils. Since previous work of the group of Prof. Dr. T. Weil showed that the respective unprotected (KIKI)SQINM depsipeptide did not exhibit self-assembling properties, it was assumed that π-π-stacking of the protective groups contributes to the formation of higher structures.

Aside from the morphology of protected depsipeptide itself, kinetics of the cleavage of the photolabile protective group from the peptide were analysed. Since the group of Prof. Dr. T. Weil already ascertained a difference in elution time in HPLC for the (KIKI)SQINM depsipeptide and its linear analogue, an HPLC study was conducted to observe cleavage of the protective group as well the *O,N*-acyl shift of the free (KIKI)SQINM depsipeptide. Samples of protected depsipeptide were prepared from a stock solution (10 mg/mL in dimethylsulfoxide (DMSO)) and diluted with phosphate buffered saline (PBS). At a concentration of 1 mg/mL, gelation was observed, which is why the study was conducted at 0.5 mg/mL. Comparison of a t_0 sample (no irradiation, not incubated in PBS)

and another sample of protected depsipeptide that had been incubated in the buffer for 24 h without irradiation showed that the product is stable in PBS. The stock solution was irradiated at 365 nm to induce the cleavage and samples were continuously prepared from the stock solution for different hours of irradiation. To determine the elution times of cleavage product (KIKI)SQINM depsipeptide and its linear KIKISQINM analogue, samples of these seperately synthesised compounds were prepared. The study showed that the photolabile protective group is cleaved from the peptide in less than an hour. At this point (1 h of irradiation), peaks for linear and depsipeptide of KIKISQINM sequence can be observed in the HPLC chromatograms. The intensity of these peaks decreases again upon further irradiation, which raised the question whether the peptide decomposes due to irradiation.
Additionally, formation of an intermediate or side-product was observed. Absorbance of the intermediate's peak at 254 nm indicated existence of some kind of aromatic system in the compound. Repetition of the study can provide further information on the underlying mechanisms of both photoinduced cleavage of the protective group from the peptide and further desomposition of intermediates and side-products.

In addition to analysis to the differing elution times, TEM imaging of the prepared irradiated HPLC samples was conducted. The t_0 sample of protected depsipeptide showed a very dense, "rug-like" network of short and thin fibrils. After 24 h of incubation without irradiation, this network had assembled into thicker and longer strands. This assembly had already been assumed due to the gelation of the HPLC samples at concentrations of 1 mg/mL. This further strengthened the assumption that interactions of the protective groups might be one of the key factors responsible for the fibril formation in the protected depsipeptide. Furthermore it was found that upon irradiation, aggregate clusters formed that disrupted the fibrillation behaviour of the protected depsipeptide.

Since the HPLC study and TEM imaging did not provide much data about the kinetics of the photoinduced cleavage of the protective group from the depsipeptide, an additional NMR study was conducted analysing shorter irradiation times. Unfortunately, due to gelation and solubility issues, the different irradiation times could not be directly compared. However, formation of another product over time could still be observed in the spectra. Additionally, a colour change of the sample upon irradiation was observed during the first hour an even up to 24 hours of irradiation. This agreed with the aforementioned assumption during the HPLC study, that formation and decomposition of intermediates or side-products will occur for multiple hours after cleavage of the protective group from the peptide.

6 Zusammenfassung

Das Projekt dieser Arbeit bestand aus zwei Hauptzielen: Die erste Aufgabe bestand darin, ein photoresponsives Depsipeptid mit KIKISQINM Basissequenz zu synthetisieren. Dieses sollte eine Esterbindung in der Seitenkette des Serins beinhalten, um einen Knick des sonst geraden Peptidrückgrats zu erreichen. Die Aminogruppe des Serins wurde durch eine photospaltbare Gruppe geschützt. Diese Schutzgruppe sollte den pH-abhängigen *O,N*-acyl shift des Depsipeptids verhindern, durch den sonst Linearsierung und Selbstassemblierung in Fibrillen aufträte. Der zweite Teil des Projektes bestand in der Analyse des synthetisierten photoresponsiven Depsipeptids, um tiefere Einblicke in Morphologie des Peptids und Kinetik der photoinduzierten Entschützung zu gewinnen.

Um das photoresponsive Depsipeptid zu synthetisieren musste zunächst die photospaltbare Schutzgruppe separat in 6 Stufen synthetisiert werden. Zwei photolabile Verbindungen wurden mit 43 und 18 % Ausbeute über die gesamte Syntheseroute hergestellt. Zusätzlich wurde eine vergleichbare, nicht photolabile Verbindung hergestellt, um ein entsprechendes nicht photoresponsives Depsipeptid zu synthetisieren und so weitere Einblicke in die Morphologie des Peptids zu gewinnen. Die nicht-photolabile Verbindung wurde in 22 % Ausbeute über die gesamte Syntheseroute hergestellt. Die Synthese der Strukturen und Zwischenstufen wurden durch Kernspinresonanz (NMR) Spektroskopie bestätigt.

Für die Synthese des photoresponsiven Depsipeptids wurden mehrere Routen zur Optimierung getestet. Unter Verwendung von *N,N'*-Diisopropylcarbodiimid (DIC) und Hydroxyiminocyanessigsäureethylester (Oxyma) in Standardmethoden der Firma *CEM* in der Festphasenpeptidsynthese (SPPS) sowie Kupplung der Schutzgruppe mittels *N*-Hydroxysuccinimidester (NHS) Funktionalisierung ergaben die höchste Ausbeute (5 %). Synthese der Verbindungen und deren Reinheit wurden durch Massenspektrometrie gezeigt. Die Synthese eines vergleichbaren, nicht photolabilen Depsipeptids für weitergehende Analysen wurde durchgeführt, jedoch konnte kein Produkt isoliert werden. Die weitere Optimierung der Synthese durch Identifikation des ausbeutenbestimmenden Schrittes kann in Zukunft weiter vertieft werden.

Die zweite Zielstellung der Arbeit beinhaltete verschiedene Analysen des synthetisierten geschützten Depsipeptids. Studien unter Verwendung von Hochleistungsflüssigchromatographie (HPLC) und NMR Spektroskopie sowie Transmissionselektronenmikroskopie wurden durchgeführt.

Erste mittels TEM aufgenommene Bilder des geschützten Depsipeptids zeigten eine Ausbildung von Fibrillen. Da vorhergehende Arbeit der Gruppe von Prof. Dr. T. Weil zeigten, dass das entsprechende ungeschützte (KIKI)SQINM Depsipeptid keine solche Selbstassemblierung zeigte wurde angenommen, dass π-π-Wechselwirkungen der Schutzgruppen zur Bildung geordneter Strukturen beitragen.

Neben der Analyse der Morphologie des geschützten Depsipeptids selbst wurde zudem die Kinetik der Abspaltung der photolabilen Schutzgruppe vom Peptid analysiert. Da durch vorhergehende Arbeit der Gruppe von Prof. Dr. T. Weil gezeigt wurde, dass (KIKI)SQINM Depsipeptid und die entprechende lineare KIKISQINM Sequenz während der HPLC Aufreinigung unterschiedliche Elution-

szeiten aufwiesen, wurde eine HPLC Studie angesetzt um die Abspaltung der photolabilen Schutzgruppe und die *O,N*-Acylverschiebung des ungeschützten Depsipeptids zu beobachten. Proben des geschützten Depsipeptids wurden aus einer 10 mg/mL in Dimethylsulfoxid (DMSO) Stocklösung vorbereitet und mit phosphatgepufferter Salzlösung (PBS) verdünnt. Bei einer Konzentration von 1 mg/mL gelierte die Probe, weshalb die Studie bei einer Konzentration von 0.5 mg/mL durchgeführt wurde. Vergleich der t_0 Probe des geschützten Depsipeptids (keine Bestrahlung, keine Inkubation in PBS) mit einer Probe, die 24 Stunden im Phosphatpuffer ohne zusätzliche Bestrahlung inkubiert wurde zeigte, dass das Produkt in PBS stabil ist. Die Stocklösung wurde bei 365 nm bestrahlt um die Spaltung der photolabilen Schutzgruppe zu induzieren. Während der Bestrahlung wurden in regelmäßigen Abständen Proben vorbereitet. Um Referenzen für die Elutionszeiten des (KIKI)SQINM Depsipeptids und dem linearen Analogon zu bestimmen, wurden Proben mit entsprechenden separat synthetisierten Verbindungen vorbereitet. Die Studie zeigte, dass die Spaltung von photolabiler Schutzgruppe und Peptid in weniger als einer Stunde abläuft. Zu diesem Zeitpunkt (1 Stunde Bestrahlung) werden entprechende Peaks für lineares KIKISQINM Peptid und Depsipeptid in den HPLC Chromatogrammen beobachtet. Die Intensität dieser Peaks nimmt mit weiterer Bestahlung wieder ab, was die Frage aufwirft, ob sich das Peptid durch die Bestrahlung zersetzt.
Des Weiteren wurde die Entstehung eines Intermediats oder Nebenprodukts beobachtet. Da der Peak im 254 nm Spektrum zu beobachten war, beinhaltete die Verbindung vermutlich ein aromatisches System. Eine Wiederholung der Studie kann weitergehende Informationen über die zugrundeliegenden Mechanismen der photoinduzierten Spaltung der Schutzgruppe sowie der Weiterreaktionen verschiedener Intermediate und Nebenprodukte liefern.

Zusätzlich zur Analyse der verschiedenen Elutionszeiten wurden Bilder der Bestrahlungsproben der HPLC Studie mittels TEM aufgenommen. Die t_0 Probe des geschützten Depsipeptids zeigte ein sehr dichtes, "teppichartiges" Netzwerk kurzer und dünner Fibrillen. Nach 24 Stunden Inkubation ohne Bestrahlung hatte sich dieses Netzwerk zu dickeren und längeren Fibrillsträngen zusammengelagert. Diese Form der Selbstassemblierung wurde nach der Gelierung der 1 mg/mL Proben, die ursprünglich für die HPLC Studie vorbereitet wurden, bereits vermutet. Dies bestätigte zudem weiter die Vermutung, dass Wechselwirkungen der Schutzgruppe einen der Hauptfaktoren in der Fibrillierung des geschützten Depsipeptids darstellen. Zudem wurde gezeigt, dass sich bei Bestrahlung Aggregate bilden, die die Fibrillierung des geschützten Depsipeptids stören.

Da HPLC Studie und TEM Bildgebung nur wenig Information über die Kinetik der photoinduzierten Spaltung der Schutzgruppe vom Depsipeptid lieferte, wurde zusätzlich eine NMR Studie mit verkürzten Bestrahlungszeiten durchgeführt. Auf Grund von Gelierung und geringer Löslichkeit des Peptids konnten die verschiedenen Spektren der Bestrahlungszeiten jedoch nicht direkt verglichen werden. Die Bildung eines anderen Produktes mit zunehmender Bestrahlungszeit konnte jedoch beobachtet werden. Außerdem zeigte die NMR Probe Farbänderungen mit zunehmender Bestrahlungszeit bis zu einer Stunde sowie nach 24 Stunden. Dies stimmt mit der zuvorgenannten Vermutung aus der HPLC Studie überein, dass Bildung und Zersetzung von Intermediaten oder Nebenprodukten weiterhin für mehrere Stunden nach der Abspaltung der Photoschutzgruppe auftritt.

Bibliography

[1] V. Nguyen, R. Zhu, K. Jenkins and R. Yang. 'Self-assembly of diphenylalanine peptide with controlled polarization for power generation'. Nature Communications, 7(1), **2016**.

[2] J. Wang, K. Liu, R. Xing and X. Yan. 'Peptide self-assembly: thermodynamics and kinetics'. Chemical Society Reviews, 45(20):5589–5604, **2016**.

[3] L. Sun, C. Zheng and T. Webster. 'Self-assembled peptide nanomaterials for biomedical applications: promises and pitfalls'. International Journal of Nanomedicine, Volume 12:73–86, **2016**.

[4] M. Pieszka, A. M. Sobota, J. Gačanin, T. Weil and D. Y. W. Ng. 'Orthogonally Stimulated Assembly/Disassembly of Depsipeptides by Rational Chemical Design'. ChemBioChem, **2019**. DOI: 10.1002/cbic.201800781.

[5] Y. Sohma, A. Taniguchi, T. Yoshiya, Y. Chiyomori, F. Fukao, S. Nakamura, M. Skwarczynski, T. Okada, K. Ikeda, Y. Hayashi, T. Kimura, S. Hirota, K. Matsuzaki and Y. Kiso. "Click peptide': a novel 'O-acyl isopeptide method' for peptide synthesis and chemical biology-oriented synthesis of amyloid β peptide analogues'. Journal of Peptide Science, 12(12):823–828, **2006**.

[6] J. Gačanin, J. Hedrich, S. Sieste, G. Glaßer, I. Lieberwirth, C. Schilling, S. Fischer, H. Barth, B. Knöll, C. V. Synatschke and T. Weil. 'Autonomous Ultrafast Self-Healing Hydrogels by pH-Responsive Functional Nanofiber Gelators as Cell Matrices'. Advanced Materials, 31(2):1805 044, **2018**.

[7] S. V. Wegner, O. I. Sentürk and J. P. Spatz. 'Photocleavable linker for the patterning of bioactive molecules'. Scientific Reports, 5(1), **2015**.

[8] H. Mizuta, S. Watanabe, Y. Sakurai, K. Nishiyama, T. Furuta, Y. Kobayashi and M. Iwamura. 'Design, synthesis, photochemical properties and cytotoxic activities of water-Soluble caged l-Leucyl-l-leucine methyl esters that control apoptosis of immune cells'. Bioorganic & Medicinal Chemistry, 10(3):675–683, **2002**.

[9] S. Kaneko, H. Nakayama, Y. Yoshino, D. Fushimi, K. Yamaguchi, Y. Horiike and J. Nakanishi. 'Photocontrol of cell adhesion on amino-bearing surfaces by reversible conjugation of poly(ethylene glycol) via a photocleavable linker'. Physical Chemistry Chemical Physics, 13(9):4051, **2011**.

[10] D. Voet and J. G. Voet. Biochemistry. John Wiley & Sons Inc, USA, 3rd edition, **2004**.

[11] D. L. Nelson and M. M. Cox. Lehninger Principles of Biochemistry. W. H. Freeman, New York, **2004**.

[12] C. J. C. Edwards-Gayle and I. W. Hamley. 'Self-assembly of bioactive peptides, peptide conjugates, and peptide mimetic materials'. Organic & Biomolecular Chemistry, 15(28):5867–5876, **2017**.

[13] G. Wei, Z. Su, N. P. Reynolds, P. Arosio, I. W. Hamley, E. Gazit and R. Mezzenga. 'Self-assembling peptide and protein amyloids: from structure to tailored function in nanotechnology'. Chemical Society Reviews, 46(15):4661–4708, **2017**.

[14] R. Nelson, M. R. Sawaya, M. Balbirnie, A. Ø. Madsen, C. Riekel, R. Grothe and D. Eisenberg. 'Structure of the cross-β spine of amyloid-like fibrils'. Nature, 435(7043):773–778, **2005**.

[15] J. T. Berryman, S. E. Radford and S. A. Harris. 'Systematic Examination of Polymorphism in Amyloid Fibrils by Molecular-Dynamics Simulation'. Biophysical Journal, 100(9):2234–2242, **2011**.

[16] J. D. Sipe and A. S. Cohen. 'Review: History of the Amyloid Fibril'. Journal of Structural Biology, 130(2-3):88–98, **2000**.

[17] E. M. Ahmed. 'Hydrogel: Preparation, characterization, and applications: A review'. Journal of Advanced Research, 6(2):105–121, **2015**.

[18] I. Coin, M. Beyermann and M. Bienert. 'Solid-phase peptide synthesis: from standard procedures to the synthesis of difficult sequences'. Nature Protocols, 2(12):3247–3256, **2007**.

[19] H.-A. Klok. 'Protein-Inspired Materials: Synthetic Concepts and Potential Applications'. Angewandte Chemie International Edition, 41(9):1509–1513, **2002**.

[20] H. Lu, J. Wang, Z. Song, L. Yin, Y. Zhang, H. Tang, C. Tu, Y. Lin and J. Cheng. 'Recent advances in amino acid N-carboxyanhydrides and synthetic polypeptides: chemistry, self-assembly and biological applications'. Chem. Commun., 50(2):139–155, **2014**.

[21] E. Fischer. 'Synthese von Derivaten der Polypeptide'. In 'Untersuchungen über Aminosäuren, Polypeptide und Proteïne (1899–1906)', pp. 302–314. Springer Berlin Heidelberg, **1906**.

[22] V. du Vigneaud, C. Ressler, J. M. Swan, C. W. Roberts and P. G. Katsoyannis. 'The Synthesis of Oxytocin'. Journal of the American Chemical Society, 76(12):3115–3121, **1954**.

[23] R. B. Merrifield. 'Solid Phase Peptide Synthesis. I. The Synthesis of a Tetrapeptide'. Journal of the American Chemical Society, 85(14):2149–2154, **1963**.

[24] J. M. Collins. 'Microwave-Enhanced Synthesis of Peptides, Proteins, and Peptidomimetics'. In 'Microwaves in Organic Synthesis', pp. 897–959. Wiley-VCH Verlag GmbH & Co. KGaA, **2013**.

[25] L. A. Carpino and G. Y. Han. '9-Fluorenylmethoxycarbonyl amino-protecting group'. The Journal of Organic Chemistry, 37(22):3404–3409, **1972**.

[26] J. Clayden, N. Greeves, S. Warren and P. Wothers. Organic Chemistry. Oxford University Press, New York, **2000**.

[27] E. Frérot, J. Coste, A. Pantaloni, M.-N. Dufour and P. Jouin. 'PyBOP® and PyBroP: Two reagents for the difficult coupling of the α,α-dialkyl amino acid, Aib.' Tetrahedron, 47(2):259–270, **1991**.

[28] R. Subirós-Funosas, R. Prohens, R. Barbas, A. El-Faham and F. Albericio. 'Oxyma: An Efficient Additive for Peptide Synthesis to Replace the Benzotriazole-Based HOBt and HOAt with a Lower Risk of Explosion'. Chemistry - A European Journal, 15(37):9394–9403, **2009**.

[29] S.-F. R., K. S. N., N.-R. L., E.-F. A. and A. F. 'Advances in Acylation Methodologies Enabled by Oxyma-Based Reagents'. Aldrichimica Acta, 46(1):21–41, **2013**.

[30] P. Sieber. 'A new acid-labile anchor group for the solid-phase synthesis of C-terminal peptide amides by the Fmoc method.' Tetrahedron Letters, 28(19):2107–2110, **1987**.

[31] C. A. Guy and G. B. Fields. '[5] Trifluoroacetic acid cleavage and deprotection of resin-bound peptides following synthesis by Fmoc chemistry'. In 'Solid-Phase Peptide Synthesis', pp. 67–83. Elsevier, **1997**.

[32] D. A. Pearson, M. Blanchette, M. L. Baker and C. A. Guindon. 'Trialkylsilanes as scavengers for the trifluoroacetic acid deblocking of protecting groups in peptide synthesis'. Tetrahedron Letters, 30(21):2739–2742, **1989**.

[33] M. Nič, J. Jirát, B. Košata, A. Jenkins and A. McNaught (editors) IUPAC Compendium of Chemical Terminology. IUPAC, **2009**.

[34] H. Jakubke. Amino Acids, Peptides and Proteins: An Introduction. Palgrave, Berlin, **2014**.

[35] 'Nomenclature and Symbolism for Amino Acids and Peptides. Recommendations 1983'. European Journal of Biochemistry, 138(1):9–37, **1984**.

[36] I. Coin, R. Dölling, E. Krause, M. Bienert, M. Beyermann, C. D. Sferdean and L. A. Carpino. 'Depsipeptide Methodology for Solid-Phase Peptide Synthesis: Circumventing Side Reactions and Development of an Automated Technique via Depsidipeptide Units†,‡'. The Journal of Organic Chemistry, 71(16):6171–6177, **2006**.

[37] R. G. W. Norrish and F. W. Kirkbride. '204. Primary photochemical processes. Part I. The decomposition of formaldehyde'. Journal of the Chemical Society (Resumed), p. 1518, **1932**.

[38] S. E. Braslavsky. 'Glossary of terms used in photochemistry, 3rd edition (IUPAC Recommendations 2006)'. Pure and Applied Chemistry, 79(3):293–465, **2007**.

[39] T. Laue and A. Plagens. Named Organic Reactions. John Wiley & Sons, Ltd, Wolfsburg, Germany, **2005**.

[40] C. G. Bochet. 'Photolabile protecting groups and linkers'. Journal of the Chemical Society, Perkin Transactions 1, (2):125–142, **2001**.

[41] N. Marturi. Vision and visual servoing for nanomanipulation and nanocharacterization in scanning electron microscope. Ph.D. thesis, Université de Franche-Comté, **2013**.

[42] C. B. C. David B. Williams. Transmission Electron Microscopy. Springer-Verlag New York Inc., **2009**. URL https://www.ebook.de/de/product/7130081/david_b_williams_c_barry_carter_transmission_electron_microscopy.html.

[43] G. T. Hermanson. ‘The Reactions of Bioconjugation’. In ‘Bioconjugate Techniques’, pp. 229–258. Elsevier, **2013**.

[44] G. Mattson, E. Conklin, S. Desai, G. Nielander, M. D. Savage and S. Morgensen. ‘A practical approach to crosslinking’. Molecular Biology Reports, 17(3):167–183, **1993**.

[45] M. Skwarczynski and Y. Kiso. ‘Application of the O-N Intramolecular Acyl Migration Reaction in Medicinal Chemistry’. Current Medicinal Chemistry, 14(26):2813–2823, **2007**.

[46] U. Sezer, P. Geyer, M. Kriegleder, M. Debiossac, A. Shayeghi, M. Arndt, L. Felix and M. Mayor. ‘Selective photodissociation of tailored molecular tags as a tool for quantum optics’. Beilstein Journal of Nanotechnology, 8:325–333, **2017**.

[47] A. Sobota. Synthese und Charakterisierung von selbstassemblierenden Peptiden. Master’s thesis, Johannes Gutenberg-Universität Mainz, **2018**.

[48] X. J. Wang. Design, Syntheses, and Bioactivities of Conformationally Locked Pin1 Ground State Inhibitors. Ph.D. thesis, Virginia Polytechnic Institute and State University, **2005**.

Appendix

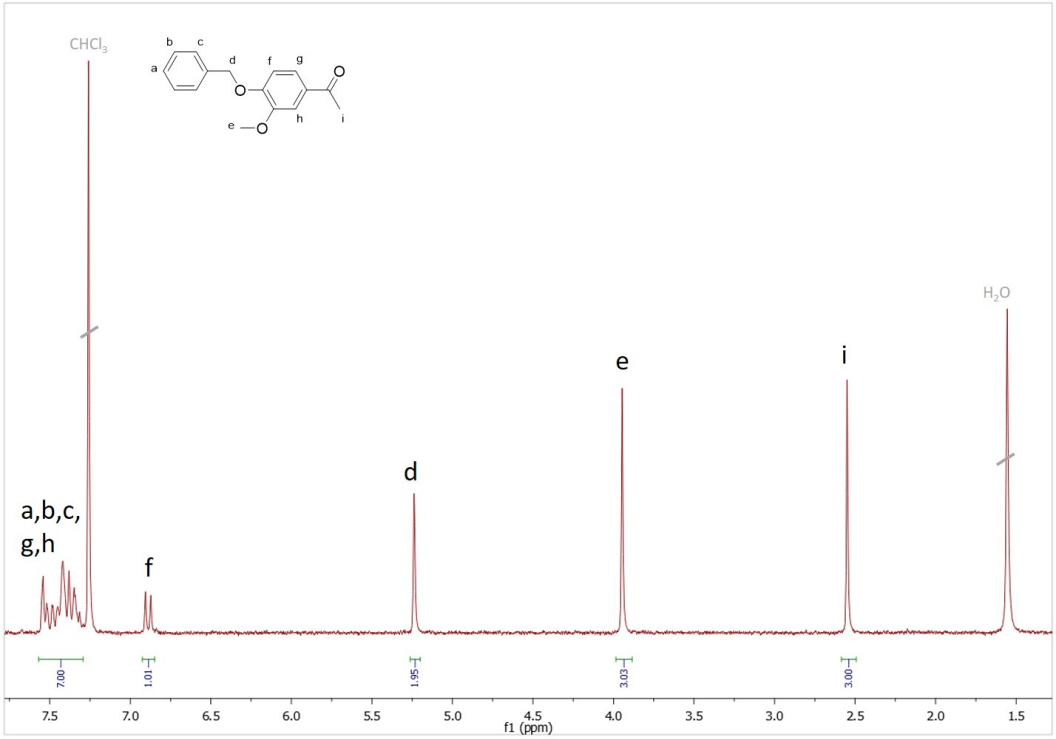

^{1}H-NMR of **PhotoSG1** (250 MHz, $CDCl_3$): δ [ppm] 7.57 to 7.29 (m, 7 H; a, b, c, g, h), 6.89 (d, J = 8.2 Hz, 1 H; f), 5.25 (s, 2 H; d), 3.95 (s, 3 H; e), 2.55 (s, 3 H; i).

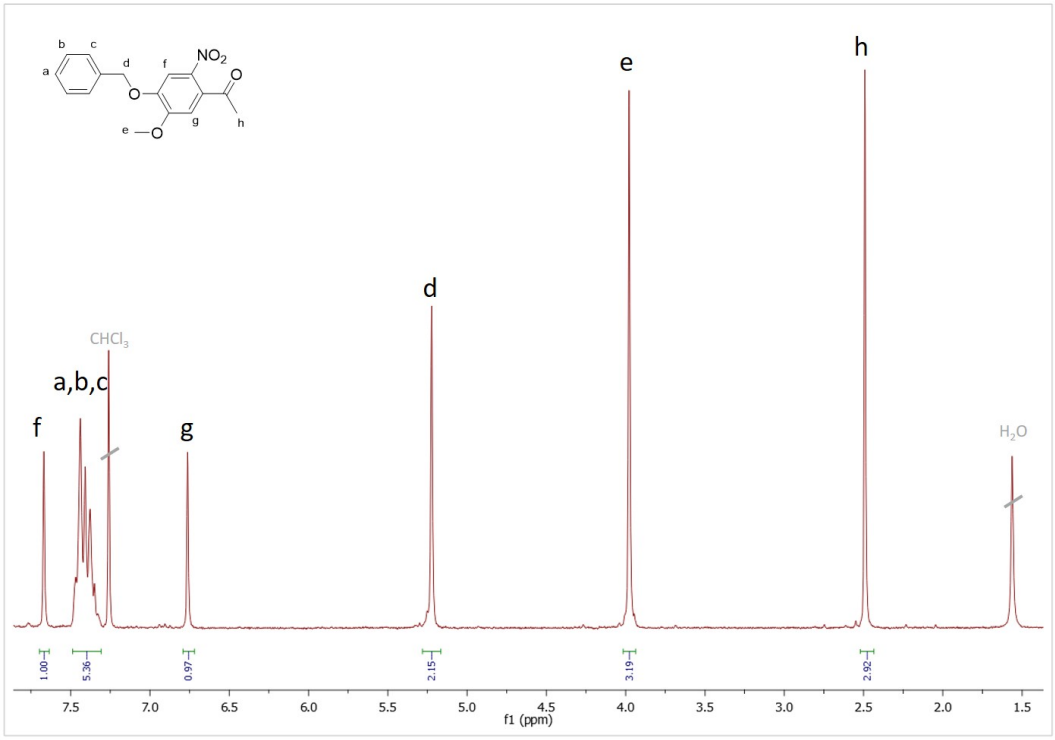

^{1}H-NMR of **PhotoSG2** (250 MHz, $CDCl_3$): δ [ppm] 7.69 (s, 1 H; f), 7.53 to 7.32 (m, 5 H; a, b, c), 6.79 (s, 1 H; g), 5.25 (s, 2 H; d), 4.00 (s, 3 H; e), 2.52 (s, 3 H; h).

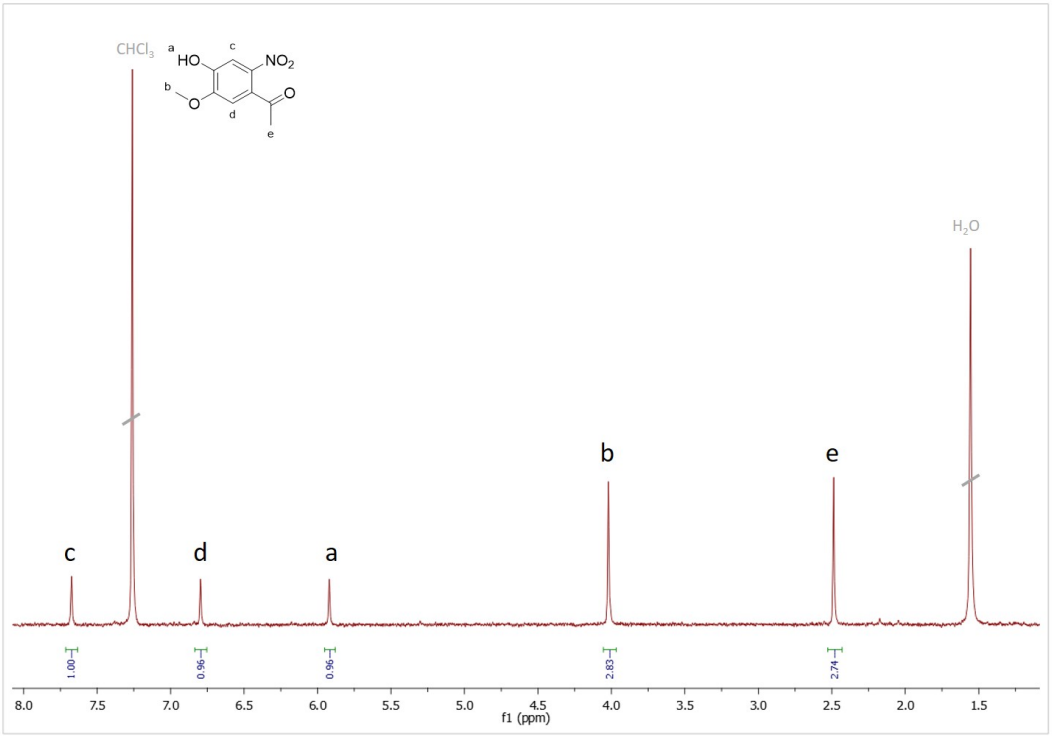

^{1}H-NMR of **PhotoSG3** (250 MHz, $CDCl_3$): δ [ppm] 7.67 (s, 1 H; c), 6.80 (s, 1 H; d), 5.92 (s, 1 H; a), 4.02 (s, 3 H; b), 2.49 (s, 3 H; e).

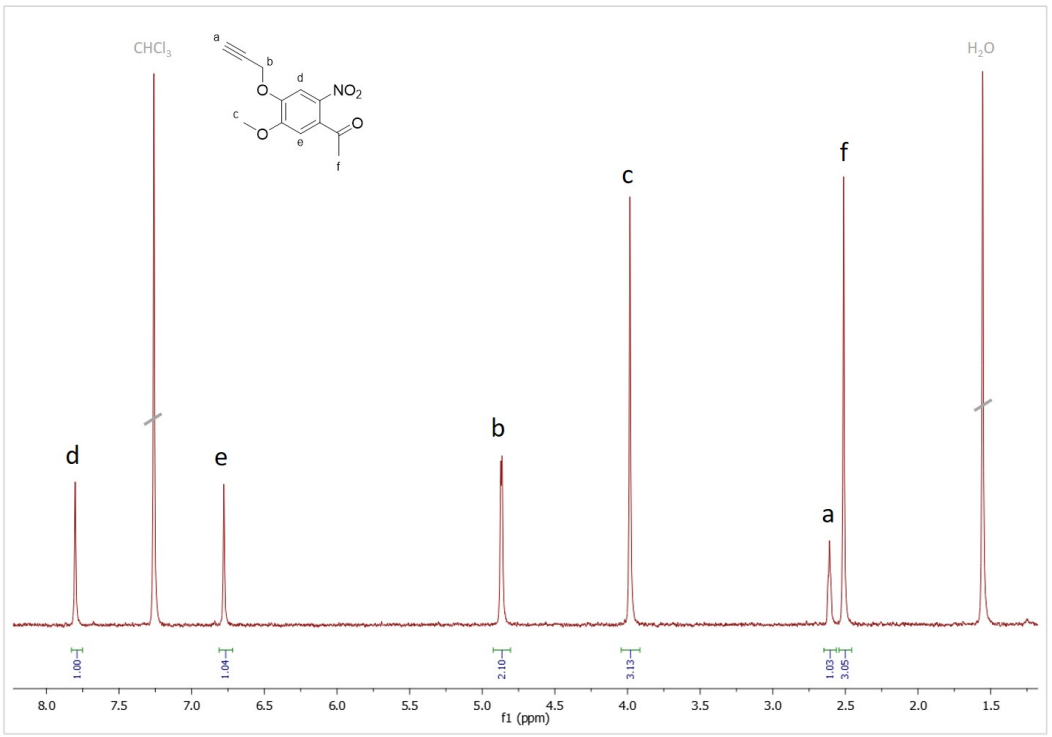

^{1}H-NMR of **PhotoSG4** (250 MHz, $CDCl_3$): δ [ppm] 7.80 (s, 1 H; d), 6.78 (s, 1 H; e), 4.87 (d, J = 2.4 Hz, 2 H; b), 3.98 (s, 3 H; c), 2.61 (t, J = 2.5 Hz, 1 H; a), 2.51 (s, 3 H; f).

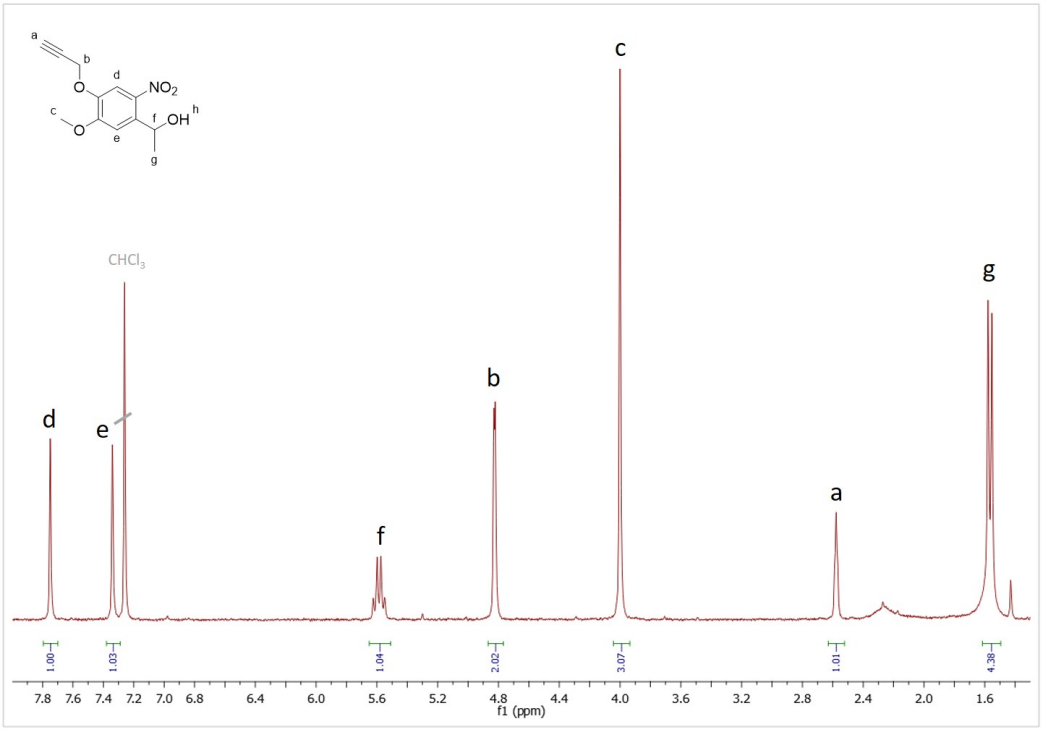

^{1}H-NMR of **PhotoSG5** (250 MHz, $CDCl_3$): δ [ppm] 7.75 (s, 1 H; d), 7.34 (s, 1 H; e), 5.59 (q, J = 6.3 Hz, 1 H; f), 4.83 (d, J = 2.4 Hz, 2 H; b), 4.00 (s, 3 H; c), 2.57 (t, J = 2.5 Hz, 1 H; a), 1.57 (d, J = 6.3 Hz, 3 H; g).

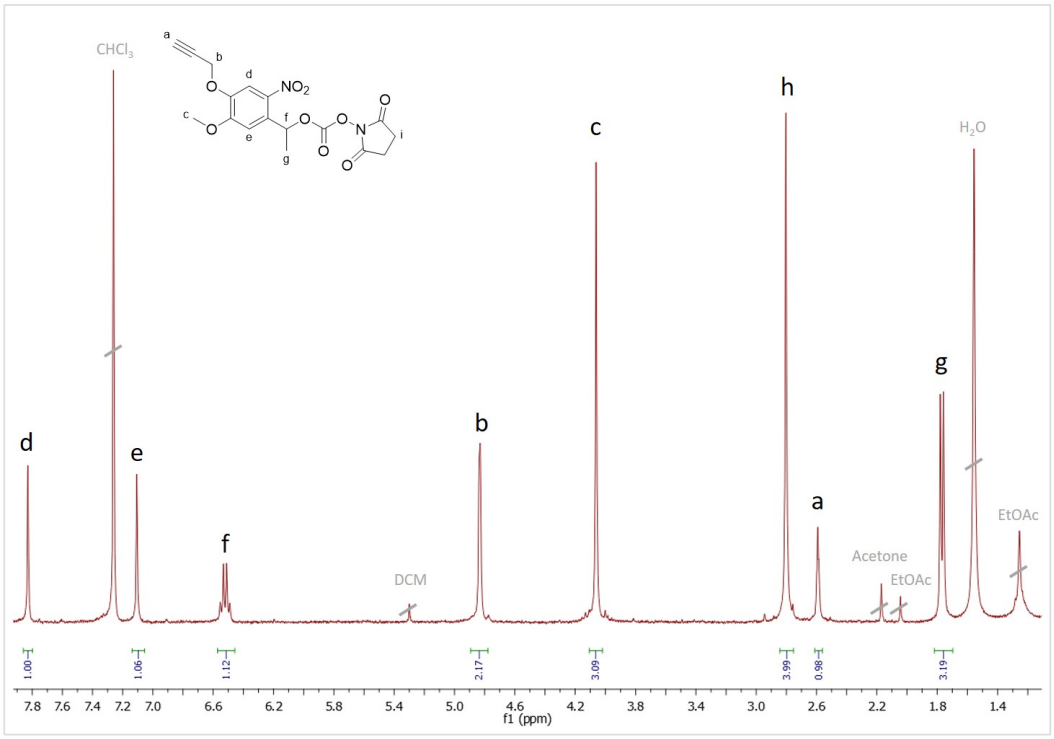

^{1}H-NMR of **PhotoSG6a** (300 MHz, $CDCl_3$): δ [ppm] 7.83 (s, 1 H; d), 7.11 (s, 1 H; e), 6.52 (q, J = 6.4 Hz, 1 H; f), 4.83 (d, J = 2.0 Hz, 2 H; b), 4.03 (s, 3 H; c), 2.78 (s, 4 H; h), 2.59 (s, 1 H; a), 1.77 (d, J = 6.3 Hz, 3 H; g).

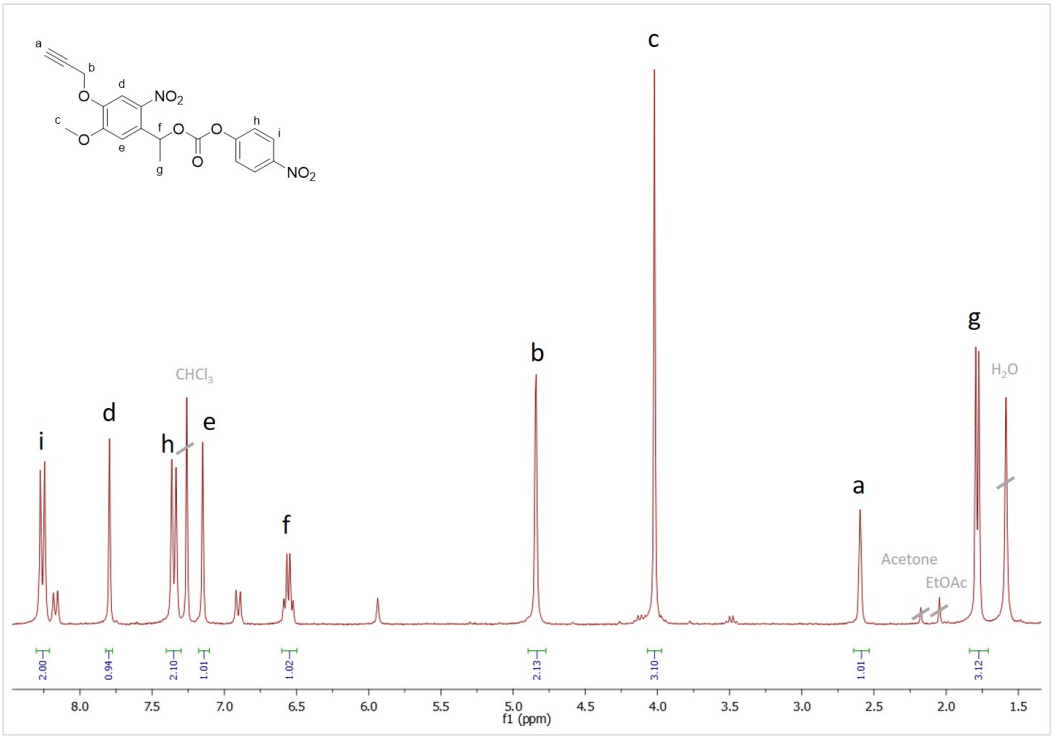

[1]H-NMR of **PhotoSG6b** (300 MHz, $CDCl_3$): δ [ppm] 8.26 (d, J = 8.8 Hz, 2 H; i), 7.80 (s, 1 H; d), 7.35 (d, J = 9.1 Hz, 2 H; h), 7.15 (s, 1 H; e), 6.56 (q, J = 6.4 Hz, 1 H; f), 4.84 (d, J = 2.4 Hz, 2 H; b), 4.02 (s, 3 H; c), 2.59 (d, J = 2.6 Hz, 1 H; a), 1.78 (d, J = 6.4 Hz, 3 H; g).

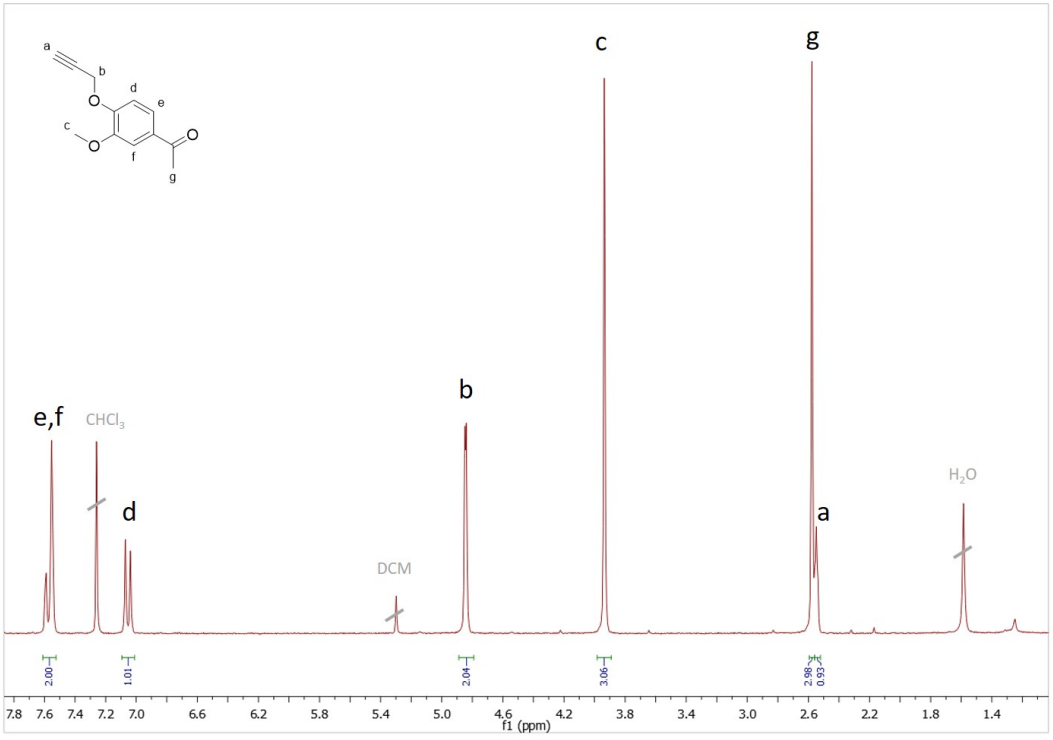

[1]H-NMR of **NSG1** (250 MHz, $CDCl_3$): δ [ppm] 7.57 (d, J = 8.9 Hz, 2 H; e, f), 7.05 (d, J = 8.2 Hz, 1 H; d), 4.84 (d, J = 2.4 Hz, 2 H; b), 3.94 (s, 3 H; c), 2.58 (s, 3 H; g), 2.55 (d, J = 3.3 Hz, 1 H; a).

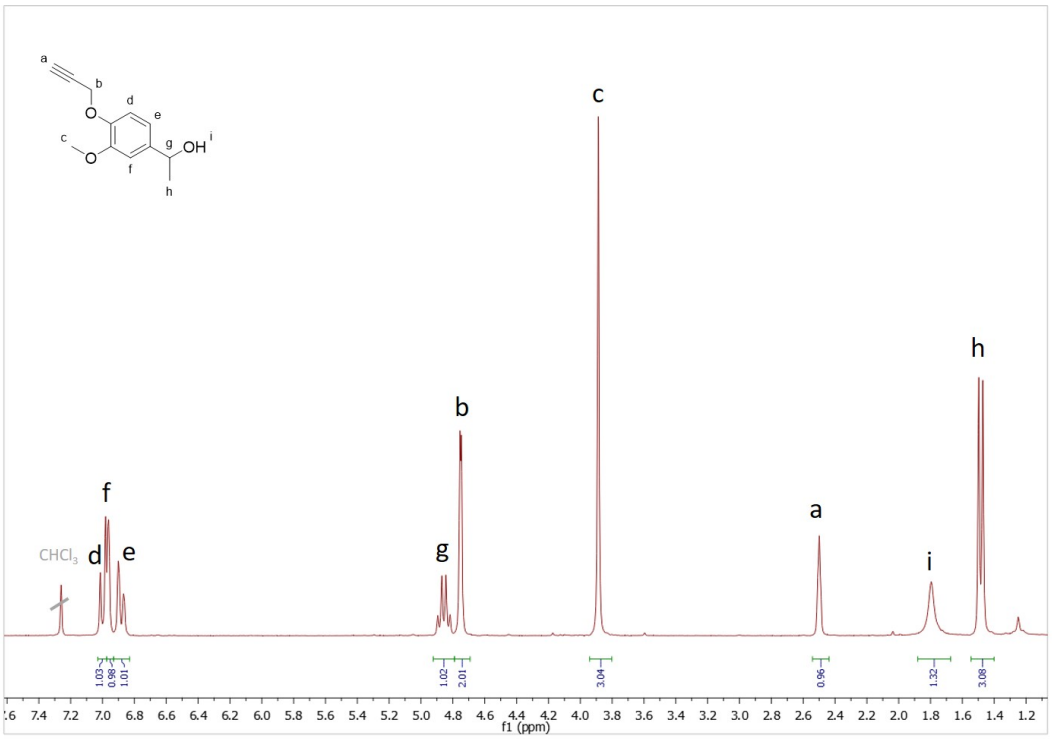

^{1}H-NMR of **NSG2** (250 MHz, $CDCl_3$): δ [ppm] 7.00 (d, J = 8.3 Hz, 1 H; d), 6.96 (d, J = 1.9 Hz, 1 H; f), 6.88 (dd, J = 8.2, 2.0 Hz, 1 H; e), 4.86 (q, J = 6.4 Hz, 1 H; g), 4.75 (d, J = 1.6 Hz, 2 H; b), 3.89 (s, 3 H; c), 2.53 to 2.46 (m, 1 H; a), 1.80 (s, 1 H; i), 1.48 (d, J = 6.4 Hz, 3 H; h).

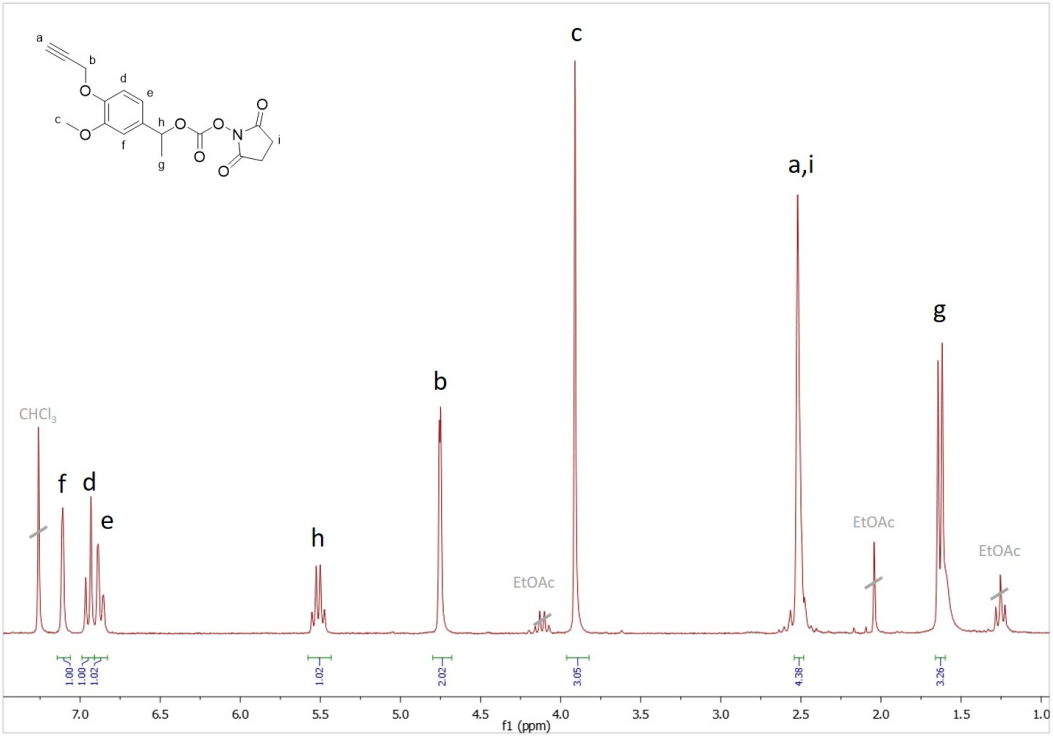

^{1}H-NMR of **NSG3** (250 MHz, $CDCl_3$): δ [ppm] 7.11 (d, J = 1.9 Hz, 1 H; f), 6.95 (d, J = 8.2 Hz, 1 H; d), 6.87 (dd, J = 8.2, 1.9 Hz, 1 H; e), 5.51 (q, J = 6.5 Hz, 1 H; h), 4.75 (d, J = 2.4 Hz, 2 H; b), 3.91 (s, 3 H; c), 2.51 (h, J = 2.7, 2.1 Hz, 5 H; a, i), 1.63 (d, J = 6.5 Hz, 3 H; g).

Affirmation in lieu of an oath

I hereby affirm that the thesis entitled: *"Synthesis of a Depsipeptide with Photolabile Protective Group and Fluorescence Label"* is my own work, written independently and without assistance other than the resources cited.

I have indicated the bodies of work, including tables and illustrations, which originate from earlier work of other authors. In each case I have quoted the origin thereof.

This thesis has not been submitted, in either identical or similar form, to any other examination authority or university, and has not yet been published.

I did not invent nor falsify the data presented in this thesis. The data have been acquired by myself or were made available for this analysis from reliable sources as indicated. I am obliged to give the 1st reviewer access to all original data until the examination procedure is completed.

Idstein, 12.06.2019